UNIVERSIDAD DE CONCEPCIÓN

Centro de Investigación en Ingeniería Matemática (CI^{2}MA)

A priori and a posteriori error analysis of a mixed FEM for stationary convective Brinkman-Forchheimer flows with variable porosity

Sergio Caucao, Gabriel N. Gatica,
Luis F. Gatica, Cristian Inzunza

PREPRINT 2026-12

SERIE DE PRE-PUBLICACIONES

A priori and a posteriori error analysis of a mixed FEM for stationary convective Brinkman–Forchheimer flows with variable porosity *

Sergio Caucao† Gabriel N. Gatica‡ Luis F. Gatica§ Cristian Inzunza‡¶

Abstract

We propose and analyze a mixed finite element method for stationary convective Brinkman–Forchheimer flows with variable porosity in R^d, $d \in \{2, 3\}$. While the primary unknowns are the velocity and pressure, our approach is based on introducing a nonlinear pseudostress as an additional variable, which allows us to eliminate the pressure from the formulation. Nevertheless, the latter, along with other physically relevant quantities such as the velocity gradient, vorticity, and stress tensor, can be accurately recovered through postprocessing formulas that depend mainly on the pseudostress and velocity. This capability constitutes one of the most distinctive features of the proposed strategy. Owing to the convective and Forchheimer terms, the velocity must be sought in a smaller space than in the standard setting, which naturally leads to a Banach space framework. The resulting formulation exhibits a perturbed saddle-point structure and can be equivalently recast as a fixed-point equation. Under suitable small-data assumptions, the unique solvability of the continuous and discrete problems is established by combining the Banach fixed-point theorem with the Babuška–Brezzi theory in Banach spaces for perturbed saddle-point problems and the Banach–Nečas–Babuška theorem. The finite element method employs Raviart–Thomas spaces of order $k \geq 0$ and spaces of discontinuous piecewise polynomials of degree k for the nonlinear pseudostress tensor and the velocity, respectively. Stability, convergence, and *a priori* error estimates are derived. We also derive a reliable and efficient residual-based *a posteriori* error estimator on general polygonal and polyhedral domains. Finally, several numerical examples illustrate the performance of the method, confirm the theoretical convergence rates, validate the estimator, and demonstrate the behavior of the associated adaptive algorithm, including the case of flow through a two-dimensional nonconvex channel with localized low-permeability regions.

Key words: convective Brinkman–Forchheimer equations, variable porosity, Banach spaces, mixed finite element methods, fixed-point theory, *a priori* and *a posteriori* error analysis

Mathematics subject classifications (2000): 65N30, 65N12, 65N15, 35Q79, 80A19, 76R05, 76D07

*This research was partially supported by ANID-Chile through Centro de Modelamiento Matemático (FB210005), Fondecyt project 1250937, and Fondecyt Postdoctoral project 3260398; by DI-UCSC through the project FGII 06/2024; by Grupo de Investigación en Análisis Numérico y Cálculo Científico (GIANuC^2), Universidad Católica de la Santísima Concepción; and by Centro de Investigación en Ingeniería Matemática (CI^{2}MA), Universidad de Concepción.

†GIANuC^2 and Departamento de Matemática y Física Aplicadas, Universidad Católica de la Santísima Concepción, Casilla 297, Concepción, Chile, email: scaucao@ucsc.cl.

‡CI^{2}MA and Departamento de Ingeniería Matemática, Universidad de Concepción, Casilla 160-C, Concepción, Chile, email: ggatica@ci2ma.udec.cl.

§GIANuC^2 and Departamento de Matemática y Física Aplicadas, Universidad Católica de la Santísima Concepción, Casilla 297, Concepción, Chile, and CI^{2}MA, Universidad de Concepción, Casilla 160-C, Concepción, Chile, email: lgatica@ucsc.cl.

¶GIANuC^2 and Departamento de Matemática y Física Aplicadas, Universidad Católica de la Santísima Concepción, Casilla 297, Concepción, Chile, email: crinzunza@ucsc.cl

1 Introduction

The flow of fluids through porous media is a classical yet persistently challenging problem, with applications ranging from petroleum extraction and groundwater remediation to industrial filtration and the mechanics of fractured geological formations. In many of these settings, the geometry and composition of the medium are spatially heterogeneous, and the flow regime involves significant inertial effects that render simpler models inadequate. The convective Brinkman–Forchheimer (CBF) equations with variable porosity offer a physically grounded response to this challenge: by combining viscous diffusion terms of Brinkman type, nonlinear inertial corrections of Forchheimer type, convective effects associated with moderate to high velocity flows, and a spatially varying porosity field, they provide a unified framework capable of capturing the complex dynamics of heterogeneous porous structures.

The mathematical analysis of the CBF equations has evolved considerably over the past two decades. Early contributions [17, 45, 38] established foundational analytical and numerical results. In particular, [17] studied the continuous dependence of solutions with respect to the Forchheimer coefficient in the $\mathbf{H}^1$-norm, while [38] developed a mixed finite element approximation for the two-dimensional stationary problem and derived well-posedness and error estimates. More recently, the attention has shifted toward mixed formulations and their numerical analysis. In this direction, [13] developed a Banach space-based mixed finite element method and proved well-posedness at both the continuous and discrete levels. This was complemented by the corresponding *a posteriori* error analysis in [14]. In turn, [9] proposed an augmented pseudostress-velocity formulation for the stationary problem and established rigorous *a priori* and *a posteriori* error estimates, whereas [7] developed a non-augmented mixed formulation in Banach spaces for the coupled CBF/double-diffusion system. Parallel developments for Darcy–Forchheimer models have also enriched the numerical analysis of nonlinear porous-media flows [33, 39, 40, 41, 37]. For example, [33] analyzed a convergent discretization of the steady Darcy–Forchheimer equations, [39] derived existence, uniqueness, and error estimates for a mixed method in two dimensions, and [37] proposed a parameter-robust scheme for poroelasticity with Darcy–Forchheimer flow. When variable porosity is incorporated, however, the analysis becomes substantially more delicate, and the available literature remains limited. Solvability results in this setting were obtained in [42, 43], and a finite element error analysis for a Darcy–Brinkman–Forchheimer model with spatially varying porosity was carried out in [19]. In addition, a three-field mixed finite element method for the CBF problem with variable porosity, within a Banach space framework, was introduced and analyzed in [10]. Despite this progress, the development of *a posteriori* error estimation for the CBF problem with variable porosity remains largely unexplored.

The nonlinear character of the convective and Forchheimer terms, together with the variable porosity, may induce pronounced local variations in the solution, thus making *a posteriori* error estimation and adaptive mesh refinement especially relevant for an efficient numerical approximation. Such estimators have been developed for mixed formulations in several related contexts [25, 26, 23, 15, 12, 3, 29, 9, 14, 16]. In particular, [25] proposes a residual-based estimator for a three-field generalized Stokes model, [26] develops an estimator for a dual-mixed approximation of non-Newtonian flow, [15] derives both *a priori* and *a posteriori* estimates for a pseudostress-based mixed Stokes formulation with varying density, and [29] establishes *a posteriori* error estimates for a Banach spaces-based fully mixed method for Boussinesq-type models. To the best of the authors' knowledge, however, reliable and efficient residual-based *a posteriori* error estimation for Banach spaces-based mixed finite element formulations of the CBF problem with variable porosity has not yet been developed in the literature. Filling this gap constitutes one of the main contributions of the present work.

Motivated by the previous discussion, we develop and analyze a mixed formulation for the stationary CBF problem with variable porosity, and study its numerical approximation. To this end, we introduce a

nonlinear pseudostress tensor as in [5] (see also [4], [13], and [7]) and subsequently eliminate the pressure unknown by means of the incompressibility condition. The resulting problem exhibits a perturbed saddle-point structure, where the convective and Forchheimer terms naturally lead to a Banach space framework. The well-posedness of the continuous formulation is established by combining a classical fixed-point strategy with recent advances in the Babuška–Brezzi theory for perturbed saddle-point problems in a Banach space setting, as developed in [21], together with the classical Banach–Nečas–Babuška theorem [24]. Similar arguments are employed for the discrete formulation, whose solvability is also proved under a suitable smallness assumption, mainly involving the porosity. Regarding the numerical scheme, we employ Raviart–Thomas spaces of order $k \geq 0$ for the approximation of the pseudostress tensor and discontinuous piecewise polynomial spaces of degree k for the velocity. In addition, by applying an ad-hoc Strang-type lemma, we derive the corresponding *a priori* error estimates and prove that the method converges at the optimal rate. Furthermore, we propose a reliable and efficient residual-based *a posteriori* error estimator for the new numerical scheme. The proofs of reliability and efficiency follow the technique developed in [44], [30], [15], [12], [3], and [29], making use of the global inf-sup condition, Helmholtz decompositions in a Banach space setting, inverse inequalities, and well-known properties of bubble functions.

We have organized the content of this article as follows. In the remainder of this section, we introduce the standard notation and the necessary function spaces. In Section 2, we present the model problem and derive the mixed formulation. Section 3 is devoted to the well-posedness analysis of the continuous problem. The corresponding Galerkin scheme is introduced and analyzed in Section 4 for generic finite-dimensional subspaces. There, the discrete counterpart of the continuous theory is employed to establish existence and uniqueness of the solution, together with an *a priori* estimate. We conclude the section by specifying particular finite element spaces that satisfy the stability hypotheses and by deriving the corresponding theoretical convergence rates. In Section 5, we establish a reliable and efficient residual-based *a posteriori* error estimator. Then, in Section 6, we present several numerical experiments illustrating the accuracy and flexibility of the proposed mixed finite element method, as well as the reliability and efficiency of the *a posteriori* error estimator. Finally, other variables of interest recovered through postprocessing are analyzed in Appendix A, while further properties used in the derivation of the reliability and efficiency estimates are provided in Appendices B and C.

Preliminary notations

Let $\Omega \subset \mathrm{R}^d, d \in \{2,3\}$, be a bounded domain with polyhedral boundary Γ, and let $\mathbf{n}$ be the outward unit normal vector on Γ. Standard notation will be adopted for Lebesgue spaces $\mathrm{L}^p(\Omega)$ and Sobolev spaces $\mathrm{W}^{s,p}(\Omega)$, with $s \in \mathrm{R}$ and $p > 1$, whose corresponding norms, either for the scalar, vectorial, or tensorial case, are written as $\|\cdot\|_{0,p;\Omega}$ and $\|\cdot\|_{s,p;\Omega}$, respectively. In addition, given a non-negative integer m, $\mathrm{W}^{m,2}(\Omega)$ is also denoted by $\mathrm{H}^m(\Omega)$, and the notations of its norm and seminorm are simplified to $\|\cdot\|_{m,\Omega}$ and $|\cdot|_{m,\Omega}$, respectively. Furthermore, $\mathbf{H}^{1/2}(\Gamma)$ is the space of traces of functions of $\mathbf{H}^1(\Omega)$ and $\mathbf{H}^{-1/2}(\Gamma)$ is its dual, whereas $\langle\cdot,\cdot\rangle_\Gamma$ stands for the corresponding product of duality between $\mathbf{H}^{-1/2}(\Gamma)$ and $\mathbf{H}^{1/2}(\Gamma)$. By $\mathbf{M}$ and $\mathbb{M}$ we mean the corresponding vectorial and tensorial counterparts of the generic scalar functional space M, whereas M' represents its dual space, whose norm is defined by $\|f\|_{\mathrm{M}'} := \sup_{0 \neq v \in \mathrm{M}} \dfrac{|f(v)|}{\|v\|_{\mathrm{M}}}$. In particular, we set $\mathbf{R} := \mathrm{R}^d$ and $\mathbb{R} := \mathrm{R}^{d\times d}$. In turn, for any vector fields $\mathbf{v} = (v_i)_{i=1,d}$ and $\mathbf{w} = (w_i)_{i=1,d}$, we define the gradient, divergence, and tensor product operators, as

$$\nabla \mathbf{v} := \left(\frac{\partial v_i}{\partial x_j}\right)_{i,j=1,d}, \quad \mathrm{div}(\mathbf{v}) := \sum_{j=1}^{d} \frac{\partial v_j}{\partial x_j}, \quad \text{and} \quad \mathbf{v} \otimes \mathbf{w} := (v_i w_j)_{i,j=1,d}\,.$$

Also, for any tensor fields $\boldsymbol{\tau} = (\tau_{ij})_{i,j=1,d}$ and $\boldsymbol{\zeta} = (\zeta_{ij})_{i,j=1,d}$, we let $\mathbf{div}(\boldsymbol{\tau})$ be the usual divergence operator div acting along the rows of $\boldsymbol{\tau}$, and define the transpose, the trace, the tensor inner product, and the deviatoric tensor, respectively, as

$$\boldsymbol{\tau}^{\mathrm{t}} := (\tau_{ji})_{i,j=1,d}\,, \quad \mathrm{tr}(\boldsymbol{\tau}) := \sum_{i=1}^{d} \tau_{ii}\,, \quad \boldsymbol{\tau} : \boldsymbol{\zeta} := \sum_{i,j=1}^{d} \tau_{ij}\,\zeta_{ij}, \text{ and } \boldsymbol{\tau}^{\mathtt{d}} := \boldsymbol{\tau} - \frac{1}{d}\,\mathrm{tr}(\boldsymbol{\tau})\,\mathbb{I}\,,$$

where $\mathbb{I}$ is the identity matrix in $\mathbb{R}$. In what follows, when no confusion arises, $|\cdot|$ denotes the Euclidean norm in $\mathbf{R}$ or $\mathbb{R}$.

2 The continuous formulation

In this section, we introduce the model problem, derive the corresponding weak formulation, and establish the stability bounds satisfied by the bilinear forms and functionals appearing in the variational formulation.

2.1 The model problem

In what follows we consider the model introduced in [42] (see also [43, 19, 10]), which is given by the convective Brinkman–Forchheimer equations with varying porosity ρ. More precisely, we are interested in finding a velocity field $\mathbf{u}$ and a pressure field p, such that

$$\begin{aligned} -\,\mathbf{div}\Big(\rho\,\Big\{\mu\,\nabla\mathbf{u} - (\mathbf{u}\otimes\mathbf{u})\Big\}\Big) + \rho\,\nabla p + \mathtt{D}(\rho)\,\mathbf{u} + \mathtt{F}(\rho)\,|\mathbf{u}|^{m-2}\mathbf{u} &= \rho\,\mathbf{f} \quad \text{in} \quad \Omega\,, \\ \mathrm{div}(\rho\,\mathbf{u}) &= 0 \quad \text{in} \quad \Omega\,, \\ \mathbf{u} &= \mathbf{u}_{\mathrm{D}} \quad \text{on} \quad \Gamma\,, \end{aligned} \tag{2.1}$$

where $\mu = \mathtt{Re}^{-1}$, $\mathtt{Re}$ is the Reynolds number, $\mathtt{D}(\rho)$ is the Darcy coefficient, $\mathtt{F}(\rho)$ is the Forchheimer coefficient, m is a given number in $[3,4]$, $\mathbf{f}$ is a given external force, and $\mathbf{u}_{\mathrm{D}} \in \mathbf{H}^{1/2}(\Gamma)$ is a Dirichlet datum. In addition, the distribution porosity function $\rho \in \mathrm{W}^{1,4}(\Omega) \cap \mathrm{L}^{\infty}(\Omega)$ satisfies

$$0 < \rho_0 \leq \rho(\mathbf{x}) \leq 1 \quad \text{a.e.} \quad \text{in} \quad \Omega\,, \tag{2.2}$$

where ρ_0 is a positive constant. In turn, we assume that both the porosity-dependent Darcy and Forchheimer coefficients are positive and bounded functions, that is, there exists positive constants $\mathtt{D}_0, \mathtt{D}_1, \mathtt{F}_0$, and $\mathtt{F}_1$, such that

$$0 < \mathtt{D}_0 \leq \mathtt{D}(s) \leq \mathtt{D}_1 \quad \text{and} \quad 0 < \mathtt{F}_0 \leq \mathtt{F}(s) \leq \mathtt{F}_1 \quad \forall\, s \in [\rho_0, 1)\,. \tag{2.3}$$

We emphasize that one always has $\mathtt{D}(1) = \mathtt{F}(1) = 0$ and thus the standard Navier–Stokes equation is recovered from (2.1) when $\rho = 1$. In addition, due to the first equation of (2.1), and in order to guarantee uniqueness of the pressure p, this unknown will be sought in the space

$$\mathrm{L}^2_0(\Omega) := \left\{ q \in \mathrm{L}^2(\Omega) : \quad \int_\Omega q = 0 \right\}.$$

Next, in order to derive a mixed formulation for (2.1), in which the Dirichlet boundary condition for the velocity becomes a natural one, we first recall the identities

$$\mathrm{div}(\varrho\,\mathbf{v}) = \varrho\,\mathrm{div}(\mathbf{v}) + \mathbf{v}\cdot\nabla\varrho \quad \text{and} \quad \mathbf{div}(\varrho\,\boldsymbol{\tau}) = \varrho\,\mathbf{div}(\boldsymbol{\tau}) + \boldsymbol{\tau}\,\nabla\varrho\,, \tag{2.4}$$

for sufficiently smooth scalar, vector and tensor functions ϱ, $\mathbf{v}$ and $\boldsymbol{\tau}$, respectively. Then, using the second equation of (2.1) and the first identity in (2.4) with $\varrho = \rho$ and $\mathbf{v} = \mathbf{u}$, we deduce that

$$\mathrm{div}(\mathbf{u}) = -\left(\mathbf{u}\cdot\frac{\nabla\rho}{\rho}\right) \quad \text{in} \quad \Omega\,. \tag{2.5}$$

We observe that owing to the Dirichlet boundary condition $\mathbf{u} = \mathbf{u}_{\mathrm{D}}$ on Γ and (2.5), $\mathbf{u}_{\mathrm{D}}$ must satisfy the compatibility condition

$$\int_{\Gamma}\mathbf{u}_{\mathrm{D}}\cdot\mathbf{n} = -\int_{\Omega}\left(\mathbf{u}\cdot\frac{\nabla\rho}{\rho}\right)\,. \tag{2.6}$$

Now, proceeding as in [5] (see similar approaches in [4], [13], [7]), we introduce as a further unknown the nonlinear pseudostress tensor $\boldsymbol{\sigma}$, which is defined by

$$\boldsymbol{\sigma} := \mu\,\nabla\mathbf{u} - (\mathbf{u}\otimes\mathbf{u}) - p\,\mathbb{I} \quad \text{in} \quad \Omega\,. \tag{2.7}$$

In this way, applying the matrix trace operator to $\boldsymbol{\sigma}$ and utilizing again (2.5), one arrives at

$$p = -\frac{1}{d}\left\{\mathrm{tr}(\boldsymbol{\sigma}+\mathbf{u}\otimes\mathbf{u}) + \mu\left(\mathbf{u}\cdot\frac{\nabla\rho}{\rho}\right)\right\} \quad \text{in} \quad \Omega\,. \tag{2.8}$$

Thus, applying the deviatoric operator to $\boldsymbol{\sigma}$ in (2.7), and using (2.5) to find $\big(\nabla\mathbf{u}\big)^{\mathtt{d}}$, we obtain

$$\boldsymbol{\sigma}^{\mathtt{d}} \;=\; \mu\nabla\mathbf{u} - (\mathbf{u}\otimes\mathbf{u})^{\mathtt{d}} + \frac{\mu}{d}\left(\mathbf{u}\cdot\frac{\nabla\rho}{\rho}\right)\mathbb{I}\,. \tag{2.9}$$

In turn, using the second identity in (2.4) with $\varrho = \rho$ and $\boldsymbol{\tau} = \mu\,\nabla\mathbf{u} - (\mathbf{u}\otimes\mathbf{u})$, and noting that $\rho\,\nabla p = \rho\,\mathbf{div}(p\,\mathbb{I})$, we find that

$$-\,\mathbf{div}\Big(\rho\left\{\mu\,\nabla\mathbf{u} - (\mathbf{u}\otimes\mathbf{u})\right\}\Big) + \rho\,\nabla p \;=\; -\,\rho\,\mathbf{div}(\boldsymbol{\sigma}) \;-\; \Big(\mu\,\nabla\mathbf{u} - (\mathbf{u}\otimes\mathbf{u})\Big)\,\nabla\rho\,. \tag{2.10}$$

Consequently, employing (2.9) and (2.10), we find that (2.1) can be rewritten, equivalently, as follows: Find $(\boldsymbol{\sigma},\mathbf{u})$ in suitable spaces to be indicated below such that

$$\begin{aligned}
\frac{1}{\mu}\,\boldsymbol{\sigma}^{\mathtt{d}} + \frac{1}{\mu}\,(\mathbf{u}\otimes\mathbf{u})^{\mathtt{d}} - \frac{1}{d}\left(\mathbf{u}\cdot\frac{\nabla\rho}{\rho}\right)\mathbb{I} - \nabla\mathbf{u} = \mathbf{0} \quad &\text{in} \quad \Omega\,,\\
\frac{\mathtt{D}(\rho)}{\rho}\mathbf{u} + \frac{\mathtt{F}(\rho)}{\rho}|\mathbf{u}|^{m-2}\mathbf{u} - \left\{\boldsymbol{\sigma}^{\mathtt{d}} - \frac{1}{d}\left(\mathrm{tr}(\mathbf{u}\otimes\mathbf{u}) + \mu\left(\mathbf{u}\cdot\frac{\nabla\rho}{\rho}\right)\right)\mathbb{I}\right\}\frac{\nabla\rho}{\rho} - \mathbf{div}(\boldsymbol{\sigma}) = \mathbf{f} \quad &\text{in} \quad \Omega\,,\\
\mathbf{u} = \mathbf{u}_{\mathrm{D}} \quad \text{on} \quad \Gamma\,, \quad \int_{\Omega}\mathrm{tr}(\boldsymbol{\sigma}+\mathbf{u}\otimes\mathbf{u}) - \mu\int_{\Gamma}\mathbf{u}_{\mathrm{D}}\cdot\mathbf{n} = 0\,.
\end{aligned} \tag{2.11}$$

At this point we stress that, as suggested by (2.8), p is eliminated from the present formulation and computed afterwards in terms of $\boldsymbol{\sigma},\mathbf{u}$, and ρ by using that identity (see Appendix A for details). This fact justifies the last equation in (2.11), which aims to ensure that the resulting p does belong to $\mathrm{L}^2_0(\Omega)$. Note that the latter was derived by combining the identities (2.8) and (2.6).

2.2 The mixed variational formulation

In this section we follow [4] and [13] (see also [6], [31], [7]) to derive a Banach spaces-based mixed formulation for the problem given by (2.11). To this end, we test the first and second equations of

(2.11) against functions $\boldsymbol{\tau}$ and $\mathbf{v}$ associated with the unknowns $\boldsymbol{\sigma}$ and $\mathbf{u}$, respectively, whence, using the identity $\boldsymbol{\sigma}^{\mathtt{d}} : \boldsymbol{\tau} = \boldsymbol{\sigma}^{\mathtt{d}} : \boldsymbol{\tau}^{\mathtt{d}}$, we formally get

$$\frac{1}{\mu}\int_\Omega \boldsymbol{\sigma}^{\mathtt{d}} : \boldsymbol{\tau}^{\mathtt{d}} - \int_\Omega \nabla\mathbf{u} : \boldsymbol{\tau} + \frac{1}{\mu}\int_\Omega (\mathbf{u}\otimes\mathbf{u})^{\mathtt{d}} : \boldsymbol{\tau} - \frac{1}{d}\int_\Omega \left(\mathbf{u}\cdot\frac{\nabla\rho}{\rho}\right)\mathrm{tr}(\boldsymbol{\tau}) = 0\,, \tag{2.12}$$

$$\int_\Omega \mathbf{v}\cdot\mathbf{div}(\boldsymbol{\sigma}) - \int_\Omega \frac{\mathtt{D}(\rho)}{\rho}\mathbf{u}\cdot\mathbf{v} - \int_\Omega \frac{\mathtt{F}(\rho)}{\rho}|\mathbf{u}|^{m-2}\mathbf{u}\cdot\mathbf{v} + \int_\Omega \left(\boldsymbol{\sigma}^{\mathtt{d}}\frac{\nabla\rho}{\rho}\right)\cdot\mathbf{v}$$
$$-\frac{1}{d}\int_\Omega \left(\mathrm{tr}(\mathbf{u}\otimes\mathbf{u}) + \mu\left(\mathbf{u}\cdot\frac{\nabla\rho}{\rho}\right)\right)\left(\mathbf{v}\cdot\frac{\nabla\rho}{\rho}\right) = -\int_\Omega \mathbf{f}\cdot\mathbf{v}\,. \tag{2.13}$$

Notice here that the first term of (2.12) is well-defined for $\boldsymbol{\sigma}$, $\boldsymbol{\tau} \in \mathbb{L}^2(\Omega)$. In turn, using the fact that ρ and $\mathtt{F}(\rho)$ are bounded (cf. (2.2), (2.3)), with $\rho \in \mathrm{W}^{1,4}(\Omega)\cap\mathrm{L}^\infty(\Omega)$, and applying the Hölder and Cauchy–Schwarz inequalities, and the Sobolev embedding of $\mathbf{L}^4(\Omega)$ into $\mathbf{L}^{2(m-2)}(\Omega)$, with $m \in [3,4]$, we find that the third and fourth terms in (2.12) and the third, fourth, fifth and sixth terms in (2.13), can be bounded, respectively, as

$$\left|\int_\Omega (\mathbf{w}\otimes\mathbf{u})^{\mathtt{d}} : \boldsymbol{\tau}\right| \leq \|\mathbf{w}\|_{0,4;\Omega}\,\|\mathbf{u}\|_{0,4;\Omega}\,\|\boldsymbol{\tau}\|_{0,\Omega}\,, \tag{2.14}$$

$$\left|\int_\Omega \left(\mathbf{u}\cdot\frac{\nabla\rho}{\rho}\right)\mathrm{tr}(\boldsymbol{\tau})\right| \leq \sqrt{d}\left\|\frac{\nabla\rho}{\rho}\right\|_{0,4;\Omega}\|\mathbf{u}\|_{0,4;\Omega}\,\|\boldsymbol{\tau}\|_{0,\Omega}\,, \tag{2.15}$$

$$\left|\int_\Omega \frac{\mathtt{F}(\rho)}{\rho}|\mathbf{w}|^{m-2}\mathbf{u}\cdot\mathbf{v}\right| \leq \frac{\mathtt{F}_1}{\rho_0}\,|\Omega|^{(4-m)/4}\,\|\mathbf{w}\|^{m-2}_{0,4;\Omega}\,\|\mathbf{u}\|_{0,4;\Omega}\,\|\mathbf{v}\|_{0,4;\Omega}\,, \tag{2.16}$$

$$\left|\int_\Omega \left(\boldsymbol{\sigma}^{\mathtt{d}}\frac{\nabla\rho}{\rho}\right)\cdot\mathbf{v}\right| \leq \left\|\frac{\nabla\rho}{\rho}\right\|_{0,4;\Omega}\|\boldsymbol{\sigma}\|_{0,\Omega}\,\|\mathbf{v}\|_{0,4;\Omega}\,, \tag{2.17}$$

$$\left|\int_\Omega \mathrm{tr}(\mathbf{w}\otimes\mathbf{u})\left(\mathbf{v}\cdot\frac{\nabla\rho}{\rho}\right)\right| \leq \sqrt{d}\left\|\frac{\nabla\rho}{\rho}\right\|_{0,4;\Omega}\|\mathbf{w}\|_{0,4;\Omega}\,\|\mathbf{u}\|_{0,4;\Omega}\,\|\mathbf{v}\|_{0,4;\Omega}\,, \tag{2.18}$$

and

$$\left|\int_\Omega \left(\mathbf{u}\cdot\frac{\nabla\rho}{\rho}\right)\left(\mathbf{v}\cdot\frac{\nabla\rho}{\rho}\right)\right| \leq \left\|\frac{\nabla\rho}{\rho}\right\|^2_{0,4;\Omega}\|\mathbf{u}\|_{0,4;\Omega}\,\|\mathbf{v}\|_{0,4;\Omega}\,, \tag{2.19}$$

which shows that they are well-defined for all $\mathbf{w}$, $\mathbf{u}$, $\mathbf{v} \in \mathbf{L}^4(\Omega)$ and for all $\boldsymbol{\sigma}, \boldsymbol{\tau} \in \mathbb{L}^2(\Omega)$. In addition, since $\mathtt{D}(\rho)$ is bounded (cf. (2.3)) and $\mathbf{L}^4(\Omega)$ is certainly contained in $\mathbf{L}^2(\Omega)$, it is clear that the second term in (2.13) makes sense as well. Next, knowing the space to which $\mathbf{v}$ belongs, the first and source terms in (2.13) are well defined if $\mathbf{div}(\boldsymbol{\sigma}) \in \mathbf{L}^{4/3}(\Omega)$ and $\mathbf{f} \in \mathbf{L}^{4/3}(\Omega)$, which we assume henceforth. Thus, initially we look for $\boldsymbol{\sigma}$ in the Banach space

$$\mathbb{H}(\mathbf{div}_{4/3};\Omega) := \left\{\boldsymbol{\zeta} \in \mathbb{L}^2(\Omega) : \quad \mathbf{div}(\boldsymbol{\zeta}) \in \mathbf{L}^{4/3}(\Omega)\right\},$$

which is equipped with the norm

$$\|\boldsymbol{\zeta}\|_{\mathbf{div}_{4/3};\Omega} := \|\boldsymbol{\zeta}\|_{0,\Omega} + \|\mathbf{div}(\boldsymbol{\zeta})\|_{0,4/3;\Omega}\,.$$

Moreover, choosing $\mathbb{H}(\mathbf{div}_{4/3};\Omega)$ as the corresponding space of test functions, and assuming originally that $\mathbf{u} \in \mathbf{H}^1(\Omega)$, we can integrate by parts the second term in (2.12), so that, using the Dirichlet boundary condition $\mathbf{u} = \mathbf{u}_{\mathrm{D}}$ on Γ, that equation becomes

$$\frac{1}{\mu}\int_\Omega \boldsymbol{\sigma}^{\mathtt{d}} : \boldsymbol{\tau}^{\mathtt{d}} + \int_\Omega \mathbf{u}\cdot\mathbf{div}(\boldsymbol{\tau}) + \frac{1}{\mu}\int_\Omega (\mathbf{u}\otimes\mathbf{u})^{\mathtt{d}} : \boldsymbol{\tau} - \frac{1}{d}\int_\Omega \left(\mathbf{u}\cdot\frac{\nabla\rho}{\rho}\right)\mathrm{tr}(\boldsymbol{\tau}) = \langle\boldsymbol{\tau}\mathbf{n}, \mathbf{u}_{\mathrm{D}}\rangle_\Gamma \tag{2.20}$$

for all $\boldsymbol{\tau} \in \mathbb{H}(\mathbf{div}_{4/3};\Omega)$. In turn, similarly as in [4] (see also [20], [13], [7]), it is convenient to consider the decomposition

$$\mathbb{H}(\mathbf{div}_{4/3};\Omega) \;=\; \mathbb{H}_0(\mathbf{div}_{4/3};\Omega) \oplus \mathrm{R}\,\mathbb{I}\,, \tag{2.21}$$

where

$$\mathbb{H}_0(\mathbf{div}_{4/3};\Omega) \;:=\; \left\{ \boldsymbol{\tau} \in \mathbb{H}(\mathbf{div}_{4/3};\Omega) : \quad \int_\Omega \mathrm{tr}(\boldsymbol{\tau}) = 0 \right\},$$

thanks to which each $\boldsymbol{\tau} \in \mathbb{H}(\mathbf{div}_{4/3};\Omega)$ can be uniquely decomposed as

$$\boldsymbol{\tau} = \boldsymbol{\tau}_0 + c_{\boldsymbol{\tau}}\,\mathbb{I} \quad \text{with} \quad \boldsymbol{\tau}_0 \in \mathbb{H}_0(\mathbf{div}_{4/3};\Omega) \quad \text{and} \quad c_{\boldsymbol{\tau}} := \frac{1}{d\,|\Omega|}\int_\Omega \mathrm{tr}(\boldsymbol{\tau}) \in \mathrm{R}\,.$$

In particular, using from the last equation of (2.11) that $\displaystyle\int_\Omega \mathrm{tr}(\boldsymbol{\sigma}) \;=\; -\int_\Omega \mathrm{tr}(\mathbf{u}\otimes\mathbf{u}) + \mu\int_\Gamma \mathbf{u}_{\mathrm{D}}\cdot\mathbf{n}$, we obtain $\boldsymbol{\sigma} = \boldsymbol{\sigma}_0 + c_{\boldsymbol{\sigma}}\,\mathbb{I}$ with

$$\boldsymbol{\sigma}_0 \in \mathbb{H}_0(\mathbf{div}_{4/3};\Omega) \quad \text{and} \quad c_{\boldsymbol{\sigma}} := -\frac{1}{d\,|\Omega|}\left\{\int_\Omega \mathrm{tr}(\mathbf{u}\otimes\mathbf{u}) - \mu\int_\Gamma \mathbf{u}_{\mathrm{D}}\cdot\mathbf{n}\right\} \in \mathrm{R}\,,$$

which says that $c_{\boldsymbol{\sigma}}$ is know explicitly in terms of $\mathbf{u}$ and $\mathbf{u}_{\mathrm{D}}$. Therefore, in order to fully determine $\boldsymbol{\sigma}$, it only remains to find its $\mathbb{H}_0(\mathbf{div}_{4/3};\Omega)$-component $\boldsymbol{\sigma}_0$, which is renamed from now on simply as $\boldsymbol{\sigma}$.

Furthermore, using the compatibility condition (2.6), we observe that both sides of (2.20) explicitly vanish when $\boldsymbol{\tau} \in \mathrm{R}\mathbb{I}$, and therefore testing against $\boldsymbol{\tau} \in \mathbb{H}(\mathbf{div}_{4/3};\Omega)$ is equivalent to doing it against $\boldsymbol{\tau} \in \mathbb{H}_0(\mathbf{div}_{4/3};\Omega)$. Hence, based on (2.13) and (2.20), and bearing in mind the foregoing discussion, we arrive at the following Banach spaces-based mixed formulation for the convective Brinkman–Forchheimer equations with varying porosity: Find $(\boldsymbol{\sigma},\mathbf{u}) \in \mathbb{H}_0(\mathbf{div}_{4/3};\Omega)\times\mathbf{L}^4(\Omega)$ such that

$$\begin{aligned}
a(\boldsymbol{\sigma},\boldsymbol{\tau}) + b(\boldsymbol{\tau},\mathbf{u}) + \frac{1}{\mu}\int_\Omega (\mathbf{u}\otimes\mathbf{u})^{\mathtt{d}} : \boldsymbol{\tau} - \frac{1}{d}\int_\Omega \left(\mathbf{u}\cdot\frac{\nabla\rho}{\rho}\right)\mathrm{tr}(\boldsymbol{\tau}) \qquad &= \quad \langle \boldsymbol{\tau}\mathbf{n}, \mathbf{u}_{\mathrm{D}}\rangle_\Gamma\,, \\
b(\boldsymbol{\sigma},\mathbf{v}) - c_{\mathbf{u}}(\mathbf{u},\mathbf{v}) - \frac{1}{d}\int_\Omega \mathrm{tr}(\mathbf{u}\otimes\mathbf{u})\left(\mathbf{v}\cdot\frac{\nabla\rho}{\rho}\right) + \int_\Omega \left(\boldsymbol{\sigma}^{\mathtt{d}}\frac{\nabla\rho}{\rho}\right)\cdot\mathbf{v} \quad &= \quad -\int_\Omega \mathbf{f}\cdot\mathbf{v}\,,
\end{aligned} \tag{2.22}$$

for all $(\boldsymbol{\tau},\mathbf{v}) \in \mathbb{H}_0(\mathbf{div}_{4/3};\Omega)\times\mathbf{L}^4(\Omega)$, where given $\mathbf{w} \in \mathbf{L}^4(\Omega)$, the bilinear forms $a : \mathbb{H}_0(\mathbf{div}_{4/3};\Omega)\times\mathbb{H}_0(\mathbf{div}_{4/3};\Omega) \to \mathrm{R}$, $b : \mathbb{H}_0(\mathbf{div}_{4/3};\Omega)\times\mathbf{L}^4(\Omega) \to \mathrm{R}$, and $c_{\mathbf{w}} : \mathbf{L}^4(\Omega)\times\mathbf{L}^4(\Omega) \to \mathrm{R}$, are defined, respectively, as

$$a(\boldsymbol{\zeta},\boldsymbol{\tau}) := \frac{1}{\mu}\int_\Omega \boldsymbol{\zeta}^{\mathtt{d}} : \boldsymbol{\tau}^{\mathtt{d}}\,, \quad b(\boldsymbol{\tau},\mathbf{v}) := \int_\Omega \mathbf{v}\cdot\mathbf{div}(\boldsymbol{\tau})\,, \tag{2.23}$$

and

$$c_{\mathbf{w}}(\mathbf{z},\mathbf{v}) := \int_\Omega \frac{\mathtt{D}(\rho)}{\rho}\mathbf{z}\cdot\mathbf{v} + \int_\Omega \frac{\mathtt{F}(\rho)}{\rho}|\mathbf{w}|^{m-2}\mathbf{z}\cdot\mathbf{v} + \frac{\mu}{d}\int_\Omega \left(\mathbf{z}\cdot\frac{\nabla\rho}{\rho}\right)\left(\mathbf{v}\cdot\frac{\nabla\rho}{\rho}\right), \tag{2.24}$$

for all $(\boldsymbol{\zeta},\mathbf{z}),(\boldsymbol{\tau},\mathbf{v}) \in \mathbb{H}_0(\mathbf{div}_{4/3};\Omega)\times\mathbf{L}^4(\Omega)$. Equivalently, defining the space $\mathbf{X} := \mathbb{H}_0(\mathbf{div}_{4/3};\Omega)\times\mathbf{L}^4(\Omega)$ equipped with the product norm

$$\|(\boldsymbol{\tau},\mathbf{v})\|_{\mathbf{X}} \;:=\; \|\boldsymbol{\tau}\|_{\mathbf{div}_{4/3};\Omega} \;+\; \|\mathbf{v}\|_{0,4;\Omega} \quad \forall\,(\boldsymbol{\tau},\mathbf{v}) \in \mathbf{X}\,,$$

and introducing, for each $\mathbf{w} \in \mathbf{L}^4(\Omega)$, the bilinear form $\mathbf{A}_{\rho,\mathbf{w}} : \mathbf{X}\times\mathbf{X} \to \mathrm{R}$ defined by

$$\mathbf{A}_{\rho,\mathbf{w}}((\boldsymbol{\zeta},\mathbf{z}),(\boldsymbol{\tau},\mathbf{v})) \;:=\; \mathbf{A}_{\mathbf{w}}((\boldsymbol{\zeta},\mathbf{z}),(\boldsymbol{\tau},\mathbf{v})) + \mathbf{B}_{\mathbf{w}}((\boldsymbol{\zeta},\mathbf{z}),(\boldsymbol{\tau},\mathbf{v})) + \mathbf{C}_{\rho}((\boldsymbol{\zeta},\mathbf{z}),(\boldsymbol{\tau},\mathbf{v}))\,, \tag{2.25}$$

where

$$\mathbf{A}_{\mathbf{w}}((\boldsymbol{\zeta},\mathbf{z}),(\boldsymbol{\tau},\mathbf{v})) := a(\boldsymbol{\zeta},\boldsymbol{\tau}) + b(\boldsymbol{\tau},\mathbf{z}) + b(\boldsymbol{\zeta},\mathbf{v}) - c_{\mathbf{w}}(\mathbf{z},\mathbf{v}), \tag{2.26}$$

$$\mathbf{B}_{\mathbf{w}}((\boldsymbol{\zeta},\mathbf{z}),(\boldsymbol{\tau},\mathbf{v})) := \frac{1}{\mu}\int_\Omega (\mathbf{w}\otimes\mathbf{z})^{\mathtt{d}} : \boldsymbol{\tau} - \frac{1}{d}\int_\Omega \mathrm{tr}(\mathbf{w}\otimes\mathbf{z})\left(\mathbf{v}\cdot\frac{\nabla\rho}{\rho}\right), \tag{2.27}$$

$$\mathbf{C}_\rho((\boldsymbol{\zeta},\mathbf{z}),(\boldsymbol{\tau},\mathbf{v})) := -\frac{1}{d}\int_\Omega \left(\mathbf{z}\cdot\frac{\nabla\rho}{\rho}\right)\mathrm{tr}(\boldsymbol{\tau}) + \int_\Omega \left(\boldsymbol{\zeta}^{\mathtt{d}}\frac{\nabla\rho}{\rho}\right)\cdot\mathbf{v}, \tag{2.28}$$

for all $(\boldsymbol{\zeta},\mathbf{z}),(\boldsymbol{\tau},\mathbf{v})\in\mathbf{X}$, we deduce that (2.22) can be re-stated as: Find $(\boldsymbol{\sigma},\mathbf{u})\in\mathbf{X}$ such that

$$\mathbf{A}_{\rho,\mathbf{u}}((\boldsymbol{\sigma},\mathbf{u}),(\boldsymbol{\tau},\mathbf{v})) \,=\, \mathbf{F}(\boldsymbol{\tau},\mathbf{v}) \quad \forall\,(\boldsymbol{\tau},\mathbf{v})\in\mathbf{X}\,, \tag{2.29}$$

where $\mathbf{F}\in\mathbf{X}'$ is defined by

$$\mathbf{F}(\boldsymbol{\tau},\mathbf{v}) \,:=\, \langle\boldsymbol{\tau}\mathbf{n},\mathbf{u}_{\mathrm{D}}\rangle_\Gamma - \int_\Omega \mathbf{f}\cdot\mathbf{v} \quad \forall\,(\boldsymbol{\tau},\mathbf{v})\in\mathbf{X}\,. \tag{2.30}$$

2.3 Stability bounds

We now establish the stability properties of the bilinear forms (2.23)–(2.28) and of the functional (2.30). We begin by observing that, as a consequence of the Cauchy–Schwarz and Hölder inequalities, and the estimates (2.16) and (2.19), the bilinear forms $a : \mathbb{H}_0(\mathbf{div}_{4/3};\Omega)\times\mathbb{H}_0(\mathbf{div}_{4/3};\Omega)\to\mathrm{R}$, $b : \mathbb{H}_0(\mathbf{div}_{4/3};\Omega)\times\mathbf{L}^4(\Omega)\to\mathrm{R}$, and $c_{\mathbf{w}} : \mathbf{L}^4(\Omega)\times\mathbf{L}^4(\Omega)\to\mathrm{R}$ are bounded. More precisely, the following continuity estimates hold:

$$\begin{aligned}
|a(\boldsymbol{\zeta},\boldsymbol{\tau})| \,&\leq\, \frac{1}{\mu}\,\|\boldsymbol{\zeta}\|_{\mathbf{div}_{4/3};\Omega}\,\|\boldsymbol{\tau}\|_{\mathbf{div}_{4/3};\Omega}\,,\\
|b(\boldsymbol{\tau},\mathbf{v})| \,&\leq\, \|\boldsymbol{\tau}\|_{\mathbf{div}_{4/3};\Omega}\,\|\mathbf{v}\|_{0,4;\Omega}\,,\\
|c_{\mathbf{w}}(\mathbf{z},\mathbf{v})| \,&\leq\, \|c\|\left\{1+\|\mathbf{w}\|_{0,4;\Omega}^{m-2}+\left\|\frac{\nabla\rho}{\rho}\right\|_{0,4;\Omega}^2\right\}\|\mathbf{z}\|_{0,4;\Omega}\,\|\mathbf{v}\|_{0,4;\Omega}\,,
\end{aligned} \tag{2.31}$$

with $\|c\|$ a positive constant depending on $\mathtt{D}_1$, ρ_0, $|\Omega|$, $\mathtt{F}_1$, μ and d. In consequence, combining these bounds with the definition of the bilinear form $\mathbf{A}_{\mathbf{w}}$ (cf. (2.26)) and straightforward estimates, we infer that there exists a positive constant $\mathcal{C}_{\mathbf{A}}$, depending only on μ, $\mathtt{D}_1$, ρ_0, $\mathtt{F}_1$, $|\Omega|$, and d, such that

$$\left|\mathbf{A}_{\mathbf{w}}((\boldsymbol{\zeta},\mathbf{z}),(\boldsymbol{\tau},\mathbf{v}))\right| \,\leq\, \mathcal{C}_{\mathbf{A}}\left\{1\,+\,\|\mathbf{w}\|_{0,4;\Omega}^{m-2}\,+\,\left\|\frac{\nabla\rho}{\rho}\right\|_{0,4;\Omega}^2\right\}\|(\boldsymbol{\zeta},\mathbf{z})\|_{\mathbf{X}}\,\|(\boldsymbol{\tau},\mathbf{v})\|_{\mathbf{X}} \tag{2.32}$$

for all $(\boldsymbol{\zeta},\mathbf{z}),(\boldsymbol{\tau},\mathbf{v})\in\mathbf{X}$. Moreover, using (2.14) and (2.18), and after straightforward algebraic manipulations, we deduce from (2.27) that, for each $\mathbf{w}\in\mathbf{L}^4(\Omega)$, the bilinear form $\mathbf{B}_{\mathbf{w}}$ is bounded. More precisely, there holds

$$\left|\mathbf{B}_{\mathbf{w}}((\boldsymbol{\zeta},\mathbf{z}),(\boldsymbol{\tau},\mathbf{v}))\right| \,\leq\, \left(\frac{1}{\mu}+\frac{1}{d^{1/2}}\left\|\frac{\nabla\rho}{\rho}\right\|_{0,4;\Omega}\right)\|\mathbf{w}\|_{0,4;\Omega}\,\|(\boldsymbol{\zeta},\mathbf{z})\|_{\mathbf{X}}\,\|(\boldsymbol{\tau},\mathbf{v})\|_{\mathbf{X}}, \tag{2.33}$$

for all $(\boldsymbol{\zeta},\mathbf{z}),(\boldsymbol{\tau},\mathbf{v})\in\mathbf{X}$. Analogously, using (2.15) and (2.17) we find from (2.28) that the bilinear form $\mathbf{C}_\rho$ satisfies

$$|\mathbf{C}_\rho((\boldsymbol{\zeta},\mathbf{z}),(\boldsymbol{\tau},\mathbf{v}))| \,\leq\, \left(\frac{1}{d^{1/2}}+1\right)\left\|\frac{\nabla\rho}{\rho}\right\|_{0,4;\Omega}\|(\boldsymbol{\zeta},\mathbf{z})\|_{\mathbf{X}}\,\|(\boldsymbol{\tau},\mathbf{v})\|_{\mathbf{X}} \tag{2.34}$$

for all $(\boldsymbol{\zeta},\mathbf{z}),(\boldsymbol{\tau},\mathbf{v}) \in \mathbf{X}$. Consequently, by the continuity bounds (2.32)–(2.34), it follows that the bilinear form $\mathbf{A}_{\rho,\mathbf{w}}$ is bounded. More precisely, there exists a positive constant $\widetilde{\mathcal{C}}_{\mathbf{A}}$, depending on μ, $\mathtt{D}_1$, ρ_0, $\mathtt{F}_1$, $|\Omega|$, and d, such that

$$|\mathbf{A}_{\rho,\mathbf{w}}((\boldsymbol{\zeta},\mathbf{z}),(\boldsymbol{\tau},\mathbf{v}))| \,\leq\, \widetilde{\mathcal{C}}_{\mathbf{A}} \left\{ 1 + \|\mathbf{w}\|_{0,4;\Omega}^{m-2} + \left\| \frac{\nabla\rho}{\rho} \right\|_{0,4;\Omega} + \left\| \frac{\nabla\rho}{\rho} \right\|_{0,4;\Omega}^2 \right\} \|(\boldsymbol{\zeta},\mathbf{z})\|_{\mathbf{X}} \, \|(\boldsymbol{\tau},\mathbf{v})\|_{\mathbf{X}} \tag{2.35}$$

for all $(\boldsymbol{\zeta},\mathbf{z}),(\boldsymbol{\tau},\mathbf{v}) \in \mathbf{X}$. Finally, using the continuity of the normal trace operator in $\mathbb{H}(\mathbf{div}_{4/3};\Omega)$, and applying Hölder's inequality, it is readily seen that $\mathbf{F}$ (cf. (2.30)) is bounded as well, that is

$$\big|\mathbf{F}(\boldsymbol{\tau},\mathbf{v})\big| \,\leq\, C_{\mathbf{F}} \left\{ \|\mathbf{f}\|_{0,4/3;\Omega} + \|\mathbf{u}_{\mathrm{D}}\|_{1/2,\Gamma} \right\} \|(\boldsymbol{\tau},\mathbf{v})\|_{\mathbf{X}} \quad \forall\, (\boldsymbol{\tau},\mathbf{v}) \,\in\, \mathbf{X}\,, \tag{2.36}$$

where $C_{\mathbf{F}} := \max\{1, \|\mathbf{i}_4\|\}$ and $\|\mathbf{i}_4\|$ is the norm of the continuous injection $\mathbf{i}_4$ of $\mathbf{H}^1(\Omega)$ into $\mathbf{L}^4(\Omega)$.

3 Analysis of the continuous problem

In this section, we follow a strategy similar to that employed in [28] (see also [7, 8, 31]), combining a fixed-point argument with recent solvability results for perturbed saddle-point problems in Banach spaces in order to establish the well-posedness of (2.29) (equivalently of (2.22)).

3.1 A fixed-point strategy

To solve (2.29), we introduce the operator $\mathbf{T} : \mathbf{L}^4(\Omega) \to \mathbf{L}^4(\Omega)$ defined by

$$\mathbf{T}(\mathbf{w}) := \bar{\mathbf{u}} \quad \forall\, \mathbf{w} \in \mathbf{L}^4(\Omega), \tag{3.1}$$

where $(\bar{\boldsymbol{\sigma}},\bar{\mathbf{u}}) \in \mathbf{X}$ denotes the unique solution (to be established below) of the linear problem

$$\mathbf{A}_{\rho,\mathbf{w}}((\bar{\boldsymbol{\sigma}},\bar{\mathbf{u}}),(\boldsymbol{\tau},\mathbf{v})) \,=\, \mathbf{F}(\boldsymbol{\tau},\mathbf{v}) \quad \forall\, (\boldsymbol{\tau},\mathbf{v}) \in \mathbf{X}. \tag{3.2}$$

Accordingly, problem (2.29) can be reformulated as the fixed-point problem: find $\mathbf{u} \in \mathbf{L}^4(\Omega)$ such that

$$\mathbf{T}(\mathbf{u}) = \mathbf{u}. \tag{3.3}$$

Indeed, if $(\bar{\boldsymbol{\sigma}},\bar{\mathbf{u}})$ denotes the solution of (3.2) with $\mathbf{w} := \mathbf{u}$, then $(\boldsymbol{\sigma},\mathbf{u}) := (\bar{\boldsymbol{\sigma}},\bar{\mathbf{u}}) \in \mathbf{X}$ is a solution of (2.29).

3.2 Well-definedness of the operator T

To prove that the operator $\mathbf{T}$ (cf. (3.1)) is well defined, or equivalently, that (3.2) is well posed, we fix $\mathbf{w} \in \mathbf{L}^4(\Omega)$ and verify that the bilinear forms a and b (cf. (2.23)), together with $c_{\mathbf{w}}$ (cf. (2.24)), satisfy hypotheses **(i)**–**(iii)** of [21, Theorem 3.4]. Indeed, it follows from (2.31) that the bilinear forms a, b, and $c_{\mathbf{w}}$ are bounded. Moreover, from the definitions of a and $c_{\mathbf{w}}$ (cf. (2.23) and (2.24)), we observe that both forms are symmetric and satisfy

$$a(\boldsymbol{\tau},\boldsymbol{\tau}) \,=\, \frac{1}{\mu}\,\|\boldsymbol{\tau}^{\mathtt{d}}\|_{0,\Omega}^2 \,\geq\, 0 \quad \forall\, \boldsymbol{\tau} \in \mathbb{H}_0(\mathbf{div}_{4/3};\Omega) \quad \text{and} \tag{3.4}$$

$$c_{\mathbf{w}}(\mathbf{v},\mathbf{v}) \,=\, \mathtt{D}_0 \int_\Omega |\mathbf{v}|^2 + \mathtt{F}_0 \int_\Omega |\mathbf{w}|^{m-2}|\mathbf{v}|^2 + \frac{\mu}{d} \int_\Omega \left| \mathbf{v} \cdot \frac{\nabla\rho}{\rho} \right|^2 \,\geq\, 0 \quad \forall\, \mathbf{v} \in \mathbf{L}^4(\Omega)\,.$$

Hence, hypothesis **(i)** of [21, Theorem 3.4] is satisfied.

On the other hand, we recall that a slight modification of the proof of [27, Lemma 2.3] (see also [2, Proposition IV.3.1]) allows one to show the existence of a constant $c_1 > 0$, depending only on Ω, such that (cf. [4, Lemma 3.2])

$$c_1 \|\boldsymbol{\tau}\|_{0,\Omega} \leq \|\boldsymbol{\tau}^{\mathtt{d}}\|_{0,\Omega} + \|\mathbf{div}(\boldsymbol{\tau})\|_{0,4/3;\Omega} \quad \forall\, \boldsymbol{\tau} \in \mathbb{H}_0(\mathbf{div}_{4/3};\Omega)\,. \tag{3.5}$$

In addition, letting $\mathbf{V}$ denote the null space of the linear and bounded operator induced by b (cf. (2.23)), we readily see that

$$\mathbf{V} = \Big\{ \boldsymbol{\tau} \in \mathbb{H}_0(\mathbf{div}_{4/3};\Omega) : \quad \mathbf{div}(\boldsymbol{\tau}) = \mathbf{0} \Big\}.$$

Hence, in view of (3.4) and inequality (3.5), it follows that

$$a(\boldsymbol{\tau},\boldsymbol{\tau}) = \frac{1}{\mu}\,\|\boldsymbol{\tau}^{\mathtt{d}}\|_{0,\Omega}^2 \geq \alpha\,\|\boldsymbol{\tau}\|_{\mathbf{div}_{4/3};\Omega}^2 \quad \forall\, \boldsymbol{\tau} \in \mathbf{V}\,, \tag{3.6}$$

with $\alpha := c_1^2/\mu$. Consequently, the bilinear form a satisfies the continuous inf-sup condition on $\mathbf{V}$ required by the hypothesis **(ii)** of [21, Theorem 3.4]. Also, we recall from [4, Lemma 3.3] that there exists a positive constant β, depending only on $|\Omega|$, such that

$$\sup_{\mathbf{0}\neq\boldsymbol{\tau}\in\mathbb{H}_0(\mathbf{div}_{4/3};\Omega)} \frac{b(\boldsymbol{\tau},\mathbf{v})}{\|\boldsymbol{\tau}\|_{\mathbf{div}_{4/3};\Omega}} \geq \beta\,\|\mathbf{v}\|_{0,4;\Omega} \quad \forall\, \mathbf{v} \in \mathbf{L}^4(\Omega)\,,$$

which confirms the verification of the hypothesis **(iii)** of [21, Theorem 3.4]. Next, given $\delta > 0$ such that $\|\mathbf{w}\|_{0,4;\Omega} \leq \delta$, the continuity estimate for $c_{\mathbf{w}}(\cdot,\cdot)$ (cf. (2.31)) yields

$$|c_{\mathbf{w}}(\mathbf{z},\mathbf{v})| \leq \|c\| \left(1 + \delta^{m-2} + \left\| \frac{\nabla\rho}{\rho} \right\|_{0,4;\Omega}^2 \right) \|\mathbf{z}\|_{0,4;\Omega}\,\|\mathbf{v}\|_{0,4;\Omega} \quad \forall\, \mathbf{z},\mathbf{v} \in \mathbf{L}^4(\Omega)\,. \tag{3.7}$$

Having verified hypotheses **(i)**–**(iii)** from [21, Theorem 3.4], we conclude that the bilinear form $\mathbf{A}_{\mathbf{w}}$ (cf. (2.26)), satisfies a corresponding global inf-sup condition. More precisely, a straightforward application of [21, Theorem 3.4] ensure the existence of a positive constant $\alpha_{\mathbf{A}}$, depending only on μ, α, β, $\mathtt{D}_1$, $|\Omega|$, ρ_0, $\mathtt{F}_1$, δ, d, and $\left\| \frac{\nabla\rho}{\rho} \right\|_{0,4;\Omega}$, such that for each $\mathbf{w} \in \mathbf{L}^4(\Omega)$ satisfying $\|\mathbf{w}\|_{0,4;\Omega} \leq \delta$, there holds

$$\sup_{\mathbf{0}\neq(\boldsymbol{\tau},\mathbf{v})\in\mathbf{X}} \frac{\mathbf{A}_{\mathbf{w}}((\boldsymbol{\zeta},\mathbf{z}),(\boldsymbol{\tau},\mathbf{v}))}{\|(\boldsymbol{\tau},\mathbf{v})\|_{\mathbf{X}}} \geq \alpha_{\mathbf{A}}\,\|(\boldsymbol{\zeta},\mathbf{z})\|_{\mathbf{X}} \qquad \forall\,(\boldsymbol{\zeta},\mathbf{z}) \in \mathbf{X}\,. \tag{3.8}$$

Hence, we are now in a position to establish that the fixed-point operator $\mathbf{T}$ is well-defined.

Lemma 3.1 *Let $\delta > 0$ be given and let $r \in (0, r_0]$, where*

$$r_0 := \min\left\{ \delta,\ \frac{\alpha_{\mathbf{A}}}{4} \left(\frac{1}{\mu} + \frac{\alpha_{\mathbf{A}}}{4(1+d^{1/2})} \right)^{-1} \right\}, \tag{3.9}$$

and assume that the porosity satisfies

$$\left\| \frac{\nabla\rho}{\rho} \right\|_{0,4;\Omega} \leq \left(\frac{1}{d^{1/2}} + 1 \right)^{-1} \frac{\alpha_{\mathbf{A}}}{4}\,. \tag{3.10}$$

Then, for each $\mathbf{w} \in \mathbf{L}^4(\Omega)$ satisfying $\|\mathbf{w}\|_{0,4;\Omega} \leq r$, the problem (3.2) admits a unique solution $(\bar{\boldsymbol{\sigma}},\bar{\mathbf{u}}) \in \mathbf{X}$, and hence one can define $\mathbf{T}(\mathbf{w}) = \bar{\mathbf{u}} \in \mathbf{L}^4(\Omega)$. Moreover, there exists a positive constant $\mathcal{C}_{\mathbf{T}}$, depending only on $C_{\mathbf{F}}$ and $\alpha_{\mathbf{A}}$, such that

$$\|\mathbf{T}(\mathbf{w})\|_{0,4;\Omega} = \|\bar{\mathbf{u}}\|_{0,4;\Omega} \leq \|(\bar{\boldsymbol{\sigma}},\bar{\mathbf{u}})\|_{\mathbf{X}} \leq \mathcal{C}_{\mathbf{T}} \Big\{ \|\mathbf{f}\|_{0,4/3;\Omega} + \|\mathbf{u}_{\mathrm{D}}\|_{1/2,\Gamma} \Big\}. \tag{3.11}$$

Proof. Let $\mathbf{w} \in \mathbf{L}^4(\Omega)$ be such that $\|\mathbf{w}\|_{0,4;\Omega} \leq r$. Combining the global inf-sup condition for $\mathbf{A}_{\mathbf{w}}$ (cf. (3.8)) with the boundedness estimates for $\mathbf{B}_{\mathbf{w}}$ and $\mathbf{C}_\rho$ (cf. (2.33) and (2.34), respectively), we obtain

$$\begin{aligned}&\sup_{0\neq(\boldsymbol{\tau},\mathbf{v})\in\mathbf{X}} \frac{\mathbf{A}_{\rho,\mathbf{w}}((\boldsymbol{\zeta},\mathbf{z}),(\boldsymbol{\tau},\mathbf{v}))}{\|(\boldsymbol{\tau},\mathbf{v})\|_{\mathbf{X}}} \\ &\qquad \geq \left\{\alpha_{\mathbf{A}} - \left[\left(\frac{1}{\mu}+\frac{1}{d^{1/2}}\left\|\frac{\nabla\rho}{\rho}\right\|_{0,4;\Omega}\right)\|\mathbf{w}\|_{0,4;\Omega} + \left(\frac{1}{d^{1/2}}+1\right)\left\|\frac{\nabla\rho}{\rho}\right\|_{0,4;\Omega}\right]\right\}\|(\boldsymbol{\zeta},\mathbf{z})\|_{\mathbf{X}}\,,\end{aligned} \tag{3.12}$$

for all $(\boldsymbol{\zeta},\mathbf{z}) \in \mathbf{X}$. Invoking (3.10) and using that $r \leq r_0$ (cf. (3.9)), we infer that the bracketed term in (3.12) is bounded by $\alpha_{\mathbf{A}}/2$, and therefore $\mathbf{A}_{\rho,\mathbf{w}}$ satisfies the global inf-sup condition

$$\sup_{\mathbf{0}\neq(\boldsymbol{\tau},\mathbf{v})\in\mathbf{X}} \frac{\mathbf{A}_{\rho,\mathbf{w}}((\boldsymbol{\zeta},\mathbf{z}),(\boldsymbol{\tau},\mathbf{v}))}{\|(\boldsymbol{\tau},\mathbf{v})\|_{\mathbf{X}}} \geq \frac{\alpha_{\mathbf{A}}}{2}\,\|(\boldsymbol{\zeta},\mathbf{z})\|_{\mathbf{X}} \qquad \forall\,(\boldsymbol{\zeta},\mathbf{z})\in\mathbf{X}\,. \tag{3.13}$$

Similarly, since $\mathbf{A}_{\mathbf{w}}$ is symmetric (inherited from the symmetry of a and c), the same argument, together with (2.33) and (2.34), and under the same assumptions on $\mathbf{w}$ and $\left\|\frac{\nabla\rho}{\rho}\right\|_{0,4;\Omega}$, yields

$$\sup_{\mathbf{0}\neq(\boldsymbol{\zeta},\mathbf{z})\in\mathbf{X}} \frac{\mathbf{A}_{\rho,\mathbf{w}}((\boldsymbol{\zeta},\mathbf{z}),(\boldsymbol{\tau},\mathbf{v}))}{\|(\boldsymbol{\zeta},\mathbf{z})\|_{\mathbf{X}}} \geq \frac{\alpha_{\mathbf{A}}}{2}\,\|(\boldsymbol{\tau},\mathbf{v})\|_{\mathbf{X}} \qquad \forall\,(\boldsymbol{\tau},\mathbf{v})\in\mathbf{X}\,. \tag{3.14}$$

Hence, the bilinear form $\mathbf{A}_{\rho,\mathbf{w}}$ satisfies (3.13) and (3.14) for each $\mathbf{w} \in \mathbf{L}^4(\Omega)$ with $\|\mathbf{w}\|_{0,4;\Omega} \leq r$, provided that ρ satisfies (3.10). Since $\mathbf{F} \in \mathbf{X}'$ by (2.36), the existence of a unique solution to (3.2) follows from a direct application of the Banach–Nečas–Babuška theorem (cf. [24, Theorem 2.6]). Finally, applying (3.13) to $(\boldsymbol{\zeta},\mathbf{z}) = (\bar{\boldsymbol{\sigma}},\bar{\mathbf{u}})$, and then using (3.2) together with the continuity bound for $\mathbf{F}$ (cf. (2.36)), we readily arrive at (3.11) with $\mathcal{C}_{\mathbf{T}} = 2\,C_{\mathbf{F}}/\alpha_{\mathbf{A}}$, thereby concluding the proof. □

3.3 Solvability analysis of the fixed-point equation

Having established the well-posedness of the problem (3.2), and hence the well-definedness of the operator $\mathbf{T}$, we now turn to proving the existence of a unique fixed point of $\mathbf{T}$ (cf. (3.3)). To this end, we verify in what follows the hypotheses of the Banach fixed-point theorem.

The following result, which is a straightforward consequence of Lemma 3.1, establishes that $\mathbf{T}$ maps a ball into itself.

Lemma 3.2 *Let $r \in (0, r_0]$, with r_0 given by (3.9), and define the ball*

$$\mathbf{W}_r := \left\{\mathbf{w}\in\mathbf{L}^4(\Omega)\ :\ \|\mathbf{w}\|_{0,4;\Omega}\leq r\right\}. \tag{3.15}$$

Assume that the porosity ρ satisfies (3.10) and that

$$\mathcal{C}_{\mathbf{T}}\left\{\|\mathbf{f}\|_{0,4/3;\Omega} + \|\mathbf{u}_{\mathrm{D}}\|_{1/2,\Gamma}\right\} \leq r\,. \tag{3.16}$$

Then the fixed point operator $\mathbf{T}$ maps $\mathbf{W}_r$ into itself, that is, $\mathbf{T}(\mathbf{W}_r) \subseteq \mathbf{W}_r$.

In order to prove the Lipschitz continuity of $\mathbf{T}$, we now recall from [34, Lemma 5.3] that, for every $p \geq 2$, there exists a constant $C(p) > 0$ such that

$$\left||\mathbf{z}|^{p-2}\mathbf{z} - |\mathbf{y}|^{p-2}\mathbf{y}\right| \leq C(p)\left(|\mathbf{z}|+|\mathbf{y}|\right)^{p-2}|\mathbf{z}-\mathbf{y}| \quad \forall\,\mathbf{z},\,\mathbf{y}\in\mathrm{R}^d\,. \tag{3.17}$$

Then, given arbitrary $\mathbf{w}_1$, $\mathbf{w}_2 \in \mathbf{L}^4(\Omega)$, we first embed the scalars $|\mathbf{w}_1|$ and $|\mathbf{w}_2|$ into R^d by setting $\mathbf{z} = (|\mathbf{w}_1|, \mathbf{0})$ and $\mathbf{y} = (|\mathbf{w}_2|, \mathbf{0})$, where $\mathbf{0} \in \mathrm{R}^{d-1}$. In this way, applying (3.17) with $p = m-1 \in [2,3]$, we infer that

$$\begin{aligned} \big| |\mathbf{w}_1|^{m-2} - |\mathbf{w}_2|^{m-2} \big| &= \big| |\mathbf{w}_1|^{m-3}(|\mathbf{w}_1|, \mathbf{0}) - |\mathbf{w}_2|^{m-3}(|\mathbf{w}_2|, \mathbf{0}) \big| \\ &\leq c_m \left(|\mathbf{w}_1| + |\mathbf{w}_2| \right)^{m-3} |\mathbf{w}_1 - \mathbf{w}_2| \,, \end{aligned} \tag{3.18}$$

where $c_m := C(m-1)$. The announced property for $\mathbf{T}$ is established next.

Lemma 3.3 *Let $r \in (0, r_0]$, with r_0 given by (3.9), and assume that the porosity ρ satisfies (3.10). Then, there exists a positive constant $L_{\mathbf{T}}$, such that for all $\mathbf{w}_1, \mathbf{w}_2 \in \mathbf{W}_r$ (cf. (3.15)) there holds*

$$\|\mathbf{T}(\mathbf{w}_1) - \mathbf{T}(\mathbf{w}_2)\|_{0,4;\Omega} \leq L_{\mathbf{T}} \Big\{ \|\mathbf{f}\|_{0,4/3;\Omega} + \|\mathbf{u}_{\mathrm{D}}\|_{1/2,\Gamma} \Big\} \|\mathbf{w}_1 - \mathbf{w}_2\|_{0,4;\Omega} \,. \tag{3.19}$$

Proof. Given $\mathbf{w}_1, \mathbf{w}_2 \in \mathbf{W}_r$, we let $\bar{\mathbf{u}}_1 := \mathbf{T}(\mathbf{w}_1)$ and $\bar{\mathbf{u}}_2 := \mathbf{T}(\mathbf{w}_2)$. According to the definitions of $\mathbf{T}$ (cf. (3.2)) and the forms $\mathbf{A}_{\rho,\mathbf{w}}$, $\mathbf{B}_{\mathbf{w}}$ and $\mathbf{C}_{\rho}$ (cf. (2.25), (2.27), (2.28)), it follows that

$$\begin{aligned} &\mathbf{A}_{\rho,\mathbf{w}_2}((\bar{\boldsymbol{\sigma}}_1, \bar{\mathbf{u}}_1) - (\bar{\boldsymbol{\sigma}}_2, \bar{\mathbf{u}}_2), (\boldsymbol{\tau}, \mathbf{v})) \\ &= (\mathbf{A}_{\mathbf{w}_2} - \mathbf{A}_{\mathbf{w}_1})((\bar{\boldsymbol{\sigma}}_1, \bar{\mathbf{u}}_1), (\boldsymbol{\tau}, \mathbf{v})) + (\mathbf{B}_{\mathbf{w}_2} - \mathbf{B}_{\mathbf{w}_1})((\bar{\boldsymbol{\sigma}}_1, \bar{\mathbf{u}}_1), (\boldsymbol{\tau}, \mathbf{v})) \\ &= (c_{\mathbf{w}_1} - c_{\mathbf{w}_2})(\bar{\mathbf{u}}_1, \mathbf{v}) + (\mathbf{B}_{\mathbf{w}_2} - \mathbf{B}_{\mathbf{w}_1})((\bar{\boldsymbol{\sigma}}_1, \bar{\mathbf{u}}_1), (\boldsymbol{\tau}, \mathbf{v})) \qquad \forall\, (\boldsymbol{\tau}, \mathbf{v}) \in \mathbf{X} \,. \end{aligned} \tag{3.20}$$

We now invoke (3.18), together with two applications of the Cauchy–Schwarz inequality, the continuity of the embedding $\mathbf{L}^4(\Omega) \hookrightarrow \mathbf{L}^t(\Omega)$ for $t \in (0,4]$, whose norm is bounded by $|\Omega|^{(4-t)/(4t)}$, and the fact that $\|\mathbf{w}_1\|_{0,4;\Omega}$, $\|\mathbf{w}_2\|_{0,4;\Omega} \leq r$, to conclude that

$$\begin{aligned} |(c_{\mathbf{w}_1} - c_{\mathbf{w}_2})(\bar{\mathbf{u}}_1, \mathbf{v})| &\leq \frac{\mathtt{F}_1}{\rho_0} c_m \int_\Omega \left(|\mathbf{w}_1| + |\mathbf{w}_2| \right)^{m-3} |\mathbf{w}_1 - \mathbf{w}_2| \, |\bar{\mathbf{u}}_1| \, |\mathbf{v}| \\ &\leq \frac{\mathtt{F}_1}{\rho_0} c_m \, |\Omega|^{(4-m)/4} \left(\|\mathbf{w}_1\|_{0,4;\Omega} + \|\mathbf{w}_2\|_{0,4;\Omega} \right)^{m-3} \|\mathbf{w}_1 - \mathbf{w}_2\|_{0,4;\Omega} \, \|\bar{\mathbf{u}}_1\|_{0,4;\Omega} \, \|\mathbf{v}\|_{0,4;\Omega} \\ &\leq \frac{\mathtt{F}_1}{\rho_0} c_m \, |\Omega|^{(4-m)/4} (2\,r)^{m-3} \, \|\mathbf{w}_1 - \mathbf{w}_2\|_{0,4;\Omega} \, \|\bar{\mathbf{u}}_1\|_{0,4;\Omega} \, \|\mathbf{v}\|_{0,4;\Omega} \,. \end{aligned} \tag{3.21}$$

In turn, by means of (2.33) and the assumption on the porosity ρ (cf. (3.10)), we get

$$|(\mathbf{B}_{\mathbf{w}_2} - \mathbf{B}_{\mathbf{w}_1})((\bar{\boldsymbol{\sigma}}_1, \bar{\mathbf{u}}_1), (\boldsymbol{\tau}, \mathbf{v}))| \leq \left(\frac{1}{\mu} + \frac{\alpha_{\mathbf{A}}}{4(d^{1/2}+1)} \right) \|\mathbf{w}_1 - \mathbf{w}_2\|_{0,4;\Omega} \, \|\bar{\mathbf{u}}_1\|_{0,4;\Omega} \, \|(\boldsymbol{\tau}, \mathbf{v})\|_{\mathbf{X}} \,. \tag{3.22}$$

Hence, applying (3.13) with $\mathbf{w} = \mathbf{w}_2$ and $(\boldsymbol{\zeta}, \mathbf{z}) = (\bar{\boldsymbol{\sigma}}_1, \bar{\mathbf{u}}_1) - (\bar{\boldsymbol{\sigma}}_2, \bar{\mathbf{u}}_2)$, a straightforward algebraic computation, together with (3.20), (3.21) and (3.22), yields

$$\begin{aligned} \|(\bar{\boldsymbol{\sigma}}_1, \bar{\mathbf{u}}_1) - (\bar{\boldsymbol{\sigma}}_2, \bar{\mathbf{u}}_2)\|_{\mathbf{X}} &\leq \frac{2}{\alpha_{\mathbf{A}}} \sup_{\mathbf{0} \neq (\boldsymbol{\tau}, \mathbf{v}) \in \mathbf{X}} \frac{(c_{\mathbf{w}_1} - c_{\mathbf{w}_2})(\bar{\mathbf{u}}_1, \mathbf{v}) + (\mathbf{B}_{\mathbf{w}_2} - \mathbf{B}_{\mathbf{w}_1})((\bar{\boldsymbol{\sigma}}_1, \bar{\mathbf{u}}_1), (\boldsymbol{\tau}, \mathbf{v}))}{\|(\boldsymbol{\tau}, \mathbf{v})\|_{\mathbf{X}}} \\ &\leq \frac{2}{\alpha_{\mathbf{A}}} \max \left\{ \frac{\mathtt{F}_1}{\rho_0} c_m \, |\Omega|^{(4-m)/4} (2\,r)^{m-3}, \frac{1}{\mu} + \frac{\alpha_{\mathbf{A}}}{4(d^{1/2}+1)} \right\} \|\mathbf{w}_1 - \mathbf{w}_2\|_{0,4;\Omega} \, \|\bar{\mathbf{u}}_1\|_{0,4;\Omega} \,. \end{aligned}$$

Finally, by bounding $\|\bar{\mathbf{u}}_1\|_{0,4;\Omega}$ through (3.11), we obtain (3.19) with

$$L_{\mathbf{T}} := \frac{2\,\mathcal{C}_{\mathbf{T}}}{\alpha_{\mathbf{A}}} \max \left\{ \frac{\mathtt{F}_1}{\rho_0} c_m \, |\Omega|^{(4-m)/4} (2\,r)^{m-3}, \frac{1}{\mu} + \frac{\alpha_{\mathbf{A}}}{4(d^{1/2}+1)} \right\} ,$$

which concludes the proof. □

We are now in a position to state the main result concerning the solvability of (3.3) (equivalently of (2.29)).

Theorem 3.4 *Let $r \in (0, r_0]$, with r_0 given by (3.9). Assume that the porosity ρ satisfies (3.10), and that the data satisfy (3.16) and*

$$L_{\mathbf{T}}\Big\{\|\mathbf{f}\|_{0,4/3;\Omega} + \|\mathbf{u}_{\mathrm{D}}\|_{1/2,\Gamma}\Big\} < 1\,. \tag{3.23}$$

Then, there exists a unique fixed point $\mathbf{u} \in \mathbf{W}_r$ (cf. (3.15)) of the operator $\mathbf{T}$ (cf. (3.3)). Equivalently, problem (2.29) admits a unique solution $(\boldsymbol{\sigma}, \mathbf{u}) := (\bar{\boldsymbol{\sigma}}, \bar{\mathbf{u}}) \in \mathbf{X}$ with $\mathbf{u} \in \mathbf{W}_r$, where $(\bar{\boldsymbol{\sigma}}, \bar{\mathbf{u}})$ is the unique solution of (3.2) with $\mathbf{w} = \mathbf{u}$. Moreover, the following continuous dependence estimate holds

$$\|(\boldsymbol{\sigma}, \mathbf{u})\|_{\mathbf{X}} \leq \mathcal{C}_{\mathbf{T}}\Big\{\|\mathbf{f}\|_{0,4/3;\Omega} + \|\mathbf{u}_{\mathrm{D}}\|_{1/2,\Gamma}\Big\}\,. \tag{3.24}$$

Proof. By Lemmas 3.2 and 3.3, together with assumption (3.23), the operator $\mathbf{T}$ is a contraction mapping the ball $\mathbf{W}_r$ into itself. Therefore, the classical Banach fixed-point theorem guarantees the solvability of (3.3), and hence of (2.29). Moreover, since $\mathbf{u} = \mathbf{T}(\mathbf{u})$, the estimate (3.24) follows directly from (3.11), thereby concluding the proof. □

4 The Galerkin scheme

In this section we introduce and analyze the Galerkin approximation of the mixed formulation (2.29) (equivalently of (2.22)). In particular, for the solvability analysis, we rely on the discrete counterparts of [21, Theorem 3.4] and [24, Theorem 2.6], namely [21, Theorem 3.5] and [24, Theorem 2.22], respectively.

4.1 Discrete setting

We first introduce arbitrary finite dimensional subspaces $\widetilde{\mathbb{H}}_h^{\boldsymbol{\sigma}} \subseteq \mathbb{H}(\mathbf{div}_{4/3};\Omega)$ and $\mathbf{H}_h^{\mathbf{u}} \subseteq \mathbf{L}^4(\Omega)$. Hereafter, $h := \max\{h_T : T \in \mathcal{T}_h\}$ stands for the size of a regular triangulation $\mathcal{T}_h$ of $\overline{\Omega}$ made up of triangles T (when $d = 2$) or tetrahedra T (when $d = 3$) of diameter h_T. Specific finite element subspaces satisfying suitable hypotheses to be introduced in due course will be provided later on in Section 4.4. Then, letting

$$\mathbb{H}_h^{\boldsymbol{\sigma}} := \widetilde{\mathbb{H}}_h^{\boldsymbol{\sigma}} \cap \mathbb{H}_0(\mathbf{div}_{4/3};\Omega)\,, \tag{4.1}$$

the Galerkin scheme associated with (2.22) reads: Find $(\boldsymbol{\sigma}_h, \mathbf{u}_h) \in \mathbb{H}_h^{\boldsymbol{\sigma}} \times \mathbf{H}_h^{\mathbf{u}}$ such that

$$\begin{aligned} &a(\boldsymbol{\sigma}_h, \boldsymbol{\tau}_h) + b(\boldsymbol{\tau}_h, \mathbf{u}_h) + \frac{1}{\nu}\int_\Omega (\mathbf{u}_h \otimes \mathbf{u}_h)^{\mathtt{d}} : \boldsymbol{\tau}_h - \frac{1}{d}\int_\Omega \left(\mathbf{u}_h \cdot \frac{\nabla\rho}{\rho}\right)\mathrm{tr}(\boldsymbol{\tau}_h) \qquad = \langle \boldsymbol{\tau}_h \mathbf{n}, \mathbf{u}_{\mathrm{D}}\rangle_\Gamma\,, \\ &b(\boldsymbol{\sigma}_h, \mathbf{v}_h) - c_{\mathbf{u}_h}(\mathbf{u}_h, \mathbf{v}_h) - \frac{1}{d}\int_\Omega \mathrm{tr}(\mathbf{u}_h \otimes \mathbf{u}_h)\left(\mathbf{v}_h \cdot \frac{\nabla\rho}{\rho}\right) + \int_\Omega \left(\boldsymbol{\sigma}_h^{\mathtt{d}}\frac{\nabla\rho}{\rho}\right)\cdot \mathbf{v}_h = -\int_\Omega \mathbf{f}\cdot\mathbf{v}_h\,, \end{aligned} \tag{4.2}$$

for all $(\boldsymbol{\tau}_h, \mathbf{v}_h) \in \mathbb{H}_h^{\boldsymbol{\sigma}} \times \mathbf{H}_h^{\mathbf{u}}$.

Thus, analogously to the approach adopted in Section 2.2, setting $\mathbf{X}_h := \mathbb{H}_h^{\boldsymbol{\sigma}} \times \mathbf{H}_h^{\mathbf{u}}$, the Galerkin scheme (4.2) can be equivalently reformulated as follows: Find $(\boldsymbol{\sigma}_h, \mathbf{u}_h) \in \mathbf{X}_h$ such that

$$\mathbf{A}_{\rho,\mathbf{u}_h}((\boldsymbol{\sigma}_h, \mathbf{u}_h), (\boldsymbol{\tau}_h, \mathbf{v}_h)) = \mathbf{F}(\boldsymbol{\tau}_h, \mathbf{v}_h) \quad \forall\, (\boldsymbol{\tau}_h, \mathbf{v}_h) \in \mathbf{X}_h\,, \tag{4.3}$$

where the bilinear form $\mathbf{A}_{\rho,\mathbf{w}_h}$ is defined as in (2.25), replacing $\mathbf{w}$ by $\mathbf{w}_h$, and the functional $\mathbf{F}$ is given by (2.30).

4.2 Discrete fixed-point strategy

We now introduce the discrete counterpart of the fixed-point strategy developed in Section 3.1 in order to analyze the solvability of (4.3). To this end, we define the operator $\mathbf{T}_{\mathtt{d}} : \mathbf{H}^{\mathbf{u}}_h \to \mathbf{H}^{\mathbf{u}}_h$ by

$$\mathbf{T}_{\mathtt{d}}(\mathbf{w}_h) := \bar{\mathbf{u}}_h \qquad \forall\, \mathbf{w}_h \in \mathbf{H}^{\mathbf{u}}_h \,,$$

where $(\bar{\boldsymbol{\sigma}}_h, \bar{\mathbf{u}}_h) \in \mathbf{X}_h$ denotes the unique solution of the linear problem

$$\mathbf{A}_{\rho,\mathbf{w}_h}\big((\bar{\boldsymbol{\sigma}}_h, \bar{\mathbf{u}}_h), (\boldsymbol{\tau}_h, \mathbf{v}_h)\big) \;=\; \mathbf{F}(\boldsymbol{\tau}_h, \mathbf{v}_h) \qquad \forall\, (\boldsymbol{\tau}_h, \mathbf{v}_h) \in \mathbf{X}_h \,. \tag{4.4}$$

Accordingly, solving (4.3) is equivalent to finding a fixed point of $\mathbf{T}_{\mathtt{d}}$, that is $\mathbf{u}_h \in \mathbf{H}^{\mathbf{u}}_h$ such that

$$\mathbf{T}_{\mathtt{d}}(\mathbf{u}_h) = \mathbf{u}_h \,. \tag{4.5}$$

In what follows, we derive the preliminary results needed to prove, first, that the fixed-point operator $\mathbf{T}_{\mathtt{d}}$ (cf. (4.5)) is well defined, or equivalently, that the linear problem (4.4) is well posed.

We begin by showing that, for each $\mathbf{w}_h \in \mathbf{H}^{\mathbf{u}}_h$, the bilinear forms a, b, and $c_{\mathbf{w}_h}$, when restricted to the corresponding finite element subspaces, satisfy hypotheses **(i)**–**(iii)** of [21, Theorem 3.5]. Indeed, since both a and $c_{\mathbf{w}_h}$ are symmetric and positive semi-definite on $\mathbb{H}_0(\mathbf{div}_{4/3};\Omega)$ and $\mathbf{L}^4(\Omega)$, respectively, they inherit these properties on the discrete subspaces $\mathbb{H}^{\boldsymbol{\sigma}}_h$ and $\mathbf{H}^{\mathbf{u}}_h$. Hence, hypothesis **(i)** is immediately satisfied.

To verify the remaining hypotheses, we introduce the following assumptions on the finite element subspaces:

(**H.0**) $\widetilde{\mathbb{H}}^{\boldsymbol{\sigma}}_h$ contains the multiples of the identity tensor $\mathbb{I}$,

(**H.1**) $\mathbf{div}(\widetilde{\mathbb{H}}^{\boldsymbol{\sigma}}_h) \subseteq \mathbf{H}^{\mathbf{u}}_h$.

As a consequence of (**H.0**) and the decomposition (2.21), $\mathbb{H}^{\boldsymbol{\sigma}}_h$ (cf. (4.1)) can be redefined as

$$\mathbb{H}^{\boldsymbol{\sigma}}_h := \left\{ \boldsymbol{\tau}_h - \left(\frac{1}{d\,|\Omega|} \int_\Omega \mathrm{tr}(\boldsymbol{\tau}_h) \right) \mathbb{I} : \quad \forall\, \boldsymbol{\tau}_h \in \widetilde{\mathbb{H}}^{\boldsymbol{\sigma}}_h \right\}.$$

Moreover, arguing as in Section 3 and invoking (**H.1**), the kernel $\mathbf{V}_h$ of $b|_{\mathbb{H}^{\boldsymbol{\sigma}}_h \times \mathbf{H}^{\mathbf{u}}_h}$ reduces to

$$\mathbf{V}_h := \left\{ \boldsymbol{\tau}_h \in \mathbb{H}^{\boldsymbol{\sigma}}_h : \quad \mathbf{div}(\boldsymbol{\tau}_h) = \mathbf{0} \quad \text{in} \quad \Omega \right\}. \tag{4.6}$$

Since $\mathbf{V}_h \subset \mathbf{V}$, we obtain the discrete analogue of (3.6) with the same constant as in the continuous case, namely $\alpha_{\mathtt{d}} = \alpha := c_1^2/\nu$. Therefore, hypothesis **(ii)** of [21, Theorem 3.5] follows.

To complete the verification, we now assume hypothesis **(iii)** of [21, Theorem 3.5], namely that

(**H.2**) there exists a positive constant $\beta_{\mathtt{d}}$, independent of h, such that

$$\sup_{\mathbf{0} \neq \boldsymbol{\tau}_h \in \mathbb{H}^{\boldsymbol{\sigma}}_h} \frac{b(\boldsymbol{\tau}_h, \mathbf{v}_h)}{\|\boldsymbol{\tau}_h\|_{\mathbf{div}_{4/3};\Omega}} \;\geq\; \beta_{\mathtt{d}}\, \|\mathbf{v}_h\|_{0,4;\Omega} \quad \forall\, \mathbf{v}_h \in \mathbf{H}^{\mathbf{u}}_h \,.$$

Specific finite element subspaces satisfying the above are defined later on in Section 4.4.

Next, proceeding as in the continuous case, given $\delta > 0$ such that $\|\mathbf{w}_h\|_{0,4;\Omega} \leq \delta$, the boundedness estimate for $c_{\mathbf{w}_h}$ takes exactly the form of (3.7), namely

$$|c_{\mathbf{w}_h}(\mathbf{z}_h, \mathbf{v}_h)| \leq \|c\| \left\{ 1 + \delta^{m-2} + \left\| \frac{\nabla \rho}{\rho} \right\|^2_{0,4;\Omega} \right\} \|\mathbf{z}_h\|_{0,4;\Omega} \, \|\mathbf{v}_h\|_{0,4;\Omega} \quad \forall \, \mathbf{z}_h, \mathbf{v}_h \in \mathbf{H}^{\mathbf{u}}_h \, .$$

Hence, since a, b, and $c_{\mathbf{w}_h}$ satisfy the required assumptions, an application of [21, Theorem 3.5] yields the existence of a constant $\alpha_{\mathbf{A}_\mathtt{d}} > 0$, depending only on μ, $\alpha_\mathtt{d}$, $\beta_\mathtt{d}$, $\mathtt{D}_1$, $|\Omega|$, ρ_0, $\mathtt{F}_1$, δ, d, and $\left\| \frac{\nabla \rho}{\rho} \right\|_{0,4;\Omega}$, such that for each $\mathbf{w}_h \in \mathbf{H}^{\mathbf{u}}_h$ satisfying $\|\mathbf{w}_h\|_{0,4;\Omega} \leq \delta$, there holds the discrete analogue of (3.8), namely

$$\sup_{\mathbf{0} \neq (\boldsymbol{\tau}_h, \mathbf{v}_h) \in \mathbf{X}_h} \frac{\mathbf{A}_{\mathbf{w}_h}((\boldsymbol{\zeta}_h, \mathbf{z}_h), (\boldsymbol{\tau}_h, \mathbf{v}_h))}{\|(\boldsymbol{\tau}_h, \mathbf{v}_h)\|_{\mathbf{X}}} \geq \alpha_{\mathbf{A}_\mathtt{d}} \, \|(\boldsymbol{\zeta}_h, \mathbf{z}_h)\|_{\mathbf{X}} \quad \forall \, (\boldsymbol{\zeta}_h, \mathbf{z}_h) \in \mathbf{X}_h \, . \tag{4.7}$$

We now establish the discrete analogue of Lemma 3.1.

Lemma 4.1 *Let $\delta > 0$ be given and let $r \in (0, r_{0,\mathtt{d}}]$, where*

$$r_{0,\mathtt{d}} := \min \left\{ \delta, \, \frac{\alpha_{\mathbf{A}_\mathtt{d}}}{4} \left(\frac{1}{\mu} + \frac{\alpha_{\mathbf{A}_\mathtt{d}}}{4(1 + d^{1/2})} \right)^{-1} \right\} , \tag{4.8}$$

and assume that the porosity satisfies

$$\left\| \frac{\nabla \rho}{\rho} \right\|_{0,4;\Omega} \leq \left(\frac{1}{d^{1/2}} + 1 \right)^{-1} \frac{\alpha_{\mathbf{A}_\mathtt{d}}}{4} \, . \tag{4.9}$$

Then, for each $\mathbf{w}_h \in \mathbf{H}^{\mathbf{u}}_h$ satisfying $\|\mathbf{w}_h\|_{0,4;\Omega} \leq r$, the problem (4.4) admits a unique solution $(\bar{\boldsymbol{\sigma}}_h, \bar{\mathbf{u}}_h) \in \mathbf{X}_h$, and hence one can define $\mathbf{T}(\mathbf{w}_h) = \bar{\mathbf{u}}_h \in \mathbf{H}^{\mathbf{u}}_h$. Moreover, there exists a positive constant $C_{\mathbf{T}_\mathtt{d}}$, depending only on $C_{\mathbf{F}}$ and $\alpha_{\mathbf{A}_\mathtt{d}}$, such that

$$\|\mathbf{T}(\mathbf{w}_h)\|_{0,4;\Omega} = \|\bar{\mathbf{u}}_h\|_{0,4;\Omega} \leq \|(\bar{\boldsymbol{\sigma}}_h, \bar{\mathbf{u}}_h)\|_{\mathbf{X}} \leq C_{\mathbf{T}_\mathtt{d}} \Big\{ \|\mathbf{f}\|_{0,4/3;\Omega} + \|\mathbf{u}_{\mathrm{D}}\|_{1/2,\Gamma} \Big\} \, . \tag{4.10}$$

Proof. Similarly to the proof of Lemma 3.1, we observe that, under the assumptions $\|\mathbf{w}_h\|_{0,4;\Omega} \leq r$ and (4.9), the discrete inf-sup condition for $\mathbf{A}_{\mathbf{w}_h}$ (cf. (4.7)), together with the continuity estimates for $\mathbf{B}_{\mathbf{w}_h}$ and $\mathbf{C}_\rho$, implies that the bilinear form $\mathbf{A}_{\rho,\mathbf{w}_h}$ satisfies the following global discrete inf-sup condition:

$$\sup_{\mathbf{0} \neq (\boldsymbol{\tau}_h, \mathbf{v}_h) \in \mathbf{X}_h} \frac{\mathbf{A}_{\rho,\mathbf{w}_h}((\boldsymbol{\zeta}_h, \mathbf{z}_h), (\boldsymbol{\tau}_h, \mathbf{v}_h))}{\|(\boldsymbol{\tau}_h, \mathbf{v}_h)\|_{\mathbf{X}_h}} \geq \frac{\alpha_{\mathbf{A}_\mathtt{d}}}{2} \, \|(\boldsymbol{\zeta}_h, \mathbf{z}_h)\|_{\mathbf{X}_h} \qquad \forall \, (\boldsymbol{\zeta}_h, \mathbf{z}_h) \in \mathbf{X}_h \, .$$

Therefore, the bilinear form $\mathbf{A}_{\rho,\mathbf{w}_h}$ satisfies the hypotheses of [24, Theorem 2.22] for each $\mathbf{w}_h \in \mathbf{H}^{\mathbf{u}}_h$ such that $\|\mathbf{w}_h\|_{0,4;\Omega} \leq r$. Moreover, since $\mathbf{F}|_{\mathbf{X}_h} \in \mathbf{X}_h'$, an application of this theorem yields the desired result. In addition, the estimate (4.10) is obtained analogously to its continuous counterpart (3.11), with $C_{\mathbf{T}_\mathtt{d}} := 2 \, C_{\mathbf{F}} / \alpha_{\mathbf{A}_\mathtt{d}}$. □

We now proceed to analyze the fixed-point equation (4.5). We begin with the discrete version of Lemma 3.2, whose proof follows straightforwardly from Lemma 4.1.

Lemma 4.2 *Let $r \in (0, r_{0,\mathtt{d}}]$, with $r_{0,\mathtt{d}}$ given by (4.8), and define the ball*

$$\mathbf{W}_{r,\mathtt{d}} := \Big\{ \mathbf{w}_h \in \mathbf{H}^{\mathbf{u}}_h \, : \, \|\mathbf{w}_h\|_{0,4;\Omega} \leq r \Big\} \, . \tag{4.11}$$

Assume that the porosity ρ satisfies (4.9) and that

$$C_{\mathbf{T}_\mathtt{d}} \Big\{ \|\mathbf{f}\|_{0,4/3;\Omega} + \|\mathbf{u}_{\mathrm{D}}\|_{1/2,\Gamma} \Big\} \leq r \, . \tag{4.12}$$

Then the discrete fixed-point operator $\mathbf{T}_\mathtt{d}$ maps $\mathbf{W}_{r,\mathtt{d}}$ into itself, that is, $\mathbf{T}_\mathtt{d}(\mathbf{W}_{r,\mathtt{d}}) \subseteq \mathbf{W}_{r,\mathtt{d}}$.

Next, we address the discrete counterpart of Lemma 3.3, whose proof, being almost verbatim to the continuous one, is omitted. Thus, we simply state the corresponding result as follows.

Lemma 4.3 *Let $r \in (0, r_{0,\mathtt{d}}]$, with $r_{0,\mathtt{d}}$ given by (4.8), and assume that the porosity ρ satisfies (4.9). Then, there exists a positive constant $L_{\mathbf{T}_\mathtt{d}}$, depending on $\mathtt{F}_1$, c_m, ρ_0, $|\Omega|$, μ, d, and $\alpha_{\mathbf{A}_\mathtt{d}}$, such that for all $\mathbf{w}_{h,1}, \mathbf{w}_{h,2} \in \mathbf{W}_{r,\mathtt{d}}$ (cf. (4.11)) there holds*

$$\|\mathbf{T}_\mathtt{d}(\mathbf{w}_{h,1}) - \mathbf{T}_\mathtt{d}(\mathbf{w}_{h,2})\|_{0,4;\Omega} \leq L_{\mathbf{T}_\mathtt{d}} \Big\{ \|\mathbf{f}\|_{0,4/3;\Omega} + \|\mathbf{u}_{\mathrm{D}}\|_{1/2,\Gamma} \Big\} \|\mathbf{w}_{h,1} - \mathbf{w}_{h,2}\|_{0,4;\Omega} \, .$$

We are now in position of establishing the well-posedness of (4.3) (equivalently of (4.2)).

Theorem 4.4 *Let $r \in (0, r_{0,\mathtt{d}}]$, with $r_{0,\mathtt{d}}$ given by (4.8). Assume that the porosity ρ satisfies (4.9), and that the data satisfy (4.12) and*

$$L_{\mathbf{T}_\mathtt{d}} \Big\{ \|\mathbf{f}\|_{0,4/3;\Omega} + \|\mathbf{u}_{\mathrm{D}}\|_{1/2,\Gamma} \Big\} < 1 \, . \tag{4.13}$$

Then, there exists a unique fixed point $\mathbf{u}_h \in \mathbf{W}_{r,\mathtt{d}}$ (cf. (4.11)) of the discrete operator $\mathbf{T}_\mathtt{d}$. Equivalently, the discrete problem (4.3) admits a unique solution $(\boldsymbol{\sigma}_h, \mathbf{u}_h) := (\bar{\boldsymbol{\sigma}}_h, \bar{\mathbf{u}}_h) \in \mathbf{X}_h$ with $\mathbf{u}_h \in \mathbf{W}_{r,\mathtt{d}}$, where $(\bar{\boldsymbol{\sigma}}_h, \bar{\mathbf{u}}_h)$ is the unique solution of (4.4) with $\mathbf{w}_h = \mathbf{u}_h$. Moreover, the following continuous-dependence estimate holds:

$$\|(\boldsymbol{\sigma}_h, \mathbf{u}_h)\|_{\mathbf{X}} \leq C_{\mathbf{T}_\mathtt{d}} \Big\{ \|\mathbf{f}\|_{0,4/3;\Omega} + \|\mathbf{u}_{\mathrm{D}}\|_{1/2,\Gamma} \Big\} \, . \tag{4.14}$$

Proof. It proceeds analogously to the proof of Theorem 3.4. Indeed, we recall from Lemma 4.2 and the assumption (4.13) that the discrete operator $\mathbf{T}_\mathtt{d}$ is a contraction mapping the ball $\mathbf{W}_{r,\mathtt{d}}$ into itself. Hence, a straightforward application of the Banach fixed-point theorem guarantees the solvability of the discrete fixed-point problem and of the discrete formulation (4.3). Furthermore, since $\mathbf{u}_h = \mathbf{T}_\mathtt{d}(\mathbf{u}_h)$, the estimate (4.14) follows directly from (4.10), which concludes the proof. □

At this point we observe that the solvability and stability analyses at the continuous and discrete levels rely on assumptions on the porosity ρ, namely (3.10) and (4.9), respectively. In order to unify these two settings, we henceforth assume that

$$\left\| \frac{\nabla \rho}{\rho} \right\|_{0,4;\Omega} \leq \frac{1}{4} \left(\frac{1}{d^{1/2}} + 1 \right)^{-1} \min \{ \alpha_{\mathbf{A}}, \, \alpha_{\mathbf{A}_\mathtt{d}} \} \, . \tag{4.15}$$

Throughout the remainder of the analysis, this condition will be assumed to hold, thereby ensuring the validity of both the continuous and discrete results established above.

4.3 A priori error analysis

In this section, we consider arbitrary finite element subspaces satisfying assumptions (**H.0**), (**H.1**), and (**H.2**), introduced in Section 4.2, and derive a Céa-type estimate for the global error

$$\|(\boldsymbol{\sigma}, \mathbf{u}) - (\boldsymbol{\sigma}_h, \mathbf{u}_h)\|_{\mathbf{X}} \, = \, \|\boldsymbol{\sigma} - \boldsymbol{\sigma}_h\|_{\mathbf{div}_{4/3};\Omega} + \|\mathbf{u} - \mathbf{u}_h\|_{0,4;\Omega} \, ,$$

where $(\boldsymbol{\sigma}, \mathbf{u}) \in \mathbf{X}$, with $\mathbf{u} \in \mathbf{W}_r$, denotes the unique solution of (2.29), and $(\boldsymbol{\sigma}_h, \mathbf{u}_h) \in \mathbf{X}_h$, with $\mathbf{u}_h \in \mathbf{W}_{r,\mathtt{d}}$, is the unique solution of (4.3). To this end, we apply Strang-type estimates to the pair of continuous and discrete schemes associated with (2.13) and (4.3). Hereafter, given a subspace Z_h of an arbitrary Banach space $(Z, \|\cdot\|_Z)$, we define

$$\mathrm{dist}\,(z, Z_h) := \inf_{z_h \in Z_h} \|z - z_h\|_Z \, .$$

Thus, by applying the a priori error bound provided by [11, Lemma 5.1], and subsequently estimating the associated consistency terms, namely

$$\begin{aligned}&\|\mathbf{A}_{\mathbf{u}}((\boldsymbol{\sigma},\mathbf{u}),(\cdot,\cdot))-\mathbf{A}_{\mathbf{u}_h}((\boldsymbol{\sigma}_h,\mathbf{u}_h),(\cdot,\cdot))\|_{\mathbf{X}'}\\&\quad\leq\|c_{\mathbf{u}}(\mathbf{u},\cdot)-c_{\mathbf{u}_h}(\mathbf{u},\cdot)\|_{(\mathbf{H}^{\mathbf{u}}_h)'}+\|\mathbf{B}_{\mathbf{u}}((\boldsymbol{\sigma},\mathbf{u}),(\cdot,\cdot))-\mathbf{B}_{\mathbf{u}_h}((\boldsymbol{\sigma},\mathbf{u}),(\cdot,\cdot))\|_{\mathbf{X}'}\,,\end{aligned}$$

we infer the existence of a positive constant $\mathcal{C}_{\mathtt{st}}$, depending only on (cf. (2.35), (3.10), (4.9)) $\mathtt{D}_1$, ρ_0, $|\Omega|$, $\mathtt{F}_1$, μ, d, r, $\alpha_{\mathbf{A}}$, and $\alpha_{\mathbf{A}_{\mathtt{d}}}$, and hence independent of h, such that

$$\begin{aligned}\|(\boldsymbol{\sigma},\mathbf{u})-(\boldsymbol{\sigma}_h,\mathbf{u}_h)\|_{\mathbf{X}}\leq\mathcal{C}_{\mathtt{st}}\Big\{&\mathrm{dist}\,(\boldsymbol{\sigma},\mathbb{H}^{\boldsymbol{\sigma}}_h)+\mathrm{dist}\,(\mathbf{u},\mathbf{H}^{\mathbf{u}}_h)+\|c_{\mathbf{u}}(\mathbf{u},\cdot)-c_{\mathbf{u}_h}(\mathbf{u},\cdot)\|_{(\mathbf{H}^{\mathbf{u}}_h)'}\\&+\|\mathbf{B}_{\mathbf{u}}((\boldsymbol{\sigma},\mathbf{u}),(\cdot,\cdot))-\mathbf{B}_{\mathbf{u}_h}((\boldsymbol{\sigma},\mathbf{u}),(\cdot,\cdot))\|_{\mathbf{X}'}\Big\}\,.\end{aligned}\tag{4.16}$$

In order to bound (4.16), we first observe that for each $(\boldsymbol{\tau}_h,\mathbf{v}_h)\in\mathbf{X}_h$ there holds

$$\mathbf{B}_{\mathbf{u}}((\boldsymbol{\sigma},\mathbf{u}),(\boldsymbol{\tau}_h,\mathbf{v}_h))-\mathbf{B}_{\mathbf{u}_h}((\boldsymbol{\sigma},\mathbf{u}),(\boldsymbol{\tau}_h,\mathbf{v}_h))=\mathbf{B}_{\mathbf{u}-\mathbf{u}_h}((\boldsymbol{\sigma},\mathbf{u}),(\boldsymbol{\tau}_h,\mathbf{v}_h))\,,$$

so that invoking the boundedness property of $\mathbf{B}_{\mathbf{w}}$ (cf. (2.33)) together with the unified assumption (4.15), we infer that

$$\|\mathbf{B}_{\mathbf{u}-\mathbf{u}_h}((\boldsymbol{\sigma},\mathbf{u}),(\cdot,\cdot))\|_{\mathbf{X}'}\leq\left(\frac{1}{\mu}+\frac{1}{4\,(d^{1/2}+1)}\min\{\alpha_{\mathbf{A}},\alpha_{\mathbf{A}_{\mathtt{d}}}\}\right)\|\mathbf{u}-\mathbf{u}_h\|_{0,4;\Omega}\,\|(\boldsymbol{\sigma},\mathbf{u})\|_{\mathbf{X}}\,.\tag{4.17}$$

Moreover, arguing as in (3.21), and using that $\|\mathbf{u}\|_{0,4;\Omega}\leq r$ and $\|\mathbf{u}_h\|_{0,4;\Omega}\leq r_{\mathtt{d}}$, we obtain

$$\|c_{\mathbf{u}}(\mathbf{u},\cdot)-c_{\mathbf{u}_h}(\mathbf{u},\cdot)\|_{(\mathbf{H}^{\mathbf{u}}_h)'}\leq\frac{\mathtt{F}_1}{\rho_0}\,c_m\,|\Omega|^{(4-m)/4}(r+r_{\mathtt{d}})^{m-3}\,\|\mathbf{u}-\mathbf{u}_h\|_{0,4;\Omega}\,\|\mathbf{u}\|_{0,4;\Omega}\,.\tag{4.18}$$

In this way, using the continuous dependence estimate for the exact solution (3.24) to bound $\|(\boldsymbol{\sigma},\mathbf{u})\|_{\mathbf{X}}$ and $\|\mathbf{u}\|_{0,4;\Omega}$ in (4.17) and (4.18), respectively, and substituting these bounds into (4.16), we obtain

$$\begin{aligned}\|(\boldsymbol{\sigma},\mathbf{u})-(\boldsymbol{\sigma}_h,\mathbf{u}_h)\|_{\mathbf{X}}\leq\mathcal{C}_{\mathtt{st}}\Big\{&\mathrm{dist}\,(\boldsymbol{\sigma},\mathbb{H}^{\boldsymbol{\sigma}}_h)+\mathrm{dist}\,(\mathbf{u},\mathbf{H}^{\mathbf{u}}_h)\Big\}\\&+\widehat{\mathcal{C}}_{\mathtt{st}}\,\mathcal{C}_{\mathbf{T}}\Big\{\|\mathbf{f}\|_{0,4/3;\Omega}+\|\mathbf{u}_{\mathrm{D}}\|_{1/2,\Gamma}\Big\}\|\mathbf{u}-\mathbf{u}_h\|_{0,4;\Omega}\,,\end{aligned}\tag{4.19}$$

where $\widehat{\mathcal{C}}_{\mathtt{st}}$ is a positive constant given by

$$\widehat{\mathcal{C}}_{\mathtt{st}}:=\mathcal{C}_{\mathtt{st}}\,\max\left\{\frac{1}{\mu}+\frac{1}{4\,(d^{1/2}+1)}\min\{\alpha_{\mathbf{A}},\alpha_{\mathbf{A}_{\mathtt{d}}}\},\frac{\mathtt{F}_1}{\rho_0}\,c_m\,|\Omega|^{(4-m)/4}(r+r_{\mathtt{d}})^{m-3}\right\}\,.$$

Having established (4.19), we can now state the announced Céa estimate.

Theorem 4.5 *Assume that the data satisfy*

$$\widehat{\mathcal{C}}_{\mathtt{st}}\,\mathcal{C}_{\mathbf{T}}\Big\{\|\mathbf{f}\|_{0,4/3;\Omega}+\|\mathbf{u}_{\mathrm{D}}\|_{1/2,\Gamma}\Big\}\leq\frac{1}{2}\,.\tag{4.20}$$

Then, there exists a positive constant $\widetilde{\mathcal{C}}_{\mathtt{st}}$, independent of h, such that

$$\|(\boldsymbol{\sigma},\mathbf{u})-(\boldsymbol{\sigma}_h,\mathbf{u}_h)\|_{\mathbf{X}}\leq\widetilde{\mathcal{C}}_{\mathtt{st}}\Big\{\mathrm{dist}\,(\boldsymbol{\sigma},\mathbb{H}^{\boldsymbol{\sigma}}_h)+\mathrm{dist}\,(\mathbf{u},\mathbf{H}^{\mathbf{u}}_h)\Big\}.$$

Proof. The result follows directly from (4.19) together with assumption (4.20), yielding $\widetilde{\mathcal{C}}_{\mathtt{st}}:=2\,\mathcal{C}_{\mathtt{st}}$. □

4.4 Specific finite element subspaces and rates of converge

In this section we introduce specific finite element subspaces $\widetilde{\mathbb{H}}_h^{\boldsymbol{\sigma}}$ and $\mathbf{H}_h^{\mathbf{u}}$ satisfying the hypotheses (**H.0**), (**H.1**) and (**H.2**) that were introduced in Section 4.2. These discrete spaces arise naturally as consequence of similar analyses developed in [4] (see also [22], [13] and [31]). Then, with the same notations from Section 4.1, and given an integer $\ell \geq 0$ and a subset S of $\mathbf{R}$, we denote by $\mathrm{P}_\ell(S)$ and $\widetilde{\mathrm{P}}_\ell(S)$ the spaces of polynomials of total degree at most l and equal to ℓ, respectively, defined on S. Hence, for each integer $k \geq 0$ and for each $T \in \mathcal{T}_h$, we define the local Raviart–Thomas space of order k as

$$\mathbf{RT}_k(T) := \mathbf{P}_k(T) \oplus \widetilde{\mathrm{P}}_k(T)\,\mathbf{x}\,,$$

where $\mathbf{x} := (x_1, \ldots, x_n)^{\mathrm{t}}$ is a generic vector of $\mathbf{R}$, and, according to the convention in Section 1, we set $\mathbf{P}_k(T) := [\mathrm{P}_k(T)]^d$ and $\mathbb{P}_k(T) := [\mathrm{P}_k(T)]^{d\times d}$. Then, denoting by $\boldsymbol{\tau}_{h,i}$ the i-th row of a tensor $\boldsymbol{\tau}_h$, the finite element subspaces on Ω are defined as

$$\begin{aligned}
\widetilde{\mathbb{H}}_h^{\boldsymbol{\sigma}} &:= \Big\{ \boldsymbol{\tau}_h \in \mathbb{H}(\mathbf{div}_{4/3};\Omega) : \quad \boldsymbol{\tau}_{h,i}|_T \in \mathbf{RT}_k(T), \quad \forall\, i \in \{1,\ldots,d\}, \quad \forall\, T \in \mathcal{T}_h \Big\}\,, \\
\mathbf{H}_h^{\mathbf{u}} &:= \Big\{ \mathbf{v}_h \in \mathbf{L}^4(\Omega) : \quad \mathbf{v}_h|_T \in \mathbf{P}_k(T)\,, \quad \forall\, T \in \mathcal{T}_h \Big\}\,.
\end{aligned} \tag{4.21}$$

It is clear from (4.21) that $\widetilde{\mathbb{H}}_h^{\boldsymbol{\sigma}}$ contains the multiples of the identity tensor $\mathbb{I}$ and that $\mathbf{div}(\widetilde{\mathbb{H}}_h^{\boldsymbol{\sigma}}) \subseteq \mathbf{H}_h^{\mathbf{u}}$, whence (**H.0**) and (**H.1**) are satisfied. Next, defining $\mathbb{H}_h^{\boldsymbol{\sigma}} := \widetilde{\mathbb{H}}_h^{\boldsymbol{\sigma}} \cap \mathbb{H}_0(\mathbf{div}_{4/3};\Omega)$ as in (4.1), it follows that the bilinear form a (cf. (2.23)) satisfies the discrete version of (3.6) on $\mathbf{V}_h$ (cf. (4.6)). In turn, we know from [20, Lemma 5.5] (see also [4, Lemma 4.4] or [6, Lemma 3.3] with $p = 4/3$) that there holds (**H.2**).

We end this section by collecting next the approximation properties of the finite element subspaces $\mathbb{H}_h^{\boldsymbol{\sigma}}$ and $\mathbf{H}_h^{\mathbf{u}}$ (cf. (4.21)), whose derivations can be found in [2], [27], and [6, Section 3.1] (see also [20, Section 5.5]):

(**AP**$_h^{\boldsymbol{\sigma}}$) there exists a positive constant C, independent of h, such that for each $l \in (0, k+1]$ and for each $\boldsymbol{\tau} \in \mathbb{H}^l \cap \mathbb{H}_0(\mathbf{div}_{4/3};\Omega)$ with $\mathbf{div}(\boldsymbol{\tau}) \in \mathbf{W}^{l,4/3}(\Omega)$, there holds

$$\mathrm{dist}\,(\boldsymbol{\tau}, \mathbb{H}_h^{\boldsymbol{\sigma}}) := \inf_{\boldsymbol{\tau}_h \in \mathbb{H}_h^{\boldsymbol{\sigma}}} \|\boldsymbol{\tau} - \boldsymbol{\tau}_h\|_{\mathbf{div}_{4/3};\Omega} \leq C\, h^l \Big\{ \|\boldsymbol{\tau}\|_{l,\Omega} + \|\mathbf{div}(\boldsymbol{\tau})\|_{l,4/3;\Omega} \Big\}\,,$$

(**AP**$_h^{\mathbf{u}}$) there exists a positive constant C, independent of h, such that for each $l \in [0, k+1]$ and for each $\mathbf{v} \in \mathbf{W}^{l,4}(\Omega)$, there holds

$$\mathrm{dist}\,(\mathbf{v}, \mathbf{H}_h^{\mathbf{u}}) := \inf_{\mathbf{v}_h \in \mathbf{H}_h^{\mathbf{u}}} \|\mathbf{v} - \mathbf{v}_h\|_{0,4;\Omega} \leq C\, h^l\, \|\mathbf{v}\|_{l,4;\Omega}\,.$$

In this way, as a consequence of Theorem 4.5 and the approximation properties (**AP**$_h^{\boldsymbol{\sigma}}$) and (**AP**$_h^{\mathbf{u}}$), we derive the convergence rates of the Galerkin scheme (4.2) associated with the finite element subspaces defined in (4.21). More precisely, we have the following result.

Theorem 4.6 *In addition to the hypotheses of Theorems 3.4, 4.4, and 4.5, assume that there exists $l \in (0, k+1]$ such that $\boldsymbol{\sigma} \in \mathbb{H}^l(\Omega) \cap \mathbb{H}_0(\mathbf{div}_{4/3};\Omega)$, $\mathbf{div}(\boldsymbol{\sigma}) \in \mathbf{W}^{l,4/3}(\Omega)$, and $\mathbf{u} \in \mathbf{W}^{l,4}(\Omega)$. Then, there exists a positive constant $\mathcal{C}$, independent of h, such that*

$$\|(\boldsymbol{\sigma}, \mathbf{u}) - (\boldsymbol{\sigma}_h, \mathbf{u}_h)\|_{\mathbf{X}} \leq \mathcal{C}\, h^l \Big\{ \|\boldsymbol{\sigma}\|_{l,\Omega} + \|\mathbf{div}(\boldsymbol{\sigma})\|_{l,4/3;\Omega} + \|\mathbf{u}\|_{l,4;\Omega} \Big\}\,.$$

5 A residual-based a posteriori error estimator

In this section, we derive a reliable and efficient residual-based *a posteriori* error estimator for the Galerkin scheme (4.3) (equivalently of (4.2)). To this end, we employ the notation and auxiliary results collected in Appendix B, and assume the hypotheses of Theorems 3.4 and 4.4, which guarantee the existence of unique solutions $(\boldsymbol{\sigma},\mathbf{u})\in\mathbf{X}$ and $(\boldsymbol{\sigma}_h,\mathbf{u}_h)\in\mathbf{X}_h$ to the continuous and discrete problems (2.22) and (4.2), respectively. We begin by introducing the global residual-based error estimator

$$\Theta:=\left(\sum_{T\in\mathcal{T}_h}\Theta_{1,T}^4\right)^{1/4}+\left(\sum_{T\in\mathcal{T}_h}\Theta_{2,T}^2\right)^{1/2}+\left(\sum_{T\in\mathcal{T}_h}\Theta_{3,T}^{4/3}\right)^{3/4}\,, \tag{5.1}$$

where, for each element $T\in\mathcal{T}_h$, the local error indicators $\Theta_{1,T}$, $\Theta_{2,T}$, and $\Theta_{3,T}$ are defined as follows:

$$\Theta_{1,T}^4:=h_T^4\left\|\nabla\mathbf{u}_h-\frac{1}{\mu}(\boldsymbol{\sigma}_h+\mathbf{u}_h\otimes\mathbf{u}_h)^{\mathtt{d}}+\frac{1}{d}\left(\mathbf{u}_h\cdot\frac{\nabla\rho}{\rho}\right)\mathbb{I}\right\|_{0,4;T}^4+\sum_{e\in\mathcal{E}_{h,T}(\Gamma)}h_e\|\mathbf{u}_{\mathrm{D}}-\mathbf{u}_h\|_{0,4;e}^4\,, \tag{5.2}$$

$$\begin{aligned}\Theta_{2,T}^2:=&\,h_T^2\left\|\underline{\mathbf{curl}}\left(\frac{1}{\mu}(\boldsymbol{\sigma}_h+\mathbf{u}_h\otimes\mathbf{u}_h)^{\mathtt{d}}-\frac{1}{d}\left(\mathbf{u}_h\cdot\frac{\nabla\rho}{\rho}\right)\mathbb{I}\right)\right\|_{0,T}^2\\&+\sum_{e\in\mathcal{E}_{h,T}(\Omega)}h_e\left\|\left[\!\left[\boldsymbol{\delta}_*\left(\frac{1}{\mu}(\boldsymbol{\sigma}_h+\mathbf{u}_h\otimes\mathbf{u}_h)^{\mathtt{d}}-\frac{1}{d}\left(\mathbf{u}_h\cdot\frac{\nabla\rho}{\rho}\right)\mathbb{I}\right)\right]\!\right]\right\|_{0,e}^2\\&+\sum_{e\in\mathcal{E}_{h,T}(\Gamma)}h_e\left\|\boldsymbol{\delta}_*\left(\nabla\mathbf{u}_{\mathrm{D}}-\frac{1}{\mu}(\boldsymbol{\sigma}_h+\mathbf{u}_h\otimes\mathbf{u}_h)^{\mathtt{d}}-\frac{1}{d}\left(\mathbf{u}_h\cdot\frac{\nabla\rho}{\rho}\right)\mathbb{I}\right)\right\|_{0,e}^2\,,\end{aligned} \tag{5.3}$$

and

$$\begin{aligned}\Theta_{3,T}^{4/3}:=&\left\|\mathbf{f}+\mathbf{div}(\boldsymbol{\sigma}_h)-\frac{\mathtt{D}(\rho)}{\rho}\mathbf{u}_h-\frac{\mathtt{F}(\rho)}{\rho}|\mathbf{u}_h|^{m-2}\mathbf{u}_h\right.\\&\left.+\left\{\boldsymbol{\sigma}_h^{\mathtt{d}}-\frac{1}{d}\left(\mathrm{tr}(\mathbf{u}_h\otimes\mathbf{u}_h)+\mu\left(\mathbf{u}_h\cdot\frac{\nabla\rho}{\rho}\right)\right)\mathbb{I}\right\}\frac{\nabla\rho}{\rho}\right\|_{0,4/3;T}^{4/3}\,.\end{aligned} \tag{5.4}$$

Here, the jump operator $[\![\cdot]\!]$ and the tangential operator $\boldsymbol{\delta}_*$ are defined in (B.1) and (B.2), respectively. We note that the boundary term $\boldsymbol{\delta}_*(\nabla\mathbf{u}_{\mathrm{D}})|_e$ belongs to $\mathbf{L}^2(e)$ for all $e\in\mathcal{E}_h(\Gamma)$, which is guaranteed by assuming $\mathbf{u}_{\mathrm{D}}\in\mathbf{H}^1(\Gamma)$. More generally, it would suffice to require that $\nabla\mathbf{u}_{\mathrm{D}}|_\Gamma$ coincides with the trace of the gradient of a function in $\mathbf{H}^t(\Omega)$ for some $t>3/2$. In any case, we emphasize that the Dirichlet data employed in the numerical experiments reported in Section 6 satisfy the former assumption.

The main goal of the present section is to establish, under suitable assumptions, the existence of positive constants $\mathcal{C}_{\mathtt{eff}}$ and $\mathcal{C}_{\mathtt{rel}}$, independent of the meshsizes and the continuous and discrete solutions, such that

$$\mathcal{C}_{\mathtt{eff}}\,\Theta+\mathtt{h.o.t.}\,\leq\|(\boldsymbol{\sigma},\mathbf{u})-(\boldsymbol{\sigma}_h,\mathbf{u}_h)\|_{\mathbf{X}}\,\leq\,\mathcal{C}_{\mathtt{rel}}\,\Theta\,, \tag{5.5}$$

where `h.o.t.` is a generic expression denoting one or several terms of higher order. The upper and lower bounds in (5.5), which are known as the reliability and efficiency of Θ, are derived below in Sections 5.1 and 5.2, respectively.

5.1 Reliability of the a posteriori error estimator

In this section we derive the reliability estimate for the residual-based *a posteriori* error estimator introduced in (5.1), that is, we establish the upper bound in (5.5). To this end, we prove several auxiliary results that are instrumental for this purpose.

Lemma 5.1 *There exists a positive constant $\mathcal{C}_1$, independent of h, such that*

$$\|(\boldsymbol{\sigma},\mathbf{u})-(\boldsymbol{\sigma}_h,\mathbf{u}_h)\|_{\mathbf{X}} \leq \mathcal{C}_1\left\{\sup_{\mathbf{0}\neq(\boldsymbol{\tau},\mathbf{v})\in\mathbf{X}}\frac{|\mathcal{R}(\boldsymbol{\tau},\mathbf{v})|}{\|(\boldsymbol{\tau},\mathbf{v})\|_{\mathbf{X}}}+\left\{\|\mathbf{f}\|_{0,4/3;\Omega}+\|\mathbf{u}_{\mathrm{D}}\|_{1/2,\Gamma}\right\}\|\mathbf{u}-\mathbf{u}_h\|_{0,4;\Omega}\right\}, \tag{5.6}$$

where the residual functional $\mathcal{R}:\mathbf{X}\to\mathrm{R}$ is defined by

$$\mathcal{R}(\boldsymbol{\tau},\mathbf{v}):=\mathbf{F}(\boldsymbol{\tau},\mathbf{v})-\mathbf{A}_{\rho,\mathbf{u}_h}\big((\boldsymbol{\sigma}_h,\mathbf{u}_h),(\boldsymbol{\tau},\mathbf{v})\big)\qquad\forall\,(\boldsymbol{\tau},\mathbf{v})\in\mathbf{X}\,.$$

Proof. We first apply the inf-sup condition (3.13) with $\mathbf{w}=\mathbf{u}$ to the error pair $(\boldsymbol{\zeta},\mathbf{z}):=(\boldsymbol{\sigma},\mathbf{u})-(\boldsymbol{\sigma}_h,\mathbf{u}_h)$, adding and subtracting the term $\mathbf{A}_{\rho,\mathbf{u}_h}((\boldsymbol{\sigma}_h,\mathbf{u}_h),(\boldsymbol{\tau},\mathbf{v}))$, and invoking the continuous problem (2.29), we obtain

$$\begin{aligned}\frac{\alpha_{\mathbf{A}}}{2}\,\|(\boldsymbol{\sigma},\mathbf{u})-(\boldsymbol{\sigma}_h,\mathbf{u}_h)\|_{\mathbf{X}} \leq & \sup_{\mathbf{0}\neq(\boldsymbol{\tau},\mathbf{v})\in\mathbf{X}}\frac{|\mathcal{R}(\boldsymbol{\tau},\mathbf{v})|}{\|(\boldsymbol{\tau},\mathbf{v})\|_{\mathbf{X}}}+\sup_{\mathbf{0}\neq(\boldsymbol{\tau},\mathbf{v})\in\mathbf{X}}\frac{|(c_{\mathbf{u}}-c_{\mathbf{u}_h})(\mathbf{u}_h,\mathbf{v})|}{\|(\boldsymbol{\tau},\mathbf{v})\|_{\mathbf{X}}}\\ &+\sup_{\mathbf{0}\neq(\boldsymbol{\tau},\mathbf{v})\in\mathbf{X}}\frac{|(\mathbf{B}_{\mathbf{u}}-\mathbf{B}_{\mathbf{u}_h})((\boldsymbol{\sigma}_h,\mathbf{u}_h),(\boldsymbol{\tau},\mathbf{v}))|}{\|(\boldsymbol{\tau},\mathbf{v})\|_{\mathbf{X}}}\end{aligned} \tag{5.7}$$

Applying the estimates (3.21) and (3.22) in the context of the last two terms in (5.7), and using the continuous dependence estimate (4.14) to bound $\|(\boldsymbol{\sigma}_h,\mathbf{u}_h)\|_{\mathbf{X}}$ and $\|\mathbf{u}_h\|_{0,4;\Omega}$, respectively, we infer (5.6), where $\mathcal{C}_1$ is a positive constant depending on $C_{\mathbf{T}_{\mathtt{d}}}$, $\mathtt{F}_1$, c_m, ρ_0, $|\Omega|$, μ, d, $\alpha_{\mathbf{A}}$, and $\alpha_{\mathbf{A}_{\mathtt{d}}}$. □

We now proceed to bound the supremum appearing in (5.6). To achieve this, we decompose the residual functional $\mathcal{R}$ as

$$\mathcal{R}(\boldsymbol{\tau},\mathbf{v})=\mathcal{R}_1(\boldsymbol{\tau})+\mathcal{R}_2(\mathbf{v}),$$

where

$$\mathcal{R}_1(\boldsymbol{\tau}):=\langle\boldsymbol{\tau}\mathbf{n},\mathbf{u}_{\mathrm{D}}\rangle_{\Gamma}-\int_{\Omega}\mathbf{u}_h\cdot\mathbf{div}(\boldsymbol{\tau})-\int_{\Omega}\mathbf{M}(\boldsymbol{\sigma}_h,\mathbf{u}_h,\rho):\boldsymbol{\tau}, \tag{5.8}$$

and

$$\begin{aligned}\mathcal{R}_2(\mathbf{v}):=-\int_{\Omega}\Bigg(&\mathbf{f}+\mathbf{div}(\boldsymbol{\sigma}_h)-\frac{\mathtt{D}(\rho)}{\rho}\mathbf{u}-\frac{\mathtt{F}(\rho)}{\rho}|\mathbf{u}|^{m-2}\mathbf{u}\\ &+\left\{\boldsymbol{\sigma}^{\mathtt{d}}-\frac{1}{d}\left(\mathrm{tr}(\mathbf{u}\otimes\mathbf{u})+\mu\left(\mathbf{u}_h\cdot\frac{\nabla\rho}{\rho}\right)\right)\mathbb{I}\right\}\frac{\nabla\rho}{\rho}\Bigg)\cdot\mathbf{v}\,,\end{aligned} \tag{5.9}$$

with the tensor-valued function $\mathbf{M}$ defined by

$$\mathbf{M}(\boldsymbol{\zeta},\mathbf{z},\varrho):=\frac{1}{\mu}\big(\boldsymbol{\zeta}+\mathbf{z}\otimes\mathbf{z}\big)^{\mathtt{d}}-\frac{1}{d}\left(\mathbf{z}\cdot\frac{\nabla\varrho}{\varrho}\right)\mathbb{I}\,, \tag{5.10}$$

for all $(\boldsymbol{\zeta},\mathbf{z})\in\mathbf{X}$ and $\varrho\in\mathrm{W}^{1,4}(\Omega)\cap\mathrm{L}^{\infty}(\Omega)$. Then, the supremum in (5.6) can be bounded in terms of $\mathcal{R}_1$ and $\mathcal{R}_2$ as follows

$$\begin{aligned}\|(\boldsymbol{\sigma},\mathbf{u})-(\boldsymbol{\sigma}_h,\mathbf{u}_h)\|_{\mathbf{X}} \leq\ & \mathcal{C}_1\Big\{\|\mathcal{R}_1\|_{\mathbb{H}_0(\mathbf{div}_{4/3};\Omega)'}+\|\mathcal{R}_2\|_{\mathbf{L}^4(\Omega)'}\\ &+\Big(\|\mathbf{f}\|_{0,4/3;\Omega}+\|\mathbf{u}_{\mathrm{D}}\|_{1/2,\Gamma}\Big)\,\|\mathbf{u}-\mathbf{u}_h\|_{0,4;\Omega}\Big\}\,.\end{aligned} \tag{5.11}$$

Hence, our next goal is to derive suitable upper bounds for the first two terms appearing on the right-hand side of (5.11). We start by establishing the corresponding estimate for $\mathcal{R}_2$ (cf. (5.9)), which follows from a straightforward application of Hölder's inequality.

Lemma 5.2 *There holds*

$$\|\mathcal{R}_2\|_{\mathbf{L}^4(\Omega)'} \leq \left(\sum_{T \in \mathcal{T}_h} \Theta_{3,T}^{4/3} \right)^{3/4},$$

where $\Theta_{3,T}$ is defined in (5.4).

We now turn to the derivation of the corresponding estimate for $\|\mathcal{R}_1\|_{\mathbb{H}_0(\mathbf{div};\Omega)'}$. To this end, we observe from the definition of $\mathcal{R}_1$ (cf. (5.8)) and from the first equation of the Galerkin scheme (4.2) that $\mathcal{R}_1(\boldsymbol{\tau}_h) = 0$ for all $\boldsymbol{\tau}_h \in \mathbb{H}_h^{\boldsymbol{\sigma}}$. Consequently, in the computation of

$$\|\mathcal{R}_1\|_{\mathbb{H}_0(\mathbf{div};\Omega)'} := \sup_{\mathbf{0} \neq \boldsymbol{\tau} \in \mathbb{H}_0(\mathbf{div}_{4/3};\Omega)} \frac{|\mathcal{R}_1(\boldsymbol{\tau})|}{\|\boldsymbol{\tau}\|_{\mathbf{div}_{4/3};\Omega}},$$

we can replace $\mathcal{R}_1(\boldsymbol{\tau})$ by $\mathcal{R}_1(\boldsymbol{\tau} - \boldsymbol{\tau}_h)$, where $\boldsymbol{\tau}_h \in \mathbb{H}_h^{\boldsymbol{\sigma}}$ is suitably chosen depending on the given $\boldsymbol{\tau} \in \mathbb{H}_0(\mathbf{div}_{4/3};\Omega)$. To this end, we employ the Helmholtz decomposition provided by Lemma B.2, part (b) (or part (a) in the two-dimensional case), with $p = 4/3$, which asserts that for each $\boldsymbol{\tau} \in \mathbb{H}_0(\mathbf{div}_{4/3};\Omega)$ there exist $\boldsymbol{\zeta} \in \mathbb{W}^{1,4/3}(\Omega)$ and $\boldsymbol{\xi} \in \mathbb{H}^1(\Omega)$ such that

$$\boldsymbol{\tau} = \boldsymbol{\zeta} + \underline{\mathbf{curl}}\,(\boldsymbol{\xi}) \quad \text{in} \quad \Omega\,, \qquad \|\boldsymbol{\zeta}\|_{1,4/3;\Omega} + \|\boldsymbol{\xi}\|_{1,\Omega} \leq C_{4/3}\,\|\boldsymbol{\tau}\|_{\mathbf{div}_{4/3};\Omega}\,, \tag{5.12}$$

where $C_{4/3}$ is a positive constant independent of $\boldsymbol{\tau}$. We then define

$$\boldsymbol{\tau}_h := \boldsymbol{\Pi}_h^k(\boldsymbol{\zeta}) + \underline{\mathbf{curl}}\,\big(\boldsymbol{\mathcal{I}}_h(\boldsymbol{\xi})\big) + c_{\mathtt{H}}\,\mathbb{I}\,, \tag{5.13}$$

where $\boldsymbol{\Pi}_h^k$ and $\boldsymbol{\mathcal{I}}_h$ denote the tensor-valued Raviart–Thomas and Clément interpolation operators, respectively (cf. Appendix B). The constant $c_{\mathtt{H}}$ is chosen so that $\mathrm{tr}(\boldsymbol{\tau}_h)$ has zero mean value. More precisely,

$$c_{\mathtt{H}} := \frac{1}{d\,|\Omega|} \left(\int_\Omega \mathrm{tr}\big(\boldsymbol{\Pi}_h^k(\boldsymbol{\zeta})\big) + \int_\Omega \mathrm{tr}\big(\underline{\mathbf{curl}}\,(\boldsymbol{\mathcal{I}}_h(\boldsymbol{\xi}))\big) \right). \tag{5.14}$$

With this choice, $\boldsymbol{\tau}_h$ can be interpreted as a discrete Helmholtz decomposition of $\boldsymbol{\tau}$, and it readily follows that $\boldsymbol{\tau}_h \in \mathbb{H}_h^{\boldsymbol{\sigma}}$. Next, defining

$$\widehat{\boldsymbol{\zeta}} := \boldsymbol{\zeta} - \boldsymbol{\Pi}_h^k(\boldsymbol{\zeta})\,, \qquad \widehat{\boldsymbol{\xi}} := \boldsymbol{\xi} - \boldsymbol{\mathcal{I}}_h(\boldsymbol{\xi})\,, \tag{5.15}$$

it follows from (5.12) and (5.13) that

$$\mathcal{R}_1(\boldsymbol{\tau}) = \mathcal{R}_1(\boldsymbol{\tau} - \boldsymbol{\tau}_h) = \mathcal{R}_1(\widehat{\boldsymbol{\zeta}}) + \mathcal{R}_1\big(\underline{\mathbf{curl}}\,(\widehat{\boldsymbol{\xi}})\big) + \mathcal{R}_1(c_{\mathtt{H}}\,\mathbb{I})\,. \tag{5.16}$$

In this way, the next lemma establishes suitable bounds for each of the terms appearing on the right-hand side of (5.16).

Lemma 5.3 *Let $\mathbf{M}$ be defined as in (5.10). Then, there exist positive constants $\mathcal{C}_2$, $\mathcal{C}_3$, and $\mathcal{C}_4$, independent of h, such that*

$$|\mathcal{R}_1(\widehat{\boldsymbol{\zeta}})| \leq \mathcal{C}_2 \left\{ \sum_{T \in \mathcal{T}_h} h_T^4 \|\nabla \mathbf{u}_h - \mathbf{M}(\boldsymbol{\sigma}_h, \mathbf{u}_h, \rho)\|_{0,4;T}^4 + \sum_{e \in \mathcal{E}_h(\Gamma)} h_e \|\mathbf{u}_{\mathrm{D}} - \mathbf{u}_h\|_{0,4;e}^4 \right\}^{1/4} \|\boldsymbol{\tau}\|_{\mathbf{div}_{4/3};\Omega}\,, \tag{5.17}$$

$$|\mathcal{R}_1(\underline{\mathbf{curl}}\,(\widehat{\boldsymbol{\xi}}))| \leq \mathcal{C}_3 \Bigg(\sum_{T\in\mathcal{T}_h} h_T^2 \, \|\underline{\mathbf{curl}}\,(\mathbf{M}(\boldsymbol{\sigma}_h,\mathbf{u}_h,\rho))\|_{0,T}^2 + \sum_{e\in\mathcal{E}_h(\Omega)} h_e \, \| \, [\![\boldsymbol{\delta}_*(\mathbf{M}(\boldsymbol{\sigma}_h,\mathbf{u}_h,\rho))]\!] \, \|_{0,e}^2 \\ + \sum_{e\in\mathcal{E}_h(\Gamma)} h_e \, \|\boldsymbol{\delta}_*(\nabla\mathbf{u}_{\mathrm{D}} - \mathbf{M}(\boldsymbol{\sigma}_h,\mathbf{u}_h,\rho))\|_{0,e}^2 \Bigg)^{1/2} \|\boldsymbol{\tau}\|_{\mathbf{div}_{4/3};\Omega} \,, \tag{5.18}$$

and

$$|\mathcal{R}_1(c_{\mathtt{H}}\,\mathbb{I})| \leq \mathcal{C}_4 \left\| \frac{\nabla\rho}{\rho} \right\|_{0,4;\Omega} \|\mathbf{u}-\mathbf{u}_h\|_{0,4;\Omega} \|\boldsymbol{\tau}\|_{\mathbf{div}_{4/3};\Omega} \,. \tag{5.19}$$

Proof. Let $\boldsymbol{\tau}\in\mathbb{H}_0(\mathbf{div}_{4/3};\Omega)$ and recall (5.15). In view of the decomposition (5.16), we proceed by estimating each term separately.

Estimate for $\mathcal{R}_1(\widehat{\boldsymbol{\zeta}})$. For each $e\in\mathcal{E}_h$, identity (B.5) together with the fact that $\mathbf{u}_h|_e\in\mathbf{P}_k(e)$ yields $\int_e \widehat{\boldsymbol{\zeta}}\,\mathbf{n}\cdot\mathbf{u}_h = 0$. Hence, locally integrating by parts the second term in the definition of $\mathcal{R}_1$ (cf. (5.8)), we obtain

$$\mathcal{R}_1(\widehat{\boldsymbol{\zeta}}) = \sum_{e\in\mathcal{E}_h(\Gamma)} \int_e (\mathbf{u}_{\mathrm{D}}-\mathbf{u}_h)\cdot\widehat{\boldsymbol{\zeta}}\,\mathbf{n} + \int_\Omega (\nabla\mathbf{u}_h - \mathbf{M}(\boldsymbol{\sigma}_h,\mathbf{u}_h,\rho)) : \widehat{\boldsymbol{\zeta}} \,.$$

Applying Hölder's inequality, the approximation properties of the Raviart–Thomas interpolant $\boldsymbol{\Pi}_h^k$ (cf. Lemma B.1 with $p=4/3$ and $\ell=0$), and the stability estimate (5.12), we conclude (5.17).

Estimate for $\mathcal{R}_1(\underline{\mathbf{curl}}\,(\widehat{\boldsymbol{\xi}}))$. First, we notice that $\mathbf{div}(\underline{\mathbf{curl}}\,(\widehat{\boldsymbol{\xi}})) = \mathbf{0}$ in Ω, which implies

$$\mathcal{R}_1(\underline{\mathbf{curl}}\,(\widehat{\boldsymbol{\xi}})) = \langle \underline{\mathbf{curl}}\,(\widehat{\boldsymbol{\xi}})\mathbf{n}, \mathbf{u}_{\mathrm{D}}\rangle_\Gamma - \int_\Omega \mathbf{M}(\boldsymbol{\sigma}_h,\mathbf{u}_h,\rho) : \underline{\mathbf{curl}}\,(\widehat{\boldsymbol{\xi}}) \,. \tag{5.20}$$

In turn, using the integration by parts formula on Γ (cf. [32, Chapter I, eq. (2.17) and Theorem 2.11], and [23, Lemma 3.5] for the two-dimensional case), we have

$$\big\langle \underline{\mathbf{curl}}\,(\widehat{\boldsymbol{\xi}})\mathbf{n}, \mathbf{u}_{\mathrm{D}}\big\rangle_\Gamma = -\big\langle \nabla\mathbf{u}_{\mathrm{D}}\times\mathbf{n}, \widehat{\boldsymbol{\xi}}\big\rangle_\Gamma = -\big\langle \boldsymbol{\delta}_*(\nabla\mathbf{u}_{\mathrm{D}}), \widehat{\boldsymbol{\xi}}\big\rangle_\Gamma \,. \tag{5.21}$$

Thus, integrating by parts the second term in (5.20) and using (5.21), we obtain

$$\mathcal{R}_1(\underline{\mathbf{curl}}\,(\widehat{\boldsymbol{\xi}})) = -\sum_{T\in\mathcal{T}_h}\int_T \underline{\mathbf{curl}}\,(\mathbf{M}(\boldsymbol{\sigma}_h,\mathbf{u}_h,\rho))\cdot\widehat{\boldsymbol{\xi}} + \sum_{e\in\mathcal{E}_h(\Omega)}\int_e [\![\boldsymbol{\delta}_*(\mathbf{M}(\boldsymbol{\sigma}_h,\mathbf{u}_h,\rho))]\!]\cdot\widehat{\boldsymbol{\xi}} \\ - \sum_{e\in\mathcal{E}_h(\Gamma)}\int_e \boldsymbol{\delta}_*(\nabla\mathbf{u}_{\mathrm{D}} - \mathbf{M}(\boldsymbol{\sigma}_h,\mathbf{u}_h,\rho))\cdot\widehat{\boldsymbol{\xi}} \,.$$

Hence, by applying the Cauchy–Schwarz inequality, the approximation properties of the Clément interpolant $\boldsymbol{\mathcal{I}}_h$ (cf. Lemma B.3), and the stability estimate (5.12), we deduce from the previous inequality that (5.18) holds.

Estimate for $\mathcal{R}_1(c_{\mathtt{H}}\,\mathbb{I})$. Proceeding as in [15, Lemma 6.4, (6.18)], we employ the continuity of the interpolation operators $\boldsymbol{\Pi}_h^k \in \mathcal{L}\big(\mathbb{W}^{1,4/3}(\Omega),\mathbb{L}^{4/3}(\Omega)\big)$ and $\boldsymbol{\mathcal{I}}_h\in\mathcal{L}\big(\mathbb{H}^1(\Omega),\mathbb{H}^1(\Omega)\big)$, and use simple computations to deduce from (5.14) that

$$|c_{\mathtt{H}}| \leq \frac{\max\{1,|\Omega|^{1/4}\}}{\sqrt{d}\,|\Omega|^{3/4}} \Big(\|\boldsymbol{\Pi}_h^k(\boldsymbol{\zeta})\|_{0,4/3;\Omega} + \|\underline{\mathbf{curl}}\,(\boldsymbol{\mathcal{I}}_h(\boldsymbol{\xi}))\|_{0,\Omega} \Big) \\ \leq \frac{\max\{1,|\Omega|^{1/4}\}}{\sqrt{d}\,|\Omega|^{3/4}} \max\big\{\|\boldsymbol{\Pi}_h^k\|, \|\boldsymbol{\mathcal{I}}_h\|\big\} \Big(\|\boldsymbol{\zeta}\|_{1,4/3;\Omega} + \|\boldsymbol{\xi}\|_{1,\Omega} \Big) \,, \tag{5.22}$$

where $\|\boldsymbol{\Pi}_h^k\|$ and $\|\boldsymbol{\mathcal{I}}_h\|$ denote the respective continuity constants of $\boldsymbol{\Pi}_h^k$ and $\boldsymbol{\mathcal{I}}_h$, both independent of h. Next, owing to the compatibility condition (2.6), together with the identities $\mathbf{div}(\mathbb{I}) = \mathbf{0}$ and $\boldsymbol{\tau}^{\mathtt{d}} : \mathbb{I} = 0$, the definition of $\mathcal{R}_1$ (cf. (5.8)) and Hölder's inequality, yields

$$\mathcal{R}_1(c_{\mathtt{H}}\,\mathbb{I}) = c_{\mathtt{H}} \int_\Omega (\mathbf{u}_h - \mathbf{u}) \cdot \frac{\nabla \rho}{\rho} \;\leq\; |c_{\mathtt{H}}| \left\| \frac{\nabla \rho}{\rho} \right\|_{0,4;\Omega} \|\mathbf{u} - \mathbf{u}_h\|_{0,4/3;\Omega}\,.$$

Then, invoking (5.22) and the stability estimate (5.12), and employing the embedding $\mathbf{L}^4(\Omega) \hookrightarrow \mathbf{L}^{4/3}(\Omega)$, we readily obtain (5.19), which concludes the proof. □

We conclude this section with the main reliability theorem.

Theorem 5.4 *Assume that the data ρ, $\mathbf{f}$ and $\mathbf{u}_{\mathrm{D}}$ satisfy*

$$\mathcal{C}_1 \left(\mathcal{C}_4 \left\| \frac{\nabla \rho}{\rho} \right\|_{0,4;\Omega} + \|\mathbf{f}\|_{0,4/3;\Omega} + \|\mathbf{u}_{\mathrm{D}}\|_{1/2,\Gamma} \right) \leq \frac{1}{2}\,, \tag{5.23}$$

where $\mathcal{C}_1$ and $\mathcal{C}_4$ are such that (5.6) and (5.19) hold, respectively. Then, there exists a positive constant $\mathcal{C}_{\mathtt{rel}}$, independent of h, such that

$$\|(\boldsymbol{\sigma}, \mathbf{u}) - (\boldsymbol{\sigma}_h, \mathbf{u}_h)\|_{\mathbf{X}} \leq \mathcal{C}_{\mathtt{rel}}\, \Theta\,. \tag{5.24}$$

Proof. The reliability estimate (5.24) is obtained by combining the preliminary inequality (5.6) with the local bounds established in Lemmas 5.2 and 5.3, and invoking the smallness condition (5.23). Further details are omitted. □

5.2 Efficiency of the a posteriori error estimator

We now turn to the derivation of the efficiency estimate for the global a posteriori error estimator Θ (cf. (5.1)), that is, we establish the lower bound in (5.5). We rely heavily on the notation and auxiliary results collected in Appendix C, as well as on the original system of equations given in (2.11). The latter is recovered from the mixed continuous formulation (2.22) by choosing appropriate test functions and reversing the integration by parts argument.

Throughout this section we assume, without loss of generality, that the data $\mathbf{f}$ and $\mathbf{u}_{\mathrm{D}}$, as well as ρ, are piecewise polynomial functions. More precisely, we assume that ρ belongs to

$$\mathrm{H}_h^{\mathbf{u}} := \left\{ v_h \in \mathrm{L}^4(\Omega) : \quad v_h|_T \in \mathrm{P}_k(T)\,, \quad \forall\, T \in \mathcal{T}_h \right\}. \tag{5.25}$$

Otherwise, if $\mathbf{f}$, $\mathbf{u}_{\mathrm{D}}$, and ρ are sufficiently smooth, the analysis can be carried out along the same lines as in [15, Section 6.2]. In that case, additional higher-order terms arising from suitable polynomial approximations of these data appear in the lower bound of (5.5), which explains the presence of the `h.o.t.` term in that inequality.

We begin the derivation of the global efficiency estimate of (5.5) by establishing a sequence of local lower bounds, starting with the following estimate for the term defining $\Theta_{3,T}$ (cf. (5.4)).

Lemma 5.5 *There exists a positive constant $\mathcal{C}_5$, independent of h, such that*

$$\begin{aligned} \Theta_{3,T}^{4/3} \leq \mathcal{C}_5 \Bigg\{ & \left\| (\boldsymbol{\sigma} - \boldsymbol{\sigma}_h)^{\mathtt{d}} \frac{\nabla \rho}{\rho} \right\|_{0,4/3;T}^{4/3} + \|\mathbf{div}(\boldsymbol{\sigma} - \boldsymbol{\sigma}_h)\|_{0,4/3;T}^{4/3} + \left\| |\mathbf{u}|^{m-2}\mathbf{u} - |\mathbf{u}_h|^{m-2}\mathbf{u}_h \right\|_{0,4/3;T}^{4/3} \\ & + \|\mathbf{u} - \mathbf{u}_h\|_{0,4/3;T}^{4/3} + \left\| (\mathbf{u} \otimes \mathbf{u} - \mathbf{u}_h \otimes \mathbf{u}_h) \frac{\nabla \rho}{\rho} \right\|_{0,4/3;T}^{4/3} + \left\| \left((\mathbf{u} - \mathbf{u}_h) \cdot \frac{\nabla \rho}{\rho} \right) \frac{\nabla \rho}{\rho} \right\|_{0,4/3;T}^{4/3} \Bigg\}. \end{aligned} \tag{5.26}$$

Proof. Recalling the strong form of the momentum balance (cf. (2.11)), we have

$$\mathbf{f} = \frac{\mathtt{D}(\rho)}{\rho}\,\mathbf{u} + \frac{\mathtt{F}(\rho)}{\rho}\,|\mathbf{u}|^{m-2}\mathbf{u} - \left\{\boldsymbol{\sigma}^{\mathtt{d}} - \frac{1}{d}\left(\mathrm{tr}(\mathbf{u}\otimes\mathbf{u}) + \mu\left(\mathbf{u}\cdot\frac{\nabla\rho}{\rho}\right)\right)\mathbb{I}\right\}\frac{\nabla\rho}{\rho} - \mathbf{div}(\boldsymbol{\sigma})\,.$$

Substituting this identity into the definition of $\Theta_{3,T}$ (cf. (5.4)), and then applying the triangle and Hölder inequalities together with the bounds (2.2) and (2.3), we obtain

$$\begin{aligned}\Theta_{3,T} \leq\ & \left\|(\boldsymbol{\sigma}-\boldsymbol{\sigma}_h)^{\mathtt{d}}\frac{\nabla\rho}{\rho}\right\|_{0,4/3;T} + \|\mathbf{div}(\boldsymbol{\sigma}-\boldsymbol{\sigma}_h)\|_{0,4/3;T} + \frac{\mathtt{F}_1}{\rho_0}\left\||\mathbf{u}|^{m-2}\mathbf{u} - |\mathbf{u}_h|^{m-2}\mathbf{u}_h\right\|_{0,4/3;T} \\ &+ \frac{\mathtt{D}_1}{\rho_0}\|\mathbf{u}-\mathbf{u}_h\|_{0,4/3;T} + \frac{1}{d^{1/2}}\left\|(\mathbf{u}\otimes\mathbf{u}-\mathbf{u}_h\otimes\mathbf{u}_h)\frac{\nabla\rho}{\rho}\right\|_{0,4/3;T} + \frac{\mu}{d}\left\|\left((\mathbf{u}-\mathbf{u}_h)\cdot\frac{\nabla\rho}{\rho}\right)\frac{\nabla\rho}{\rho}\right\|_{0,4/3;T}\,,\end{aligned}$$

from which, raising the estimate to the power of $4/3$ and performing straightforward computations, we deduce (5.26). □

Now we proceed by deriving the estimates for the terms defining $\Theta_{1,T}$ (cf. (5.2)).

Lemma 5.6 *Assume that ρ, and hence $\nabla\rho$, are piecewise polynomial functions. Then, there exists a positive constant $\mathcal{C}_6$, independent of h, such that for all $T\in\mathcal{T}_h$,*

$$\begin{aligned}h_T^4\left\|\nabla\mathbf{u}_h - \frac{1}{\mu}\big(\boldsymbol{\sigma}_h+\mathbf{u}_h\otimes\mathbf{u}_h\big)^{\mathtt{d}} + \frac{1}{d}\left(\mathbf{u}_h\cdot\frac{\nabla\rho}{\rho}\right)\mathbb{I}\right\|_{0,4;T}^4 \leq\ & \mathcal{C}_6\Big\{h_T^2\|\boldsymbol{\sigma}-\boldsymbol{\sigma}_h\|_{0,T}^4 \\ &+ \|\mathbf{u}-\mathbf{u}_h\|_{0,4;T}^4 + h_T^2\|\mathbf{u}\otimes\mathbf{u}-\mathbf{u}_h\otimes\mathbf{u}_h\|_{0,T}^4 + h_T^2\left\|(\mathbf{u}-\mathbf{u}_h)\cdot\frac{\nabla\rho}{\rho}\right\|_{0,T}^4\Big\}\,.\end{aligned} \tag{5.27}$$

Proof. Given $T\in\mathcal{T}_h$, we let $\widetilde{\boldsymbol{\chi}}_T := \nabla\mathbf{u}_h - \mathbf{M}(\boldsymbol{\sigma}_h,\mathbf{u}_h,\rho)$ (cf. (5.10)) and

$$\boldsymbol{\chi}_T := \rho\,\widetilde{\boldsymbol{\chi}}_T \;=\; \rho\,\nabla\mathbf{u}_h - \frac{\rho}{\mu}\big(\boldsymbol{\sigma}_h+\mathbf{u}_h\otimes\mathbf{u}_h\big)^{\mathtt{d}} + \frac{1}{d}(\mathbf{u}_h\cdot\nabla\rho)\mathbb{I}\,,$$

which, in view of the lower bound of ρ (cf. (2.2)), yields

$$\|\widetilde{\boldsymbol{\chi}}_T\|_{0,4;T} \leq \frac{1}{\rho_0}\,\|\boldsymbol{\chi}_T\|_{0,4;T}\,. \tag{5.28}$$

Since $\mathbf{RT}_k(T)\subset\mathbf{P}_{k+1}(T)$ and ρ is actually assumed to belong to $\mathrm{H}_h^{\mathbf{u}}$ (cf. (5.25)), it readily follows that $\boldsymbol{\chi}_T\in\mathbb{P}_{\widetilde{k}}(T)$, where $\widetilde{k} := \begin{cases}1, & \text{if } k=0,\\ 3k, & \text{if } k\geq 1.\end{cases}$. Then, proceeding as in [12, Lemma 5.15], we apply the tensor-valued version of the left-hand side of (C.2) (cf. Lemma C.1), with $p=4$ and $q=4/3$, yielding

$$c_1\,\|\boldsymbol{\chi}_T\|_{0,4;T} \leq \sup_{0\neq\boldsymbol{\tau}\in\mathbb{P}_{\widetilde{k}}(T)}\frac{\displaystyle\int_T \boldsymbol{\chi}_T : (\psi_T\boldsymbol{\tau})}{\|\boldsymbol{\tau}\|_{0,4/3;T}}\,, \tag{5.29}$$

where ψ_T denotes the element bubble function introduced in (C.1). In turn, noting that

$$\int_T \boldsymbol{\chi}_T : (\psi_T\boldsymbol{\tau}) = \int_T \widetilde{\boldsymbol{\chi}}_T : (\psi_T\rho\boldsymbol{\tau})$$

and (cf. (2.2))

$$\|\boldsymbol{\tau}\|_{0,4/3;T} \,\geq\, \|\rho\boldsymbol{\tau}\|_{0,4/3;T}\,,$$

with $\rho\boldsymbol{\tau} \in \mathbb{P}_{\widehat{k}}(T)$, where $\widehat{k} = \widetilde{k} + k$, it follows from (5.28) and (5.29) that

$$\|\widetilde{\boldsymbol{\chi}}_T\|_{0,4;T} \,\leq\, \frac{1}{\rho_0\, c_1} \sup_{0\neq\boldsymbol{\tau}\in\mathbb{P}_{\widehat{k}}(T)} \frac{\displaystyle\int_T \widetilde{\boldsymbol{\chi}}_T : (\psi_T\boldsymbol{\tau})}{\|\boldsymbol{\tau}\|_{0,4/3;T}}\,. \tag{5.30}$$

Next, recalling from the first equation of (2.11) and (5.10), that

$$\nabla\mathbf{u} = \frac{1}{\mu}\big(\boldsymbol{\sigma} + \mathbf{u}\otimes\mathbf{u}\big)^{\mathtt{d}} - \frac{1}{d}\left(\mathbf{u}\cdot\frac{\nabla\rho}{\rho}\right)\mathbb{I} = \mathbf{M}(\boldsymbol{\sigma},\mathbf{u},\rho) \quad \text{in} \quad \Omega\,, \tag{5.31}$$

and integrating by parts, together with the fact that $\psi_T\boldsymbol{\tau} = \mathbf{0}$ on ∂T (cf. (C.1)), we arrive at

$$\begin{aligned}\int_T \widetilde{\boldsymbol{\chi}}_T : (\psi_T\boldsymbol{\tau}) &= \int_T (\nabla(\mathbf{u}_h - \mathbf{u}) + \mathbf{M}(\boldsymbol{\sigma}-\boldsymbol{\sigma}_h, \mathbf{u}-\mathbf{u}_h,\rho)) : (\psi_T\boldsymbol{\tau}) \\ &= \int_T (\mathbf{u}-\mathbf{u}_h)\cdot\mathbf{div}(\psi_T\boldsymbol{\tau}) + \int_T \mathbf{M}(\boldsymbol{\sigma}-\boldsymbol{\sigma}_h,\mathbf{u}-\mathbf{u}_h,\rho) : (\psi_T\boldsymbol{\tau})\,.\end{aligned} \tag{5.32}$$

Then, applying Hölder's inequality, using the bound

$$\|\mathbf{div}(\psi_T\boldsymbol{\tau})\|_{0,4/3;T} \,\leq\, \|\nabla(\psi_T\boldsymbol{\tau})\|_{0,4/3;T}\,,$$

the right-hand side estimate in (C.3), the Cauchy–Schwarz inequality to control the last term in (5.32), the fact that $0 \leq \psi_T \leq 1$, and $\|\boldsymbol{\zeta}^{\mathtt{d}}\|_{0,T} \leq \|\boldsymbol{\zeta}\|_{0,T}$ for all $\boldsymbol{\zeta} \in \mathbb{L}^2(T)$, we obtain

$$\begin{aligned}\int_T \widetilde{\boldsymbol{\chi}}_T : (\psi_T\boldsymbol{\tau}) \,\leq\, & c_3\, h_T^{-1}\, \|\mathbf{u}-\mathbf{u}_h\|_{0,4;T}\, \|\boldsymbol{\tau}\|_{0,4/3;T} \\ & + \left(\frac{1}{\mu}\Big(\|\boldsymbol{\sigma}-\boldsymbol{\sigma}_h\|_{0,T} + \|\mathbf{u}\otimes\mathbf{u} - \mathbf{u}_h\otimes\mathbf{u}_h\|_{0,T}\Big) + \frac{1}{\sqrt{d}}\left\|(\mathbf{u}-\mathbf{u}_h)\cdot\frac{\nabla\rho}{\rho}\right\|_{0,T}\right)\|\boldsymbol{\tau}\|_{0,T}\,.\end{aligned} \tag{5.33}$$

Next, by the local inverse inequality (C.4) (cf. Lemma C.2) with $d \in \{2,3\}$, $\ell = m = 0$, $r = 2$, and $s = 4/3$, and the fact that $h_T^{-d/4} \leq h_T^{-1}$ for $h_T \leq 1$, we have

$$\|\boldsymbol{\tau}\|_{0,T} \leq c\, h_T^{-d/4}\, \|\boldsymbol{\tau}\|_{0,4/3;T} \leq c\, h_T^{-1/2}\, \|\boldsymbol{\tau}\|_{0,4/3;T}\,.$$

Substituting this estimate into (5.33) yields

$$\begin{aligned}\int_T \widetilde{\boldsymbol{\chi}}_T : (\psi_T\boldsymbol{\tau}) \,\leq\, & C\Bigg\{ h_T^{-1}\, \|\mathbf{u}-\mathbf{u}_h\|_{0,4;T} \\ & + h_T^{-1/2}\left(\|\boldsymbol{\sigma}-\boldsymbol{\sigma}_h\|_{0,T} + \|\mathbf{u}\otimes\mathbf{u} - \mathbf{u}_h\otimes\mathbf{u}_h\|_{0,T} + \left\|(\mathbf{u}-\mathbf{u}_h)\cdot\frac{\nabla\rho}{\rho}\right\|_{0,T}\right)\Bigg\}\,\|\boldsymbol{\tau}\|_{0,4/3;T}\,.\end{aligned} \tag{5.34}$$

Finally, inserting (5.34) into (5.30), multiplying the resulting inequality by h_T, and raising it to the fourth power, we obtain the desired bound. □

The remaining local efficiency estimate for $\Theta_{1,T}$ (cf. (5.2)) is established as follows.

Lemma 5.7 *Assume that $\mathbf{u}_{\mathrm{D}}$, ρ, and hence $\nabla\rho$, are piecewise polynomial functions. Then, there exists a positive constant $\mathcal{C}_7$, independent of h, such that*

$$\begin{aligned} h_e\|\mathbf{u}_{\mathrm{D}}-\mathbf{u}\|^4_{0,4;e} \leq \mathcal{C}_7\Big\{ & h^2_{T_e}\|\boldsymbol{\sigma}-\boldsymbol{\sigma}_h\|^4_{0,T_e}+\|\mathbf{u}-\mathbf{u}_h\|^4_{0,4;T_e} \\ & + h^2_{T_e}\|\mathbf{u}\otimes\mathbf{u}-\mathbf{u}_h\otimes\mathbf{u}_h\|^4_{0,T_e}+h^2_{T_e}\left\|(\mathbf{u}-\mathbf{u}_h)\cdot\frac{\nabla\rho}{\rho}\right\|^4_{0,T_e}\Big\}, \end{aligned} \tag{5.35}$$

for all $e\in\mathcal{E}_h(\Gamma)$, and where T_e is the triangle/tetrahedron of $\mathcal{T}_h$ having e as an edge/face.

Proof. The proof follows as a mild modification of [29, Lemma 3.16]. Let $e\in\mathcal{E}_h(\Gamma)$ be given. We first observe that, by the local inverse inequality (C.4), where $d=1$ for boundary edges in the two-dimensional setting and $d=2$ for boundary faces in three dimensions, $l=m=0$, $r=4$, and $s=2$, together with the fact that $\mathbf{u}=\mathbf{u}_{\mathrm{D}}$ on Γ, there holds

$$\|\mathbf{u}_{\mathrm{D}}-\mathbf{u}_h\|_{0,4;e}\leq c\,h_e^{-d/4}\,\|\mathbf{u}-\mathbf{u}_h\|_{0,e}\,.$$

Raising the above inequality to the fourth power, using the fact that $h_e^{-d}\leq h_e^{-1}$ for $h_e\leq 1$, applying the vector-valued discrete trace inequality (C.5) (cf. Lemma C.3) with $p=2$, and recalling (5.31), we obtain, after applying the triangle inequality and performing straightforward algebraic manipulations,

$$h_e\|\mathbf{u}_{\mathrm{D}}-\mathbf{u}_h\|^4_{0,4;e}\leq\ C\Big\{h^{-1}_{T_e}\|\mathbf{u}-\mathbf{u}_h\|^2_{0,T_e}+h_{T_e}\,\|\mathbf{M}(\boldsymbol{\sigma},\mathbf{u},\rho)-\nabla\mathbf{u}_h\|^2_{0,T_e}\Big\}^2.$$

Next, adding and subtracting $\mathbf{M}(\boldsymbol{\sigma}_h,\mathbf{u}_h,\rho)$ (cf. (5.10)) and applying the triangle inequality once more, we deduce

$$\begin{aligned} h_e\|\mathbf{u}_{\mathrm{D}}-\mathbf{u}_h\|^4_{0,4;e}\leq\ C\Big\{ & h^{-2}_{T_e}\|\mathbf{u}-\mathbf{u}_h\|^4_{0,T_e}+h^2_{T_e}\|\boldsymbol{\sigma}-\boldsymbol{\sigma}_h\|^4_{0,T_e}+h^2_{T_e}\|\mathbf{u}\otimes\mathbf{u}-\mathbf{u}_h\otimes\mathbf{u}_h\|^4_{0,T_e} \\ & + h^2_{T_e}\left\|(\mathbf{u}-\mathbf{u}_h)\cdot\frac{\nabla\rho}{\rho}\right\|^4_{0,T_e}+h^2_{T_e}\,\|\mathbf{M}(\boldsymbol{\sigma}_h,\mathbf{u}_h,\rho)-\nabla\mathbf{u}_h\|^4_{0,T_e}\Big\}. \end{aligned} \tag{5.36}$$

Moreover, an application of the Cauchy–Schwarz inequality, together with the fact that $|T_e|\cong h^d_{T_e}$ for $d\in\{2,3\}$, yields

$$\|\mathbf{w}\|^4_{0,T_e}\leq|T_e|\|\mathbf{w}\|^4_{0,4;T_e}\leq c\,h^d_{T_e}\,\|\mathbf{w}\|^4_{0,4;T_e}\leq c\,h^2_{T_e}\,\|\mathbf{w}\|^4_{0,4;T_e}\qquad\forall\,\mathbf{w}\in\mathbf{L}^4(T_e)\,. \tag{5.37}$$

Then, applying (5.37) to the first and last terms on the right-hand side of (5.36), we obtain

$$\begin{aligned} h_e\|\mathbf{u}_{\mathrm{D}}-\mathbf{u}\|^4_{0,4;e}\ \leq\ C\Big\{ & \|\mathbf{u}-\mathbf{u}_h\|^4_{0,4;T_e}+h^2_{T_e}\|\boldsymbol{\sigma}-\boldsymbol{\sigma}_h\|^4_{0,T_e}+h^2_{T_e}\|\mathbf{u}\otimes\mathbf{u}-\mathbf{u}_h\otimes\mathbf{u}_h\|^4_{0,T_e} \\ & + h^2_{T_e}\left\|(\mathbf{u}-\mathbf{u}_h)\cdot\frac{\nabla\rho}{\rho}\right\|^4_{0,T_e}+h^4_{T_e}\,\|\nabla\mathbf{u}_h-\mathbf{M}(\boldsymbol{\sigma}_h,\mathbf{u}_h,\rho)\|^4_{0,4;T_e}\Big\}. \end{aligned} \tag{5.38}$$

Finally, the last term in (5.38) is controlled by (5.27), yielding (5.35) and completing the proof. □

The bounds for the terms defining $\Theta_{2,T}$ (cf. (5.3)) are stated next.

Lemma 5.8 *Let* $\mathbf{M}$ *be defined by* (5.10)*, and assume that* ρ*, and hence* $\nabla\rho$*, are piecewise polynomial functions. Then, there exist positive constants* $\mathcal{C}_8$ *and* $\mathcal{C}_9$*, independent of* h*, such that*

$$h_T^2 \, \|\underline{\mathbf{curl}}\,(\mathbf{M}(\boldsymbol{\sigma}_h,\mathbf{u}_h,\rho))\|_{0,T}^2 \\ \leq \mathcal{C}_8 \left\{ \|\boldsymbol{\sigma}-\boldsymbol{\sigma}_h\|_{0,T}^2 + \|\mathbf{u}\otimes\mathbf{u}-\mathbf{u}_h\otimes\mathbf{u}_h\|_{0,T}^2 + \left\|(\mathbf{u}-\mathbf{u}_h)\cdot\frac{\nabla\rho}{\rho}\right\|_{0,T}^2 \right\}, \tag{5.39}$$

for all $T\in\mathcal{T}_h$ *and*

$$h_e \, \|[\![\boldsymbol{\delta}_*\,(\mathbf{M}(\boldsymbol{\sigma}_h,\mathbf{u}_h,\rho))]\!]\|_{0,e}^2 \\ \leq \mathcal{C}_9 \left\{ \|\boldsymbol{\sigma}-\boldsymbol{\sigma}_h\|_{0,\omega_e}^2 + \|\mathbf{u}\otimes\mathbf{u}-\mathbf{u}_h\otimes\mathbf{u}_h\|_{0,\omega_e}^2 + \left\|(\mathbf{u}-\mathbf{u}_h)\cdot\frac{\nabla\rho}{\rho}\right\|_{0,\omega_e}^2 \right\}, \tag{5.40}$$

for all $e\in\mathcal{E}_h(\Omega)$*, where* ω_e *denotes the union of the two elements of* $\mathcal{T}_h$ *sharing the edge/face* e*. Additionally, if* $\mathbf{u}_{\mathrm{D}}$ *is piecewise polynomial, there exists* $\mathcal{C}_{10}>0$*, independent on* h*, such that*

$$h_e \left\|\boldsymbol{\delta}_*\big(\nabla\mathbf{u}_{\mathrm{D}}\big)-\boldsymbol{\delta}_*\,(\mathbf{M}(\boldsymbol{\sigma}_h,\mathbf{u}_h,\rho))\right\|_{0,e}^2 \\ \leq \mathcal{C}_{10} \left\{ \|\boldsymbol{\sigma}-\boldsymbol{\sigma}_h\|_{0,T_e}^2 + \|\mathbf{u}\otimes\mathbf{u}-\mathbf{u}_h\otimes\mathbf{u}_h\|_{0,T_e}^2 + \left\|(\mathbf{u}-\mathbf{u}_h)\cdot\frac{\nabla\rho}{\rho}\right\|_{0,T_e}^2 \right\} \tag{5.41}$$

for all $e\in\mathcal{E}_h(\Gamma)$*, where* T_e *is the element to which the boundary edge/face* e *belongs.*

Proof. The proof of (5.39)–(5.40) follows from a slight adaptation of [30, Lemma 4.11], taking into account that, by the definition of $\mathbf{M}$ (cf. (5.10)),

$$\underline{\mathbf{curl}}\,(\mathbf{M}(\boldsymbol{\sigma},\mathbf{u},\rho)) = \underline{\mathbf{curl}}\left(\frac{1}{\mu}\left(\boldsymbol{\sigma}+\mathbf{u}\otimes\mathbf{u}\right)^{\mathtt{d}} - \frac{1}{d}\left(\mathbf{u}\cdot\frac{\nabla\rho}{\rho}\right)\mathbb{I}\right) = \underline{\mathbf{curl}}\,(\nabla\mathbf{u}) = \mathbf{0} \quad \text{in} \quad \Omega\,,$$

together with an application of the Cauchy–Schwarz inequality. On the other hand, estimate (5.41) follows from a slight modification of [30, Lemma 4.15]. □

In order to complete the global efficiency estimate of Θ (cf. (5.1)) it remains to bound the terms

$$\left\|(\boldsymbol{\sigma}-\boldsymbol{\sigma}_h)^{\mathtt{d}}\frac{\nabla\rho}{\rho}\right\|_{0,4/3;T}^{4/3}, \quad \left\|(\mathbf{u}\otimes\mathbf{u}-\mathbf{u}_h\otimes\mathbf{u}_h)\frac{\nabla\rho}{\rho}\right\|_{0,4/3;T}^{4/3}, \quad \big\||\mathbf{u}|^{m-2}\mathbf{u}-|\mathbf{u}_h|^{m-2}\mathbf{u}_h\big\|_{0,4/3;T}^{4/3},$$

$$\big\|\mathbf{u}\otimes\mathbf{u}-\mathbf{u}_h\otimes\mathbf{u}_h\big\|_{0,T_e}^{j}, \quad \left\|(\mathbf{u}-\mathbf{u}_h)\cdot\frac{\nabla\rho}{\rho}\right\|_{0,T}^{j}, \quad j\in\{2,4\}, \quad \text{and} \quad \left\|\left((\mathbf{u}-\mathbf{u}_h)\cdot\frac{\nabla\rho}{\rho}\right)\frac{\nabla\rho}{\rho}\right\|_{0,4/3;T}^{4/3},$$

which appear in the upper bounds established in Lemmas 5.5, 5.6, 5.7, and 5.8. To this end, for the third and fourth term, we follow the arguments in [14, eqs. (3.37)–(3.39)]. For the sake of completeness, however, we reproduce the corresponding estimates below. Indeed, invoking (3.17) with $p=m$, together with the Hölder inequality with exponents $r=3/2$ and $s=3$ (so that $1/r+1/s=1$), and performing straightforward algebraic manipulations, we obtain

$$\big\||\mathbf{u}|^{m-2}\mathbf{u}-|\mathbf{u}_h|^{m-2}\mathbf{u}_h\big\|_{0,4/3;T}^{4/3} \leq \widetilde{c}_m\left(\|\mathbf{u}\|_{0,2(m-2);T}^{4(m-2)/3}+\|\mathbf{u}_h\|_{0,2(m-2);T}^{4(m-2)/3}\right)\|\mathbf{u}-\mathbf{u}_h\|_{0,4;T}^{4/3},$$

where $\widetilde{c}_m$ is a positive constant depending only on m. Summing over $T \in \mathcal{T}_h$ and applying Hölder's inequality once again, we arrive at

$$\begin{aligned}&\sum_{T\in\mathcal{T}_h} \left\| |\mathbf{u}|^{m-2}\mathbf{u} - |\mathbf{u}_h|^{m-2}\mathbf{u}_h \right\|_{0,4/3;T}^{4/3} \\ &\quad \leq \widetilde{c}_m \left(\sum_{T\in\mathcal{T}_h} \left(\|\mathbf{u}\|_{0,2(m-2);T}^{4(m-2)/3} + \|\mathbf{u}_h\|_{0,2(m-2);T}^{4(m-2)/3} \right)^{3/2} \right)^{2/3} \left(\sum_{T\in\mathcal{T}_h} \|\mathbf{u}-\mathbf{u}_h\|_{0,4;T}^4 \right)^{1/3} .\end{aligned} \tag{5.42}$$

Next, using the subadditivity of the exponent $3/2$ in (5.42) and recalling that $2(m-2) \in [2,4]$, we apply the continuous embedding $\mathbf{L}^4(\Omega) \hookrightarrow \mathbf{L}^{2(m-2)}(\Omega)$. Since $\mathbf{u} \in \mathbf{W}_r$ and $\mathbf{u}_h \in \mathbf{W}_{r,\mathtt{d}}$, the corresponding $\mathbf{L}^4$-norms are uniformly bounded. Hence, the first factor in (5.42) is bounded independently of h, and there exists $C > 0$, independent of h, such that

$$\sum_{T\in\mathcal{T}_h} \left\| |\mathbf{u}|^{m-2}\mathbf{u} - |\mathbf{u}_h|^{m-2}\mathbf{u}_h \right\|_{0,4/3;T}^{4/3} \leq C \, \|\mathbf{u}-\mathbf{u}_h\|_{0,4;\Omega}^{4/3} . \tag{5.43}$$

In turn, adding and subtracting the intermediate term $\mathbf{u} \otimes \mathbf{u}_h$ (and analogously $\mathbf{u}_h \otimes \mathbf{u}$), and applying the Cauchy–Schwarz inequality, we obtain

$$\|\mathbf{u}\otimes\mathbf{u} - \mathbf{u}_h\otimes\mathbf{u}_h\|_{0,T} \leq (\|\mathbf{u}\|_{0,4;T} + \|\mathbf{u}_h\|_{0,4;T}) \, \|\mathbf{u}-\mathbf{u}_h\|_{0,4;T} . \tag{5.44}$$

Proceeding as in (5.43), and recalling that $\mathbf{u} \in \mathbf{W}_r$ and $\mathbf{u}_h \in \mathbf{W}_{r,\mathtt{d}}$, so that their $\mathbf{L}^4$-norms are uniformly bounded, we infer that there exists a positive constant C, independent of h, such that

$$\sum_{T\in\mathcal{T}_h} \|\mathbf{u}\otimes\mathbf{u} - \mathbf{u}_h\otimes\mathbf{u}_h\|_{0,T}^4 \leq C \, \|\mathbf{u}-\mathbf{u}_h\|_{0,4;\Omega}^4 . \tag{5.45}$$

The case of (5.45) with exponent $j = 2$ is analogous. Finally, to estimate the remaining terms, we employ the appropriate Hölder inequality to obtain

$$\begin{aligned}&\sum_{T\in\mathcal{T}_h} \left\| (\boldsymbol{\sigma}-\boldsymbol{\sigma}_h)^{\mathtt{d}} \frac{\nabla\rho}{\rho} \right\|_{0,4/3;T}^{4/3} = \left\| (\boldsymbol{\sigma}-\boldsymbol{\sigma}_h)^{\mathtt{d}} \frac{\nabla\rho}{\rho} \right\|_{0,4/3;\Omega}^{4/3} \leq \|\boldsymbol{\sigma}-\boldsymbol{\sigma}_h\|_{0,\Omega}^{4/3} \left\| \frac{\nabla\rho}{\rho} \right\|_{0,4;\Omega}^{4/3} , \\ &\sum_{T\in\mathcal{T}_h} \left\| (\mathbf{u}\otimes\mathbf{u} - \mathbf{u}_h\otimes\mathbf{u}_h) \frac{\nabla\rho}{\rho} \right\|_{0,4/3;T}^{4/3} \leq \|\mathbf{u}\otimes\mathbf{u} - \mathbf{u}_h\otimes\mathbf{u}_h\|_{0,\Omega}^{4/3} \left\| \frac{\nabla\rho}{\rho} \right\|_{0,4;\Omega}^{4/3} , \\ &\sum_{T\in\mathcal{T}_h} \left\| \left((\mathbf{u}-\mathbf{u}_h)\cdot\frac{\nabla\rho}{\rho} \right) \frac{\nabla\rho}{\rho} \right\|_{0,4/3;T}^{4/3} \leq \|\mathbf{u}-\mathbf{u}_h\|_{0,4;\Omega}^{4/3} \left\| \frac{\nabla\rho}{\rho} \right\|_{0,4;\Omega}^{8/3} , \\ &\sum_{T\in\mathcal{T}_h} \left\| (\mathbf{u}-\mathbf{u}_h)\cdot\frac{\nabla\rho}{\rho} \right\|_{0,T}^{4} \leq \left(\sum_{T\in\mathcal{T}_h} \left\| (\mathbf{u}-\mathbf{u}_h)\cdot\frac{\nabla\rho}{\rho} \right\|_{0,T}^{2} \right)^2 \leq \|\mathbf{u}-\mathbf{u}_h\|_{0,4;\Omega}^4 \left\| \frac{\nabla\rho}{\rho} \right\|_{0,4;\Omega}^{4} .\end{aligned} \tag{5.46}$$

The last estimate with exponent $j = 2$ is analogous. The foregoing local estimates allow us to establish the main efficiency result of this section.

Theorem 5.9 *Assume that $\mathbf{u}_{\mathrm{D}}$, ρ, and hence $\nabla\rho$, are piecewise polynomial functions. Then, there exists a positive constant $\mathcal{C}_{\mathtt{eff}}$, independent of h, such that*

$$\mathcal{C}_{\mathtt{eff}}\Theta + \mathtt{h.o.t.} \leq \|(\boldsymbol{\sigma},\mathbf{u}) - (\boldsymbol{\sigma}_h,\mathbf{u}_h)\|_{\mathbf{X}} , \tag{5.47}$$

where `h.o.t.` *stands for one or several terms of higher order.*

Proof. The estimate (5.47) follows by combining the local lower bounds established in Lemmas 5.5–5.8 with the auxiliary estimates (5.43)–(5.46), together with the porosity bound established in (4.15). □

6 Numerical results

This section illustrates the performance and accuracy of the proposed mixed finite element scheme (4.2) (see also (4.3)), as well as the reliability and efficiency of the *a posteriori* error estimator Θ (cf. (5.1)) in both two and three dimensions. In what follows, the corresponding finite element subspaces generated by $k = 0$ and $k = 1$ are denoted by $\mathbb{RT}_0$–$\mathbf{P}_0$ and $\mathbb{RT}_1$–$\mathbf{P}_1$, respectively. The implementation is based on a `FreeFEM` code [35]. Regarding the Newton iterative method associated with (4.2), the iterations are terminated when the relative error between the coefficient vectors of two consecutive iterates, say $\mathbf{coeff}^m$ and $\mathbf{coeff}^{m+1}$, is sufficiently small, that is,

$$\frac{\|\mathbf{coeff}^{m+1} - \mathbf{coeff}^m\|_{\mathtt{DOF}}}{\|\mathbf{coeff}^{m+1}\|_{\mathtt{DOF}}} \leq \mathtt{tol}\,,$$

where $\|\cdot\|_{\mathtt{DOF}}$ denotes the standard Euclidean norm in $\mathrm{R}^{\mathtt{DOF}}$, with `DOF` representing the total number of degrees of freedom associated with the finite element subspaces $\mathbb{H}_h^{\boldsymbol{\sigma}}$ and $\mathbf{H}_h^{\mathbf{u}}$ defined in Section 4.4. Throughout the experiments, the tolerance is fixed as $\mathtt{tol} = \mathtt{1e-06}$.

The individual errors are defined as

$$\mathrm{e}(\boldsymbol{\sigma}) := \|\boldsymbol{\sigma} - \boldsymbol{\sigma}_h\|_{\mathbf{div}_{4/3};\Omega}, \qquad \mathrm{e}(\mathbf{u}) := \|\mathbf{u} - \mathbf{u}_h\|_{0,4;\Omega}, \qquad \mathrm{e}(p) := \|p - p_h\|_{0,\Omega},$$

$$\mathrm{e}(\mathbf{G}) := \|\mathbf{G} - \mathbf{G}_h\|_{0,\Omega}, \qquad \mathrm{e}(\boldsymbol{\omega}) := \|\boldsymbol{\omega} - \boldsymbol{\omega}_h\|_{0,\Omega}, \qquad \mathrm{e}(\widetilde{\boldsymbol{\sigma}}) := \|\widetilde{\boldsymbol{\sigma}} - \widetilde{\boldsymbol{\sigma}}_h\|_{0,\Omega}.$$

Here, the pressure p, the velocity gradient $\mathbf{G}$, the vorticity $\boldsymbol{\omega}$, and the shear stress tensor $\widetilde{\boldsymbol{\sigma}}$ are additional quantities of physical interest, which are recovered through the corresponding postprocessing formulas yielding p_h, $\mathbf{G}_h$, $\boldsymbol{\omega}_h$, and $\widetilde{\boldsymbol{\sigma}}_h$ (see Appendix A for details). The global error and the associated effectivity index for the estimator Θ are defined, respectively, by

$$\mathrm{e}(\boldsymbol{\sigma}, \mathbf{u}) := \mathrm{e}(\boldsymbol{\sigma}) + \mathrm{e}(\mathbf{u}) \quad \text{and} \quad \mathtt{eff}(\Theta) := \frac{\mathrm{e}(\boldsymbol{\sigma}, \mathbf{u})}{\Theta}\,.$$

Moreover, using the fact that $\mathtt{DOF}^{-1/d} \cong h$, the respective experimental rates of convergence are computed as

$$r(\star) := -d\,\frac{\log(\mathrm{e}(\star)/\mathrm{e}'(\star))}{\log(\mathtt{DOF}/\mathtt{DOF}')} \qquad \text{for each } \star \in \{\boldsymbol{\sigma}, \mathbf{u}, (\boldsymbol{\sigma}, \mathbf{u}), p, \mathbf{G}, \boldsymbol{\omega}, \widetilde{\boldsymbol{\sigma}}\}\,,$$

where `DOF` and `DOF'` denote the total degrees of freedom associated to two consecutive triangulations with errors $\mathrm{e}(\star)$ and $\mathrm{e}'(\star)$, respectively.

The examples considered in this section are introduced below. In all cases, we take $\mu = 1$, except in Example 4, where we set $\mu = 0.01$. The Darcy and Forchheimer coefficients `D` and `F` are defined as in [19, eq. (44)], namely,

$$\mathtt{D}(\rho) = 150\left(\frac{1-\rho}{\rho}\right)^2 \quad \text{and} \quad \mathtt{F}(\rho) = 1.75\,\frac{1-\rho}{\rho}\,.$$

The null mean value of $\mathrm{tr}(\boldsymbol{\sigma}_h)$ over Ω is enforced by means of a real Lagrange multiplier.

Example 1 is used to verify the theoretical rates of convergence and to corroborate the reliability and efficiency of the *a posteriori* error estimator Θ. In turn, Examples 2–4 illustrate the behavior of the associated adaptive algorithm in two and three dimensions, both with and without manufactured solutions. The adaptive procedure follows the standard strategy proposed in [44]:

(1) Start with a coarse mesh $\mathcal{T}_h$.

(2) Solve the Newton iterative method associated to (4.2) for the current mesh $\mathcal{T}_h$.

(3) Compute the local indicator Θ_T for each $T \in \mathcal{T}_h$, where

$$\Theta_T := \Theta_{1,T} + \Theta_{2,T} + \Theta_{3,T} \quad \text{(cf. (5.2), (5.3), (5.4))}\,.$$

(4) Check the stopping criterion and decide whether to finish or go to next step.

(5) Use the automatic meshing algorithm adaptmesh from [36, Section 9.1.9] to refine each $T' \in \mathcal{T}_h$ satisfying:

$$\Theta_{T'} \geq C_{\texttt{adm}} \frac{1}{\#T} \sum_{T \in \mathcal{T}_h} \Theta_T\,, \quad \text{for some } C_{\texttt{adm}} \in (0,1)\,,$$

where $\#T$ denotes the number of triangles of the mesh $\mathcal{T}_h$.

(6) Define the resulting mesh as the current mesh $\mathcal{T}_h$, and go to step (2).

In particular, $C_{\texttt{adm}}$ is chosen as 0.8 for Examples 2 and 3, while for Example 4 we consider 0.7.

Example 1: Numerical accuracy using a smooth solution on a square domain

We first validate the convergence rates and study the performance of the numerical method (4.2) in a two-dimensional domain. In particular, we analyze the behavior of the *a posteriori* error estimator through the effectivity index $\texttt{eff}(\Theta)$ under a quasi-uniform refinement strategy. We consider the square domain $\Omega = (0,1)^2$, the parameter $m = 4$, and the porosity ρ is considered as follow

$$\rho(x_1, x_2) = 0.45 + 0.55\, \exp(x_2 - 1)\,, \tag{6.1}$$

The data in (2.11) are then chosen so that the exact solution is given by the smooth functions

$$\mathbf{u}(x_1, x_2) = \frac{1}{\rho(x_1, x_2)} \begin{pmatrix} \sin(\pi x_1)\cos(\pi x_2) \\ -\cos(\pi x_1)\sin(\pi x_2) \end{pmatrix} \quad \text{and} \quad p(x_1, x_2) = \cos(\pi x_1)\sin\Big(\frac{\pi}{2} x_2\Big)\,.$$

Tables 6.1 and 6.2 display the convergence history for a sequence of quasi-uniform mesh refinements, including the average number of Newton iterations. We observe that the method is able not only to approximate the original unknowns but also the pressure field, the velocity gradient tensor, the vorticity, and the shear stress tensor through the postprocessing formula (A.2). The results illustrate that the optimal rates of convergence $\mathcal{O}(h^{k+1})$ established in Theorem 4.6 and Lemma A.1 are attained for $k = 0, 1$. In addition, the global *a posteriori* error indicator Θ and its corresponding effectivity index are also reported, showing that the latter remains uniformly bounded.

Example 2: Adaptivity in a 2D horseshoe-shaped domain

The second example is aimed at assessing the performance of the adaptive mesh refinement strategy driven by the *a posteriori* error estimator Θ (cf. (5.1)). We consider the two-dimensional horseshoe-shaped domain $\Omega := (-1,1) \times (-0.5, 1.25) \setminus (-0.75, 0.75) \times (0.25, 1.25)$, and parameter $m = 3.5$. In turn, ρ is given by (6.1). The data $\mathbf{f}$ and $\mathbf{u}_{\mathrm{D}}$ are chosen so that the exact solution is given by

$$\mathbf{u}(x_1, x_2) = \frac{1}{\rho(x_1, x_2)} \begin{pmatrix} \sin(\pi x_1)\cos(\pi x_2) \\ -\cos(\pi x_1)\sin(\pi x_2) \end{pmatrix},$$

$$p(x_1, x_2) = \frac{x_2 - 0.27}{(x_1 + 0.73)^2 + (x_2 - 0.27)^2} - \frac{x_1 - 0.73}{(x_1 - 0.73)^2 + (x_2 - 0.27)^2} - p_0\,,$$

DOF	h	iter	e($\boldsymbol{\sigma}$)	$r(\boldsymbol{\sigma})$	e($\mathbf{u}$)	$r(\mathbf{u})$	e(p)	$r(p)$	e($\mathbf{G}$)	$r(\mathbf{G})$
196	0.373	4	5.99e+00	–	3.25e-01	–	5.38e-01	–	9.36e-01	–
792	0.196	4	2.59e+00	1.31	1.43e-01	1.29	2.12e-01	1.46	4.45e-01	1.16
3074	0.097	4	1.30e+00	0.98	7.19e-02	0.97	9.75e-02	1.10	2.26e-01	0.96
12188	0.048	4	6.28e-01	1.02	3.43e-02	1.05	4.47e-02	1.10	1.13e-01	0.98
48786	0.026	4	3.15e-01	1.12	1.74e-02	1.11	2.24e-02	1.12	5.64e-02	1.13
196272	0.014	4	1.57e-01	1.19	8.66e-03	1.19	1.11e-02	1.20	2.80e-02	1.20

e($\boldsymbol{\omega}$)	$r(\boldsymbol{\omega})$	e($\widetilde{\boldsymbol{\sigma}}$)	$r(\widetilde{\boldsymbol{\sigma}})$	e($\boldsymbol{\sigma}, \mathbf{u}$)	$r(\boldsymbol{\sigma}, \mathbf{u})$	Θ	eff(Θ)
5.07e-01	–	1.74e+00	–	6.31e+00	–	1.59e+01	0.396
2.50e-01	1.11	7.94e-01	1.23	2.73e+00	1.20	7.33e+00	0.373
1.32e-01	0.91	3.92e-01	1.00	1.37e+00	1.02	3.72e+00	0.368
6.76e-02	0.94	1.91e-01	1.02	6.63e-01	1.05	1.84e+00	0.361
3.36e-02	1.13	9.57e-02	1.12	3.32e-01	1.00	9.18e-01	0.362
1.67e-02	1.20	4.76e-02	1.20	1.66e-01	1.00	4.58e-01	0.361

Table 6.1: [Example 1] $\mathbb{RT}_0 - \mathbf{P}_0$ scheme with quasi-uniform refinement.

DOF	h	iter	e($\boldsymbol{\sigma}$)	$r(\boldsymbol{\sigma})$	e($\mathbf{u}$)	$r(\mathbf{u})$	e(p)	$r(p)$	e($\mathbf{G}$)	$r(\mathbf{G})$
608	0.373	4	7.72e-01	–	3.49e-02	–	8.22e-02	–	1.34e-01	–
2496	0.196	4	1.72e-01	2.34	9.01e-03	2.12	1.47e-02	2.69	2.54e-02	2.60
9760	0.097	4	4.41e-02	1.93	2.25e-03	1.97	3.51e-03	2.02	6.57e-03	1.92
38848	0.048	4	1.08e-02	1.99	5.57e-04	1.97	8.15e-04	2.07	1.53e-03	2.06
155808	0.026	4	2.71e-03	2.25	1.40e-04	2.24	2.05e-04	2.24	3.90e-04	2.22

e($\boldsymbol{\omega}$)	$r(\boldsymbol{\omega})$	e($\widetilde{\boldsymbol{\sigma}}$)	$r(\widetilde{\boldsymbol{\sigma}})$	e($\boldsymbol{\sigma}, \mathbf{u}$)	$r(\boldsymbol{\sigma}, \mathbf{u})$	Θ	eff(Θ)
7.25e-02	–	2.54e-01	–	8.07e-01	–	2.64e+00	0.306
1.29e-02	2.69	4.84e-02	2.59	1.81e-01	2.11	6.22e-01	0.292
3.32e-03	1.93	1.24e-02	1.93	4.63e-02	2.00	1.57e-01	0.294
7.61e-04	2.08	2.90e-03	2.05	1.13e-02	2.04	3.80e-02	0.299
1.93e-04	2.23	7.36e-04	2.23	2.85e-03	1.99	9.60e-03	0.296

Table 6.2: [Example 1] $\mathbb{RT}_1 - \mathbf{P}_1$ scheme with quasi-uniform refinement.

where $p_0 \in \mathrm{R}$ is a constant chosen in such a way $\int_\Omega p = 0$. Notice that the pressure exhibits high gradients near vertex $(-0.75, 0.25)$ and $(0.75, 0.25)$.

Tables 6.3 and 6.4, together with Figure 6.1, summarize the convergence history of the method applied to a sequence of quasi-uniform and adaptively refined triangulations of the domain. Suboptimal rates are observed in the first case, whereas adaptive refinement driven by the *a posteriori* error indicator Θ yields optimal convergence and stable effectivity indices. Notice how the adaptive algorithms improve the efficiency of the method by delivering accurate solutions at a lower computational cost. In particular, it is possible to obtain a better approximation (in terms of e($\boldsymbol{\sigma}, \mathbf{u}$)) using only about 10% and 6% of the degrees of freedom of the last quasi-uniform mesh for the cases $k = 0$ and $k = 1$, respectively. Furthermore, the initial mesh and the approximate solutions obtained with the adaptive $\mathbb{RT}_1 - \mathbf{P}_1$ scheme using $560,530$ degrees of freedom, and 34,931 triangles are shown in Figure 6.2. We observe there that the pressure exhibits large gradients in the contraction regions. In turn, examples of some adapted meshes for $k = 0$ and $k = 1$ are displayed in Figure 6.3. A clear clustering of elements near the corner regions of the two-dimensional horseshoe-shaped domain can be observed, as expected.

$\mathbb{RT}_0 - \mathbf{P}_0$ scheme with quasi-uniform refinement										
DoF	h	it	e($\boldsymbol{\sigma}$)	$r(\boldsymbol{\sigma})$	e($\mathbf{u}$)	$r(\mathbf{u})$	e($\boldsymbol{\sigma}, \mathbf{u}$)	$r(\boldsymbol{\sigma}, \mathbf{u})$	Θ	eff(Θ)
368	0.373	4	3.67e+01	–	3.99e-01	–	3.71e+01	–	6.53e+01	0.568
1436	0.187	4	3.13e+01	0.234	2.01e-01	1.007	3.15e+01	0.241	4.41e+01	0.714
5582	0.099	4	2.26e+01	0.477	1.02e-01	1.003	2.27e+01	0.479	2.92e+01	0.779
23214	0.061	4	1.31e+01	0.766	4.97e-02	1.004	1.32e+01	0.767	1.66e+01	0.794
89528	0.026	3	7.28e+00	0.873	2.50e-02	1.019	7.30e+00	0.873	9.28e+00	0.787
362546	0.014	3	3.63e+00	0.994	1.24e-02	0.998	3.64e+00	0.994	4.72e+00	0.772

$\mathbb{RT}_0 - \mathbf{P}_0$ scheme with adaptive refinement									
DoF	it	e($\boldsymbol{\sigma}$)	$r(\boldsymbol{\sigma})$	e($\mathbf{u}$)	$r(\mathbf{u})$	e($\boldsymbol{\sigma}, \mathbf{u}$)	$r(\boldsymbol{\sigma}, \mathbf{u})$	Θ	eff(Θ)
368	4	3.67e+01	–	3.99e-01	–	3.71e+01	–	6.53e+01	0.568
804	4	3.19e+01	0.359	2.91e-01	0.810	3.22e+01	0.364	5.15e+01	0.625
1588	4	2.16e+01	1.144	1.97e-01	1.151	2.18e+01	1.144	3.62e+01	0.602
2802	4	1.30e+01	1.782	1.58e-01	0.761	1.32e+01	1.771	2.44e+01	0.541
4648	4	9.60e+00	1.207	1.27e-01	0.867	9.73e+00	1.202	1.88e+01	0.517
8316	4	7.30e+00	0.942	9.47e-02	1.013	7.39e+00	0.943	1.42e+01	0.522
13664	4	5.30e+00	1.286	7.77e-02	0.797	5.38e+00	1.279	1.12e+01	0.481
21872	4	4.33e+00	0.858	6.06e-02	1.055	4.39e+00	0.861	8.87e+00	0.495
34886	4	3.37e+00	1.074	4.98e-02	0.846	3.42e+00	1.070	7.12e+00	0.481
54508	3	2.67e+00	1.046	4.14e-02	0.826	2.71e+00	1.043	5.74e+00	0.472
85848	3	2.15e+00	0.956	3.36e-02	0.921	2.18e+00	1.000	4.62e+00	0.473
132304	3	1.73e+00	1.001	2.74e-02	0.936	1.76e+00	1.044	3.75e+00	0.469
204442	3	1.38e+00	1.046	2.24e-02	0.927	1.40e+00	1.044	3.02e+00	0.465
316546	3	1.12e+00	0.970	1.84e-02	0.896	1.13e+00	0.968	2.45e+00	0.463

Table 6.3: [Example 2] Comparison of the $\mathbb{RT}_0 - \mathbf{P}_0$ mixed approximation with quasi-uniform and adaptive refinements.

Example 3: Adaptivity in a 3D L-shaped domain

Here we consider the three-dimensional L-shaped domain $\Omega := (-0.5, 0.5)\times(0, 0.5)\times(-0.5, 0.5)\setminus(0, 0.5)^3$, parameter $m = 3$, and define the porosity function ρ by

$$\rho(x_1, x_2, x_3) = 0.45 + 0.55\, \exp(2 - x_2 - x_3)\,.$$

The manufactured solution is given by

$$\mathbf{u}(x_1, x_2, x_3) = \frac{1}{\rho(x_1, x_2, x_3)} \begin{pmatrix} \sin(\pi x_1)\cos(\pi x_2)\cos(\pi x_3) \\ -2\cos(\pi x_1)\sin(\pi x_2)\cos(\pi x_3) \\ \cos(\pi x_1)\cos(\pi x_2)\sin(\pi x_3) \end{pmatrix},$$
$$p(x_1, x_2, x_3) = \frac{10\, x_3}{(x_1 - 0.02)^2 + (x_3 - 0.02)^2} - p_0\,,$$

where $p_0 \in \mathrm{R}$ is a constant chosen so that $\int_\Omega p = 0$.

Table 6.5 confirms a disturbed convergence under quasi-uniform refinement and optimal convergence rates when adaptive refinement driven by the *a posteriori* error estimator Θ is employed. Furthermore, the initial mesh and the approximate solutions obtained with the adaptive $\mathbb{RT}_0$–$\mathbf{P}_0$ scheme (guided by Θ), with 867,321 degrees of freedom and 94,802 tetrahedra, are shown in Figure 6.4. In turn,

$\mathbb{RT}_1 - \mathbf{P}_1$ scheme with quasi-uniform refinement										
DoF	h	it	e($\boldsymbol{\sigma}$)	$r(\boldsymbol{\sigma})$	e($\mathbf{u}$)	$r(\mathbf{u})$	e($\boldsymbol{\sigma}, \mathbf{u}$)	$r(\boldsymbol{\sigma}, \mathbf{u})$	Θ	eff(Θ)
1132	0.373	4	2.32e+01	–	7.35e-02	–	2.32e+01	–	3.16e+01	0.735
4504	0.187	4	1.99e+01	0.223	2.79e-02	1.401	1.99e+01	0.225	2.43e+01	0.818
17680	0.099	4	1.26e+01	0.664	9.73e-03	1.542	1.26e+01	0.665	1.47e+01	0.860
73920	0.061	4	4.53e+00	1.433	2.32e-03	2.007	4.53e+00	1.433	5.33e+00	0.850
285760	0.026	3	1.49e+00	1.648	4.95e-04	2.281	1.49e+00	1.648	1.80e+00	0.825
1158688	0.014	3	3.80e-01	1.947	7.81e-05	2.638	3.81e-01	1.947	4.69e-01	0.812

$\mathbb{RT}_1 - \mathbf{P}_1$ scheme with adaptive refinement									
DoF	it	e($\boldsymbol{\sigma}$)	$r(\boldsymbol{\sigma})$	e($\mathbf{u}$)	$r(\mathbf{u})$	e($\boldsymbol{\sigma}, \mathbf{u}$)	$r(\boldsymbol{\sigma}, \mathbf{u})$	Θ	eff(Θ)
1132	4	2.32e+01	–	7.35e-02	–	2.32e+01	–	3.16e+01	0.735
2764	4	1.67e+01	0.735	4.45e-02	1.124	1.67e+01	0.736	2.18e+01	0.769
5574	4	5.24e+00	3.301	1.62e-02	2.882	5.26e+00	3.300	7.12e+00	0.739
9420	4	1.51e+00	4.745	1.22e-02	1.094	1.52e+00	4.726	2.81e+00	0.541
17806	4	8.75e-01	1.714	6.60e-03	1.918	8.81e-01	1.716	1.45e+00	0.608
30320	4	4.60e-01	2.415	3.88e-03	1.994	4.64e-01	2.411	8.71e-01	0.533
52500	4	2.84e-01	1.762	2.50e-03	1.598	2.86e-01	1.761	5.12e-01	0.559
94184	4	1.53e-01	2.103	1.35e-03	2.110	1.55e-01	2.103	2.87e-01	0.539
166770	3	8.57e-02	2.038	7.83e-04	1.910	8.65e-02	2.037	1.60e-01	0.539
304330	3	4.86e-02	1.887	4.21e-04	2.062	4.90e-02	1.888	8.91e-02	0.550
560530	3	2.53e-02	2.132	2.41e-04	1.832	2.56e-02	2.129	4.80e-02	0.533

Table 6.4: [Example 2] Comparison of the $\mathbb{RT}_1 - \mathbf{P}_1$ mixed approximation with quasi-uniform and adaptive refinements for the stationary convective Brinkman–Forchheimer model with variable porosity.

snapshots of three meshes generated through the adaptive strategy are displayed in Figure 6.5, where a clear clustering of elements around the contraction region can be observed.

Example 4: Flow through a non-convex channel with localized low permeability

We focus on studying the behavior of the adaptive scheme in the presence of both geometric and material heterogeneities. We consider the non-convex domain $\Omega := (0, 2.5) \times (0, 0.3) \setminus \big([0.6, 0.8] \times [0, 0.2]\big)$, with boundaries $\partial\Omega = \Gamma_{in} \cup \Gamma_{out} \cup \Gamma_{top} \cup \Gamma_{bottom} \cup \Gamma_{cav}$, as detailed in Figure 6.6. The boundary conditions are prescribed as follows:

$$\mathbf{u} = \begin{cases} \big(10\, x_2(0.3 - x_2),\, 0\big)^{\mathrm{t}} & \text{on } \Gamma_{\text{left}} \cup \Gamma_{\text{right}}\,, \\ \mathbf{0} & \text{on } \partial\Omega \setminus (\Gamma_{\text{left}} \cup \Gamma_{\text{right}})\,. \end{cases}$$

In other words, we impose a horizontal parabolic velocity profile on the left and right boundaries, and homogeneous Dirichlet conditions on the rest of the boundary. We consider $m = 3$ and the porosity is modeled according to

$$\rho(x_1, x_2) = \widetilde{\rho}(x_1, x_2) + \big(1 - \widetilde{\rho}(x_1, x_2)\big) \exp(x_2 - 1)\,,$$

where

$$\widetilde{\rho}(x_1, x_2) = 0.65 - \exp(-50(x_1 - 1.2)^2 - 50(x_2 - 0.25)^2) - 0.9 \exp(-70(x_1 - 1.85)^2 - 20(x_2 - 0.10)^2).$$

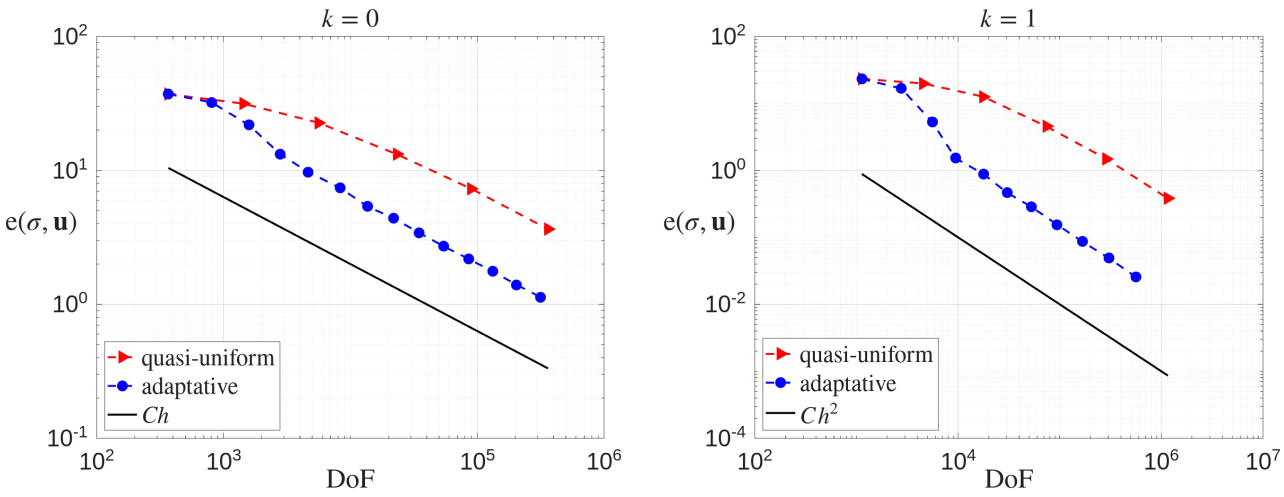

Figure 6.1: [Example 2] Log–log plots of $e(\boldsymbol{\sigma}, \mathbf{u})$ versus DOF for quasi-uniform and adaptive refinements with $k = 0$ and $k = 1$ (left and right plots, respectively).

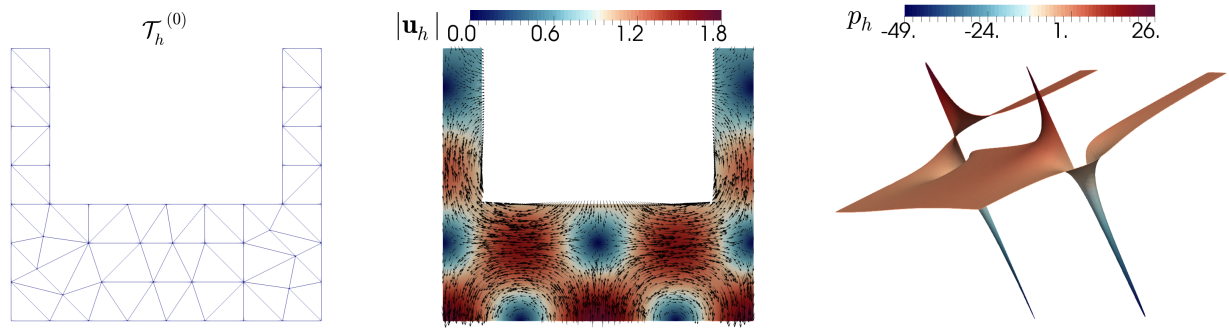

Figure 6.2: [Example 2]: Initial mesh, computed magnitude of the velocity, and pressure field.

Thus, ρ consists of a smooth background profile together with two localized depressions placed downstream of the cavity, which generate two regions of reduced effective permeability, as illustrated in the top panel of Figure 6.7.

In Table 6.6 we report the experimental convergence rate of the global estimator Θ (cf. (5.1)) for seven adapted meshes. Although the effectivity index cannot be computed for this example, the optimal convergence rate of Θ illustrates the reliability and efficiency of the estimator, as well as the accuracy of the proposed approximation in handling the varying porosity. In Figure 6.7 we display the porosity, the computed velocity magnitude, and the pressure, obtained using the $\mathbb{RT}_1 - \mathbf{P}_1$ scheme on a mesh with 108,022 triangular elements (corresponding to 1,732,924 degrees of freedom) generated through the adaptive procedure driven by Θ. The results confirm the expected behavior of the scheme. In particular, the two low-porosity patches generate regions of reduced effective permeability, so that the flow is diverted around them and preferential channels are formed in the surrounding areas. At the same time, the cavity induces an additional local acceleration above its upper boundary. In turn, the pressure distribution is consistent with the heterogeneous structure of the medium. More precisely, p_h exhibits a global drop along the channel together with stronger local variations near the low-porosity patches, where the resistance to the flow is higher. Finally, snapshots of three adapted meshes generated using Θ are shown in Figure 6.8. As expected, refinement is mainly concentrated near the upper

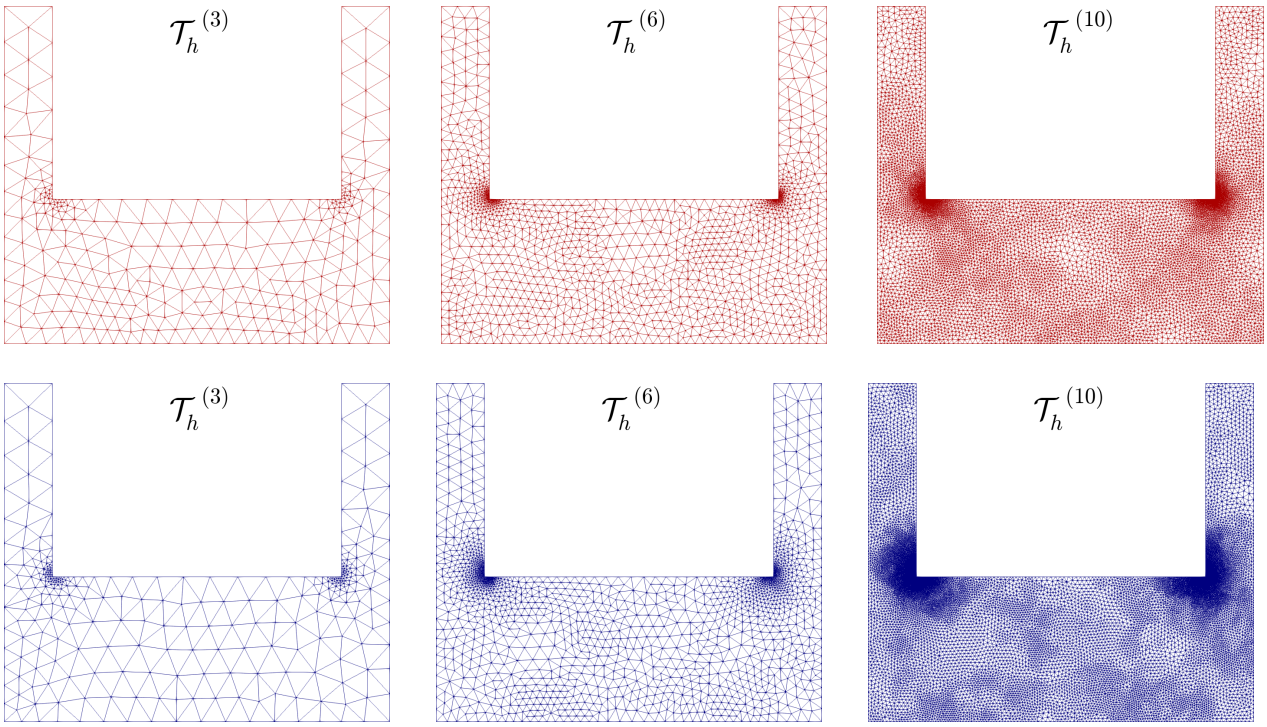

Figure 6.3: [Example 2] Three snapshots of adapted meshes according to the indicator Θ for $k = 0$ and $k = 1$ (top and bottom plots, respectively).

corners of the cavity and around the low-porosity regions, where the solution exhibits the strongest spatial variations.

A Computing other variables of interest

In this appendix we introduce suitable approximations for additional variables of interest, such as the pressure p, the velocity gradient $\mathbf{G} := \nabla\mathbf{u}$, the vorticity $\boldsymbol{\omega} := \frac{1}{2}\big(\nabla\mathbf{u} - (\nabla\mathbf{u})^{\mathrm{t}}\big)$, the shear stress tensor $\widetilde{\boldsymbol{\sigma}} := \mu\big(\nabla\mathbf{u} + (\nabla\mathbf{u})^{\mathrm{t}}\big) - p\,\mathbb{I}$, and the scalar constant $c_{\boldsymbol{\sigma}}$ associated with the decomposition $\mathbb{H}(\mathbf{div}_{4/3};\Omega) = \mathbb{H}_0(\mathbf{div}_{4/3};\Omega) \oplus \mathrm{R}\,\mathbb{I}$. All these quantities can be readily computed in terms of $\boldsymbol{\sigma}$, $\mathbf{u}$, and ρ, namely

$$p = -\frac{1}{d}\left\{\mathrm{tr}(\boldsymbol{\sigma} + \mathbf{u}\otimes\mathbf{u}) + d\,c_{\boldsymbol{\sigma}} + \mu\left(\mathbf{u}\cdot\frac{\nabla\rho}{\rho}\right)\right\}, \quad \mathbf{G} = \frac{1}{\mu}\,\boldsymbol{\sigma}^{\mathtt{d}} + \frac{1}{\mu}\,(\mathbf{u}\otimes\mathbf{u})^{\mathtt{d}} - \frac{1}{d}\left(\mathbf{u}\cdot\frac{\nabla\rho}{\rho}\right)\mathbb{I},$$

$$\boldsymbol{\omega} = \frac{1}{2\,\mu}\left(\boldsymbol{\sigma} - \boldsymbol{\sigma}^{\mathrm{t}}\right), \quad \widetilde{\boldsymbol{\sigma}} = \boldsymbol{\sigma}^{\mathtt{d}} + (\mathbf{u}\otimes\mathbf{u})^{\mathtt{d}} + \boldsymbol{\sigma}^{\mathrm{t}} + (\mathbf{u}\otimes\mathbf{u}) - \left\{\frac{\mu}{d}\left(\mathbf{u}\cdot\frac{\nabla\rho}{\rho}\right) - c_{\boldsymbol{\sigma}}\right\}\mathbb{I}, \tag{A.1}$$

$$\text{with} \quad c_{\boldsymbol{\sigma}} = -\frac{1}{d\,|\Omega|}\left\{\int_\Omega \mathrm{tr}(\mathbf{u}\otimes\mathbf{u}) - \mu\int_\Gamma \mathbf{u}_{\mathrm{D}}\cdot\mathbf{n}\right\}.$$

Hence, provided the discrete solution $(\boldsymbol{\sigma}_h, \mathbf{u}_h) \in \mathbb{H}_h^{\boldsymbol{\sigma}} \times \mathbf{H}_h^{\mathbf{u}}$ of problem (4.2), we propose the following approximations for the aforementioned variables:

$$p_h = -\frac{1}{d}\left\{\mathrm{tr}(\boldsymbol{\sigma}_h + \mathbf{u}_h\otimes\mathbf{u}_h) + d\,c_{\boldsymbol{\sigma},h} + \mu\left(\mathbf{u}_h\cdot\frac{\nabla\rho}{\rho}\right)\right\},$$

$\mathbb{RT}_0 - \mathbf{P}_0$ scheme with quasi-uniform refinement										
DoF	h	it	e($\boldsymbol{\sigma}$)	$r(\boldsymbol{\sigma})$	e($\mathbf{u}$)	$r(\mathbf{u})$	e($\boldsymbol{\sigma},\mathbf{u}$)	$r(\boldsymbol{\sigma},\mathbf{u})$	Θ	eff(Θ)
1464	0.433	4	1.21e+02	–	7.60e-01	–	1.21e+02	–	1.41e+02	0.862
11040	0.217	4	1.10e+02	0.142	5.52e-01	0.474	1.10e+02	0.144	1.14e+02	0.969
57624	0.124	4	9.66e+01	0.231	3.94e-01	0.612	9.70e+01	0.232	9.64e+01	1.006
285984	0.072	3	7.20e+01	0.548	2.23e-01	1.062	7.23e+01	0.550	7.14e+01	1.012
1518804	0.041	3	4.66e+01	0.782	1.10e-01	1.266	4.67e+01	0.783	4.63e+01	1.010

$\mathbb{RT}_0 - \mathbf{P}_0$ scheme with adaptive refinement									
DoF	it	e($\boldsymbol{\sigma}$)	$r(\boldsymbol{\sigma})$	e($\mathbf{u}$)	$r(\mathbf{u})$	e($\boldsymbol{\sigma},\mathbf{u}$)	$r(\boldsymbol{\sigma},\mathbf{u})$	Θ	eff(Θ)
1464	4	1.21e+02	–	7.60e-01	–	1.21e+02	–	1.41e+02	0.862
5691	4	1.05e+02	0.314	5.20e-01	0.840	1.05e+02	0.317	1.16e+02	0.907
28371	3	6.73e+01	0.826	2.17e-01	1.633	6.75e+01	0.829	7.33e+01	0.920
163644	3	3.16e+01	1.294	1.07e-01	1.204	3.17e+01	1.294	3.59e+01	0.882
867321	3	1.78e+01	1.033	5.60e-02	1.168	1.78e+01	1.034	2.01e+01	0.889

Table 6.5: [Example 3] Comparison of the $\mathbb{RT}_0 - \mathbf{P}_0$ mixed approximation with quasi-uniform and adaptive refinements.

DoF	19,496	48,138	107,428	210,892	426,664	857,154	1,732,924
it	4	4	4	4	4	4	4
Θ	2.95e+01	7.26e+00	2.57e+00	1.36e+00	6.77e-01	3.81e-01	1.88e-01
$r(\Theta)$	–	3.11	2.58	1.90	1.97	1.65	2.01

Table 6.6: [Example 4] Number of degrees of freedom, Newton iteration count, global estimator, and experimental rate of convergence of the global estimator.

$$\mathbf{G}_h = \frac{1}{\mu}\,\boldsymbol{\sigma}_h^{\mathtt{d}} + \frac{1}{\mu}\,(\mathbf{u}_h \otimes \mathbf{u}_h)^{\mathtt{d}} - \frac{1}{d}\left(\mathbf{u}_h \cdot \frac{\nabla \rho}{\rho}\right)\mathbb{I}\,, \quad \boldsymbol{\omega}_h = \frac{1}{2\,\mu}\left(\boldsymbol{\sigma}_h - \boldsymbol{\sigma}_h^{\mathtt{t}}\right)\,, \tag{A.2}$$

$$\widetilde{\boldsymbol{\sigma}}_h = \boldsymbol{\sigma}_h^{\mathtt{d}} + (\mathbf{u}_h \otimes \mathbf{u}_h)^{\mathtt{d}} + \boldsymbol{\sigma}_h^{\mathtt{t}} + (\mathbf{u}_h \otimes \mathbf{u}_h) - \left\{\frac{\mu}{d}\left(\mathbf{u}_h \cdot \frac{\nabla \rho}{\rho}\right) - c_{\boldsymbol{\sigma},h}\right\}\mathbb{I}\,,$$

$$\text{with} \quad c_{\boldsymbol{\sigma},h} = -\frac{1}{d\,|\Omega|}\left\{\int_\Omega \mathrm{tr}(\mathbf{u}_h \otimes \mathbf{u}_h) - \mu \int_\Gamma \mathbf{u}_{\mathrm{D}} \cdot \mathbf{n}\right\}\,.$$

The following result, which follows directly from Theorem 4.6, provides the corresponding approximation properties of the postprocessing procedure.

Lemma A.1 *Let $(\boldsymbol{\sigma},\mathbf{u}) \in \mathbb{H}_0(\mathbf{div}_{4/3};\Omega) \times \mathbf{L}^4(\Omega)$ be the unique solution of the continuous problem (2.22), and let p, $\mathbf{G}$, $\boldsymbol{\omega}$, and $\widetilde{\boldsymbol{\sigma}}$ be the postprocessed variables defined in (A.1). In addition, let p_h, $\mathbf{G}_h$, $\boldsymbol{\omega}_h$, and $\widetilde{\boldsymbol{\sigma}}_h$ denote their discrete counterparts introduced in (A.2). Let $l \in (0, k+1]$ and assume that the hypotheses of Theorem 4.6 hold. Then there exists a constant $\mathcal{C} > 0$, independent of h, such that*

$$\|p - p_h\|_{0,\Omega} + \|\mathbf{G} - \mathbf{G}_h\|_{0,\Omega} + \|\boldsymbol{\omega} - \boldsymbol{\omega}_h\|_{0,\Omega} + \|\widetilde{\boldsymbol{\sigma}} - \widetilde{\boldsymbol{\sigma}}_h\|_{0,\Omega}$$
$$\leq \mathcal{C}\, h^l \Big\{ \|\boldsymbol{\sigma}\|_{l,\Omega} + \|\mathbf{div}(\boldsymbol{\sigma})\|_{l,4/3;\Omega} + \|\mathbf{u}\|_{l,4;\Omega} \Big\}.$$

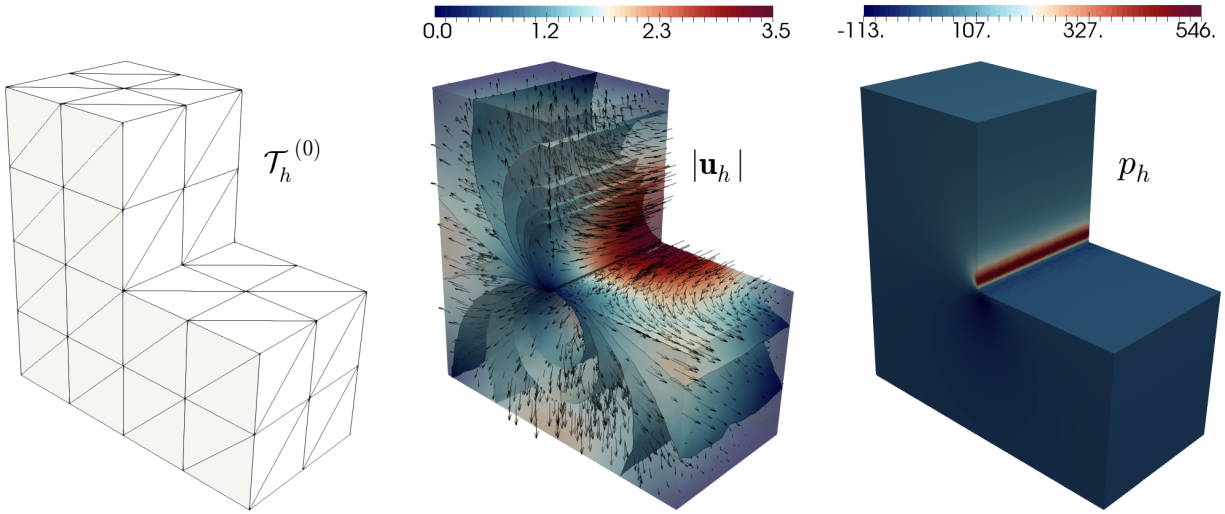

Figure 6.4: [Example 3] Initial mesh, computed magnitude of the velocity, and pressure field.

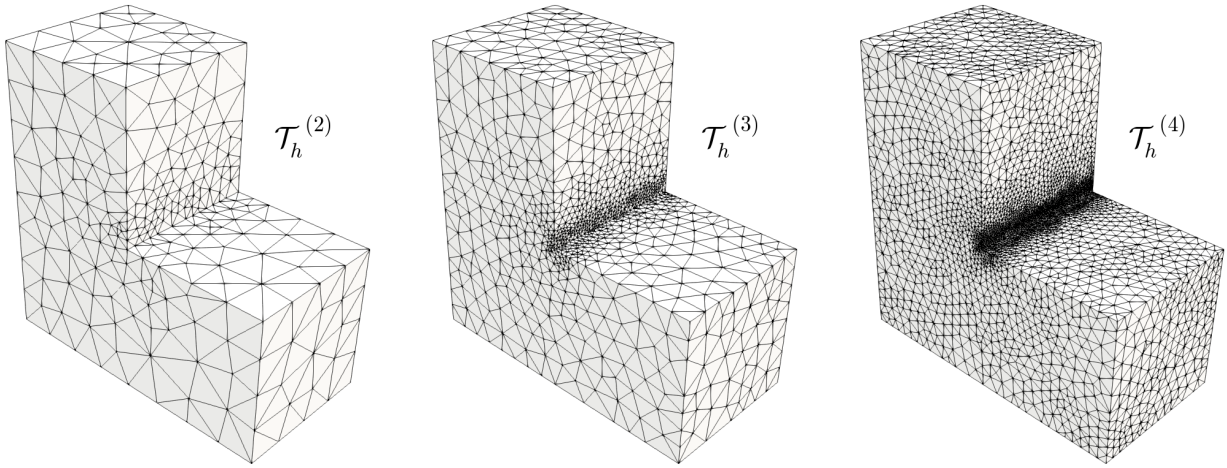

Figure 6.5: [Example 3] Three snapshots of adapted meshes according to the indicator Θ for $k = 0$.

Proof. From (A.1) and (A.2), by adding and subtracting $\mathbf{u} \otimes \mathbf{u}_h$ and applying the triangle and Hölder inequalities, we obtain that there exists a constant $C > 0$, depending only on the data and other constants independent of h, such that

$$\begin{aligned}
&\|p - p_h\|_{0,\Omega} + \|\mathbf{G} - \mathbf{G}_h\|_{0,\Omega} + \|\boldsymbol{\omega} - \boldsymbol{\omega}_h\|_{0,\Omega} + \|\widetilde{\boldsymbol{\sigma}} - \widetilde{\boldsymbol{\sigma}}_h\|_{0,\Omega} \\
&\leq C \left\{ \|\boldsymbol{\sigma} - \boldsymbol{\sigma}_h\|_{0,\Omega} + \left(\|\mathbf{u}\|_{0,4;\Omega} + \|\mathbf{u}_h\|_{0,4;\Omega} + \left\| \frac{\nabla \rho}{\rho} \right\|_{0,4;\Omega} \right) \|\mathbf{u} - \mathbf{u}_h\|_{0,4;\Omega} \right\}.
\end{aligned}$$

Then, using that $\mathbf{u} \in \mathbf{W}_r$ and $\mathbf{u}_h \in \mathbf{W}_{r,\mathrm{d}}$, together with assumption (4.15), the result follows directly from Theorem 4.6. □

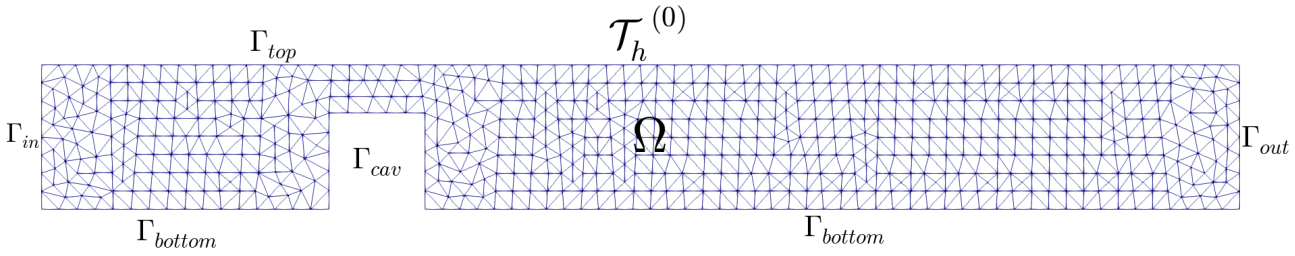

Figure 6.6: [Example 4]: Initial mesh of the non-convex channel.

B Preliminaries for reliability

We start by introducing a few useful notations for describing local information on elements and edges or faces depending on wether $d = 2$ or $d = 3$, respectively. Let $\mathcal{E}_h$ be the set of edges or faces of $\mathcal{T}_h$, whose corresponding diameters are denoted by h_e, and define

$$\mathcal{E}_h(\Omega) := \{e \subseteq \mathcal{E}_h : \quad e \subseteq \Omega\} \quad \text{and} \quad \mathcal{E}_h(\Gamma) := \{e \subseteq \mathcal{E}_h : \quad e \subseteq \Gamma\}\,.$$

For each $T \in \mathcal{T}_h$, we let $\mathcal{E}_{h,T}$ be the set of edges or faces of T, and denote

$$\mathcal{E}_{h,T}(\Omega) := \{e \subseteq \partial T : \quad e \subseteq \mathcal{E}_h(\Omega)\} \quad \text{and} \quad \mathcal{E}_{h,T}(\Gamma) := \{e \subseteq \partial T : \quad e \subseteq \mathcal{E}_h(\Gamma)\}\,.$$

We also define the unit normal vector $\mathbf{n}_e$ on each edge or face by

$$\mathbf{n}_e := (n_1, \ldots, n_d)^{\mathrm{t}} \quad \forall\, e \in \mathcal{E}_h\,.$$

Hence, when $d = 2$ we can define the tangential vector $\mathbf{s}_e$ by

$$\mathbf{s}_e := (-n_2, n_1)^{\mathrm{t}} \quad \forall\, e \in \mathcal{E}_h\,.$$

However, when no confusion arises, we will simply write $\mathbf{n}$ and $\mathbf{s}$ instead of $\mathbf{n}_e$ and $\mathbf{s}_e$, respectively.

The usual jump operator $[\![\cdot]\!]$ across internal edges or faces is defined for piecewise continuous tensor, vector, or scalar-valued functions $\boldsymbol{\zeta}$, by

$$[\![\boldsymbol{\zeta}]\!] = \big(\boldsymbol{\zeta}|_{T_+}\big)\,|_e - \big(\boldsymbol{\zeta}|_{T_-}\big)\,|_e \quad \text{with} \quad e = \partial T_+ \cap \partial T_-\,, \tag{B.1}$$

where T_+ and T_- are the elements of $\mathcal{T}_h$ having e as a common edge or face. Finally, for sufficiently smooth vector $\mathbf{v} := (v_1, \ldots, v_d)^{\mathrm{t}}$ and tensor fields $\boldsymbol{\tau} := (\tau_{ij})_{i,j=1,d}$, we let

$$\boldsymbol{\delta}_*(\boldsymbol{\tau}) = \begin{cases} \boldsymbol{\tau}\,\mathbf{s} & , \quad \text{for } d = 2, \\ \begin{pmatrix} (\boldsymbol{\tau}_1^{\mathrm{t}} \times \mathbf{n})^{\mathrm{t}} \\ (\boldsymbol{\tau}_2^{\mathrm{t}} \times \mathbf{n})^{\mathrm{t}} \\ (\boldsymbol{\tau}_3^{\mathrm{t}} \times \mathbf{n})^{\mathrm{t}} \end{pmatrix} & , \quad \text{for } d = 3, \end{cases} \qquad \mathbf{curl}\,(\mathbf{v}) := \begin{pmatrix} \dfrac{\partial v_1}{\partial x_2} & -\dfrac{\partial v_1}{\partial x_1} \\ \dfrac{\partial v_2}{\partial x_2} & -\dfrac{\partial v_2}{\partial x_1} \end{pmatrix} \quad \text{for } d = 2\,, \tag{B.2}$$

$$\underline{\mathrm{curl}}\,(\mathbf{v}) := \begin{cases} \dfrac{\partial v_2}{\partial x_1} - \dfrac{\partial v_1}{\partial x_2} & , \quad \text{for } d = 2\,, \\ \nabla \times \mathbf{v} & , \quad \text{for } d = 3\,, \end{cases} \qquad \underline{\mathbf{curl}}\,(\boldsymbol{\tau}) = \begin{cases} \begin{pmatrix} \underline{\mathrm{curl}}\,(\boldsymbol{\tau}_1^{\mathrm{t}}) \\ \underline{\mathrm{curl}}\,(\boldsymbol{\tau}_2^{\mathrm{t}}) \end{pmatrix} & , \quad \text{for } d = 2, \\ \begin{pmatrix} \underline{\mathrm{curl}}\,(\boldsymbol{\tau}_1^{\mathrm{t}})^{\mathrm{t}} \\ \underline{\mathrm{curl}}\,(\boldsymbol{\tau}_2^{\mathrm{t}})^{\mathrm{t}} \\ \underline{\mathrm{curl}}\,(\boldsymbol{\tau}_3^{\mathrm{t}})^{\mathrm{t}} \end{pmatrix} & , \quad \text{for } d = 3, \end{cases}$$

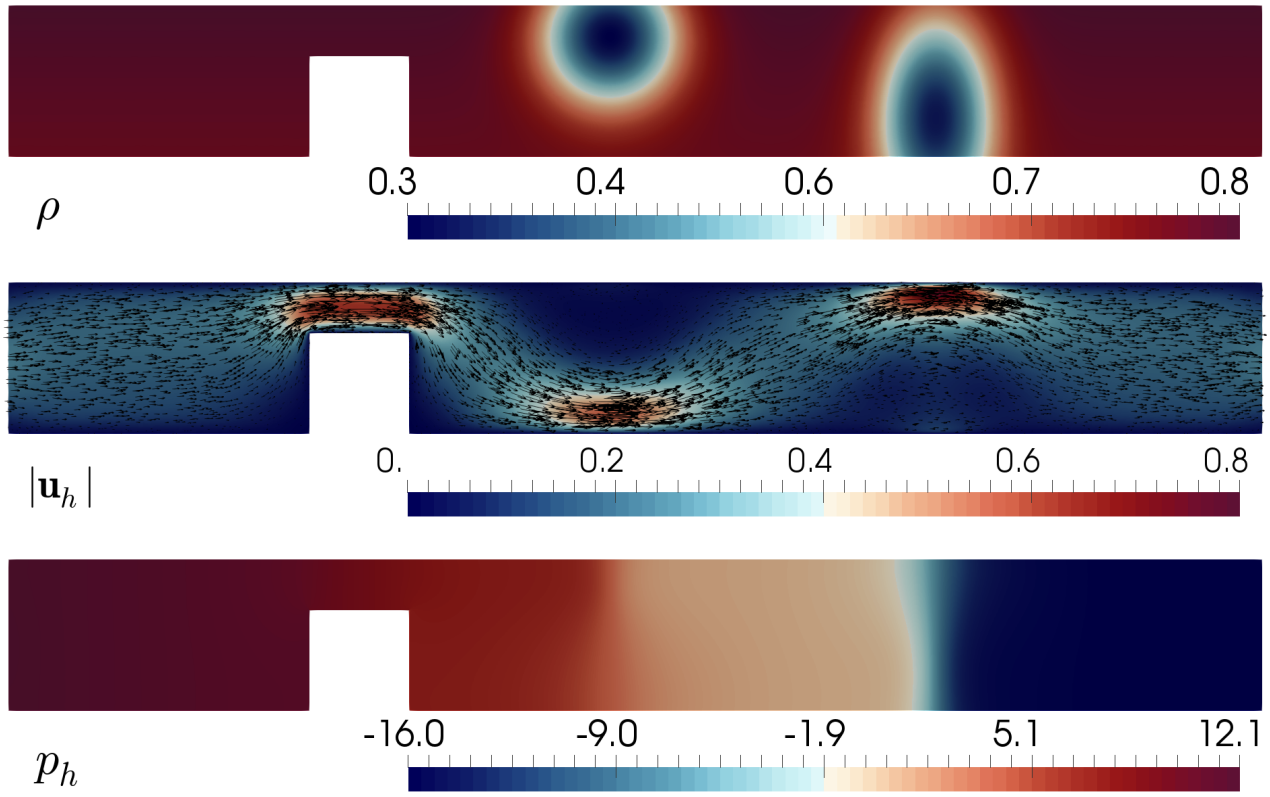

Figure 6.7: [Example 4]: Porosity (top), velocity magnitude (middle), and pressure (bottom).

where $\boldsymbol{\tau}_i$ is the i-th row of $\boldsymbol{\tau}$ and the derivatives involved are taken in the distributional sense.

Let us now recall the main properties of the Raviart–Thomas and Clément interpolation operators (cf. [24], [18]). We begin by defining for each $p \geq \frac{2\,d}{d+2}$ the spaces

$$\mathbf{H}_p := \left\{ \boldsymbol{\tau} \in \mathbf{H}(\mathrm{div}_p;\Omega) : \quad \boldsymbol{\tau}|_T \in \mathbf{W}^{1,p}(T) \quad \forall\, T \in \mathcal{T}_h \right\}, \tag{B.3}$$

and

$$\widehat{\mathbf{H}}_h^{\boldsymbol{\sigma}} := \left\{ \boldsymbol{\tau} \in \mathbf{H}(\mathrm{div}_p;\Omega) : \quad \boldsymbol{\tau}|_T \in \mathbf{RT}_k(T) \quad \forall\, T \in \mathcal{T}_h \right\}. \tag{B.4}$$

In addition, we let $\Pi_h^k : \mathbf{H}_p \to \widehat{\mathbf{H}}_h^{\boldsymbol{\sigma}}$ be the Raviart–Thomas interpolation operator, which is characterized for each $\boldsymbol{\tau} \in \mathbf{H}_p$ by the identities (see, e.g. [24, Section 1.2.7])

$$\int_e (\Pi_h^k(\boldsymbol{\tau})\cdot\mathbf{n})\,\xi \;=\; \int_e (\boldsymbol{\tau}\cdot\mathbf{n})\,\xi \quad \forall\, \xi \in \mathrm{P}_k(e), \quad \forall\, \text{edge or face } e \text{ of } \mathcal{T}_h\,, \tag{B.5}$$

when $k \geq 0$, and

$$\int_T \Pi_h^k(\boldsymbol{\tau})\cdot\boldsymbol{\psi} \;=\; \int_T \boldsymbol{\tau}\cdot\boldsymbol{\psi} \quad \forall\, \boldsymbol{\psi} \in \mathbf{P}_{k-1}(T), \quad \forall\, T \in \mathcal{T}_h\,,$$

when $k \geq 1$. In turn, given $q > 1$ such that $1/p + 1/q = 1$, we let

$$\mathrm{H}_h^{\mathbf{u}} := \left\{ v \in \mathrm{L}^q(\Omega) : \quad v|_T \in \mathrm{P}_k(T) \quad \forall\, T \in \mathcal{T}_h \right\}, \tag{B.6}$$

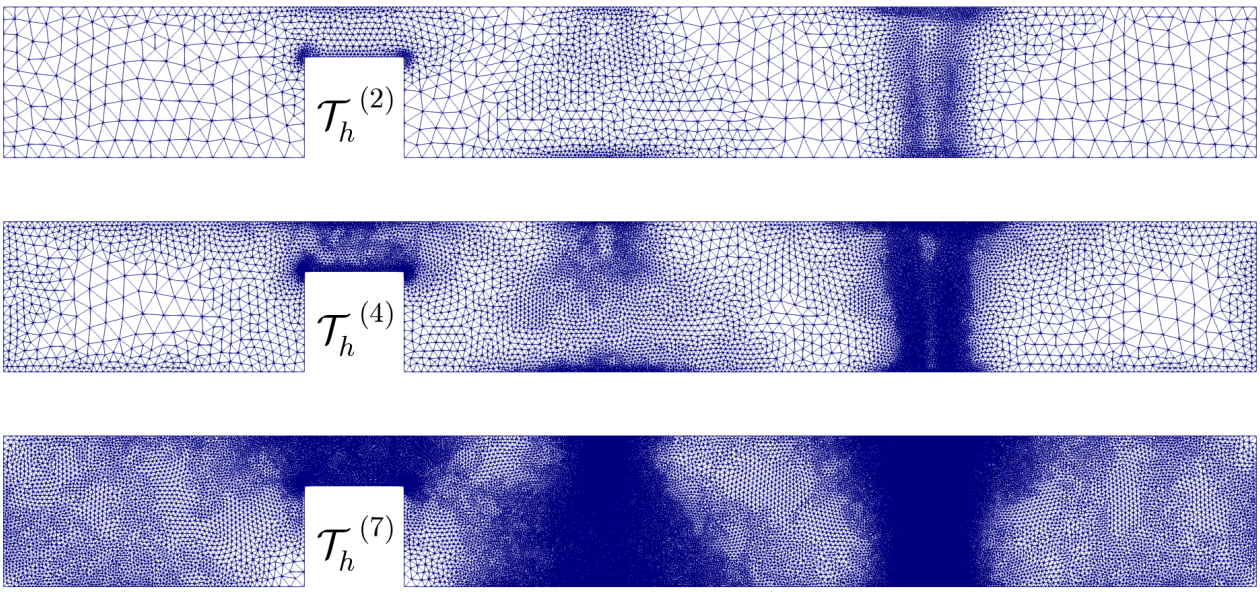

Figure 6.8: [Example 4] Three snapshots of adapted meshes according to the indicator Θ for $k = 1$.

and recall from [24, Lemma 1.41] that there holds

$$\mathrm{div}\big(\Pi_h^k(\boldsymbol{\tau})\big) = \mathcal{P}_h^k\big(\mathrm{div}(\boldsymbol{\tau})\big) \quad \forall\, \boldsymbol{\tau} \in \mathbf{H}_p\,, \tag{B.7}$$

where $\mathcal{P}_h^k : \mathrm{L}^p(\Omega) \to \mathrm{H}_h^{\mathbf{u}}$ is the usual orthogonal projector with respect to the $\mathrm{L}^2(\Omega)$-inner product, which satisfies the following error estimate (see [24, Proposition 1.135]): there exists a positive constant C_0, independent of h, such that for $0 \leq \ell \leq k+1$ and $1 \leq p \leq \infty$ there holds

$$\|w - \mathcal{P}_h^k(w)\|_{0,p;\Omega} \,\leq\, C_0\, h^\ell\, \|w\|_{\ell,p;\Omega} \quad \forall\, w \in \mathrm{W}^{\ell,p}(\Omega)\,. \tag{B.8}$$

We stress that $\mathcal{P}_h^k(w)|_T = \mathcal{P}_T^k(w|_T)\ \forall\, w \in \mathrm{L}^p(\Omega)$, where $\mathcal{P}_T^k : \mathrm{L}^p(T) \to \mathrm{P}_k(T)$ is the corresponding local orthogonal projector. In addition, denoting by $\mathbf{H}_h^{\mathbf{u}}$ the vector version of $\mathrm{H}_h^{\mathbf{u}}$ (cf. (B.6)), we let $\boldsymbol{\mathcal{P}}_h^k : \mathbf{L}^p(\Omega) \to \mathbf{H}_h^{\mathbf{u}}$ be the vector version of $\mathcal{P}_h^k$.

Next, we collect some approximation properties of Π_h^k.

Lemma B.1 *Given $p > 1$, there exist positive constants C_1, C_2, independent of h, such that for $0 \leq \ell \leq k$ and for each $T \in \mathcal{T}_h$ there holds*

$$\|\boldsymbol{\tau} - \Pi_h^k(\boldsymbol{\tau})\|_{0,p;T} \,\leq\, C_1\, h_T^{\ell+1}\, |\boldsymbol{\tau}|_{\ell+1,p;T} \quad \forall\, \boldsymbol{\tau} \in \mathbf{W}^{\ell+1,p}(T)\,, \tag{B.9}$$

and

$$\|\boldsymbol{\tau}\cdot\mathbf{n} - \Pi_h^k(\boldsymbol{\tau})\cdot\mathbf{n}\|_{0,p;e} \leq C_2\, h_e^{1-1/p}\, |\boldsymbol{\tau}|_{1,p;T} \quad \forall\, \boldsymbol{\tau} \in \mathbf{W}^{1,p}(T), \quad \forall\, e \in \mathcal{E}_h(T)\,. \tag{B.10}$$

Proof. For the estimate (B.9) we refer to [29, Lemma 3.1], whereas the proof of (B.10) can be found in [3, Lemma 4.2]. □

Furthermore, denoting by $\mathbb{H}_p$ and $\widehat{\mathbb{H}}_h^{\boldsymbol{\sigma}}$ the tensor versions of $\mathbf{H}_p$ (cf. (B.3)) and $\widehat{\mathbf{H}}_h^{\boldsymbol{\sigma}}$ (cf. (B.4)), respectively, we let $\boldsymbol{\Pi}_h^k : \mathbb{H}_p \to \widehat{\mathbb{H}}_h^{\boldsymbol{\sigma}}$ be the operator Π_h^k acting row-wise. Then, according to the decomposition (2.21), for each $\boldsymbol{\tau} \in \mathbb{H}_p$ there holds (cf. (4.1))

$$\boldsymbol{\Pi}_h^k(\boldsymbol{\tau}) \,=\, \boldsymbol{\Pi}_{h,0}^k(\boldsymbol{\tau}) + \jmath\,\mathbb{I}, \quad \text{with} \quad \boldsymbol{\Pi}_{h,0}^k(\boldsymbol{\tau}) \in \mathbb{H}_h^{\boldsymbol{\sigma}} \quad \text{and} \quad \jmath := \frac{1}{d\,|\Omega|}\int_\Omega \mathrm{tr}(\boldsymbol{\Pi}_h^k(\boldsymbol{\tau})) \in \mathrm{R}\,.$$

Other approximation properties of Π_h^k and $\mathbf{\Pi}_h^k$, in particular those involving the div and **div** operators, can also be derived using (B.7) and (B.8), as well as their tensorial counterparts with $\mathbf{\Pi}_h^k$ and $\boldsymbol{\mathcal{P}}_h^k$.

We now recall from [3, Lemma 4.4] a stable Helmholtz decomposition for the nonstandard Banach space $\mathbb{H}(\mathbf{div}_p;\Omega)$, whose particular case given by $p = 4/3$ is considered in the present paper. More precisely, we have the following result.

Lemma B.2 *Let $1 < p \leq 2$ when $d = 2$ and $6/5 \leq p \leq 2$ when $d = 3$. Then, for each $\boldsymbol{\tau} \in \mathbb{H}(\mathbf{div}_p;\Omega)$, there exist*

(a) $\boldsymbol{\zeta} \in \mathbb{W}^{1,p}(\Omega)$ and $\boldsymbol{\xi} \in \mathbf{H}^1(\Omega)$ such that $\boldsymbol{\tau} = \boldsymbol{\zeta} + \mathbf{curl}\,(\boldsymbol{\xi})$ in Ω when $d = 2$,

(b) $\boldsymbol{\zeta} \in \mathbb{W}^{1,p}(\Omega)$ and $\boldsymbol{\xi} \in \mathbb{H}^1(\Omega)$ such that $\boldsymbol{\tau} = \boldsymbol{\zeta} + \underline{\mathbf{curl}}\,(\boldsymbol{\xi})$ in Ω when $d = 3$.

In addition, in both cases there holds

$$\|\boldsymbol{\zeta}\|_{1,p;\Omega} + \|\boldsymbol{\xi}\|_{1,\Omega} \leq C_p\,\|\boldsymbol{\tau}\|_{\mathbf{div}_p;\Omega}\,,$$

where C_p is a positive constant independent of all the foregoing variables.

On the other hand, defining $X_h := \big\{v_h \in C(\overline{\Omega}) : \quad v_h|_T \in \mathrm{P}_1(T) \quad \forall\, T \in \mathcal{T}_h\big\}$ and denoting by $\mathbf{X}_h$ its tensor version, we let $\mathcal{I}_h : \mathrm{H}^1(\Omega) \to X_h$ and $\boldsymbol{\mathcal{I}}_h : \mathbb{H}^1(\Omega) \to \mathbf{X}_h$ be the usual Clément interpolation operator and its tensor version, respectively. Some local properties of $\mathcal{I}_h$, and hence of $\boldsymbol{\mathcal{I}}_h$, are established in the following lemma (cf. [18]):

Lemma B.3 *There exist positive constants C_1 and C_2, such that*

$$\|v - \mathcal{I}_h(v)\|_{0,T} \;\leq\; C_1\,h_T\,\|v\|_{1,\Delta(T)} \quad \forall\, T \in \mathcal{T}_h\,,$$

and

$$\|v - \mathcal{I}_h(v)\|_{0,e} \;\leq\; C_2\,h_e^{1/2}\,\|v\|_{1,\Delta(e)} \quad \forall\, e \in \mathcal{E}_h\,,$$

where $\Delta(T) := \cup\big\{T' \in \mathcal{T}_h : \quad T' \cap T \neq \emptyset\big\}$ and $\Delta(e) := \cup\big\{T' \in \mathcal{T}_h : \quad T' \cap e \neq \emptyset\big\}$.

C Preliminaries for efficiency

For the efficiency analysis of Θ (cf. (5.1)), we proceed as in [30], [12], [3] and [29], and apply the localization technique based on bubble functions, along with inverse and discrete trace inequalities. For the former, given $T \in \mathcal{T}_h$, we let T be the usual element-bubble function (cf. [44, eqs. (1.5) and (1.6)]), which satisfies

$$\psi_T \in \mathrm{P}_3(T), \quad \mathrm{supp}(\psi_T) \subseteq T, \quad \psi_T = 0 \quad \text{on} \quad \partial T \quad \text{and} \quad 0 \leq \psi_T \leq 1 \quad \text{in} \quad T\,. \tag{C.1}$$

The specific properties of ψ_T to be employed in what follows, are collected in the following lemma, for whose proof we refer to [44, Lemma 3.3 and Remark 3.2].

Lemma C.1 *Let k be a non-negative integer, and let $p, q \in (1, +\infty)$ conjugate to each other, that is such that $1/p + 1/q = 1$, and $T \in \mathcal{T}_h$. Then, there exist positive constants c_1, c_2, and c_3, independent of h and T, but depending on the shape-regularity of the triangulations (minimum angle condition) and k, such that for each $u \in \mathrm{P}_k(T)$ there hold*

$$c_1\|u\|_{0,p;T} \;\leq\; \sup_{0 \neq v \in \mathrm{P}_k(T)} \frac{\displaystyle\int_T u\,\psi_T v}{\|v\|_{0,q;T}} \;\leq\; \|u\|_{0,p;T} \tag{C.2}$$

and

$$c_2\, h_T^{-1}\|\psi_T u\|_{0,q;T} \,\leq\, \|\nabla(\psi_T u)\|_{0,q;T} \,\leq\, c_3\, h_T^{-1}\|\psi_T u\|_{0,q;T}\,. \tag{C.3}$$

In turn, the aforementioned inverse inequality is stated as follows (cf. [24, Lemma 1.138]).

Lemma C.2 *Let d, k, ℓ, and m be non-negative integers such that $m \leq \ell$, and let $r, s \in [1, +\infty]$, and $T \in \mathcal{T}_h$. Then, there exists $c > 0$, independent of h, T, r, and s, but depending on d, k, ℓ, m, and the shape regularity of the triangulations, such that*

$$\|v\|_{\ell,r;T} \,\leq\, c\, h_T^{m-\ell+d(1/r-1/s)}\|v\|_{m,s;T} \quad \forall\, v \in \mathrm{P}_k(T)\,. \tag{C.4}$$

Finally, proceeding as in [1, Theorem 3.10], that is employing the usual scaling estimates with respect to a fixed reference element $\widehat{T}$, and applying the trace inequality in $\mathrm{W}^{1,p}(\widehat{T})$, for a given $p \in (1, +\infty)$, one is able to establish the following discrete trace inequality.

Lemma C.3 *Let $p \in (1, +\infty)$. Then, there exits $c > 0$, depending only on the shape regularity of the triangulations, such that for each $T \in \mathcal{T}_h$ and $e \in \mathcal{E}(T)$, there holds*

$$\|v\|^p_{0,p;e} \,\leq\, c\left\{h_T^{-1}\,\|v\|^p_{0,p;T} + h_T^{p-1}\,|v|^p_{1,p;T}\right\} \quad \forall\, v \in \mathrm{W}^{1,p}(T)\,. \tag{C.5}$$

References

[1] S. Agmon, *Lectures on elliptic boundary value problems*. Van Nostrand, Princeton, NJ, 1965.

[2] F. Brezzi and M. Fortin, *Mixed and hybrid finite element methods*. Springer Series in Computational Mathematics, 15. Springer-Verlag, New York, 1991.

[3] J. Camaño, S. Caucao, R. Oyarzúa, and S. Villa-Fuentes, *A posteriori error analysis of a momentum conservative Banach spaces based mixed-FEM for the Navier–Stokes problem*. Appl. Numer. Math. 176 (2022), 134–158.

[4] J. Camaño, C. García, and R. Oyarzúa, *Analysis of a momentum conservative mixed-FEM for the stationary Navier–Stokes problem*. Numer. Methods Partial Differential Equations 37 (2021), no. 5, 2895–2923.

[5] J. Camaño, G.N. Gatica, R. Oyarzúa, and G. Tierra, *An augmented mixed finite element method for the Navier–Stokes equations with variable viscosity*. SIAM J. Numer. Anal. 54 (2016), no. 2, 1069–1092.

[6] J. Camaño, C. Muñoz, and R. Oyarzúa, *Numerical analysis of a dual-mixed problem in non-standard Banach spaces*. Electron. Trans. Numer. Anal. 48 (2018), 114–130.

[7] S. Carrasco, S. Caucao, and G.N. Gatica, *New mixed finite element methods for the coupled convective Brinkman–Forchheimer and double-diffusion equations*. J. Sci. Comput. 97 (2023), no. 3, Article No. 61.

[8] S. Caucao, E. Colmenares, G.N. Gatica, and C. Inzunza, *A Banach spaces-based fully-mixed finite element method for the stationary chemotaxis–Navier–Stokes problem*. Comput. Math. Appl. 145 (2023), 65–89.

[9] S. Caucao and J. Esparza, *An augmented mixed FEM for the convective Brinkman–Forchheimer problem: a priori and a posteriori error analysis*. J. Comput. Appl. Math. 438 (2024), Article No. 115517.

[10] S. Caucao, G.N. Gatica, and J.P. Ortega, *A three-field mixed finite element method for the convective Brinkman–Forchheimer problem with varying porosity*. J. Comput. Appl. Math. 451 (2024), Article No. 116090.

[11] S. Caucao, G.N. Gatica, R. Oyarzúa, and N. Sánchez, *A fully-mixed formulation for the steady double-diffusive convection system based upon Brinkman–Forchheimer equations*. J. Sci. Comput. 85 (2020), no. 2, Paper No. 44, 37 pp.

[12] S. Caucao, G.N. Gatica, R. Oyarzúa, and F. Sandoval, *Residual-based a posteriori error analysis for the coupling of the Navier–Stokes and Darcy–Forchheimer equations*. ESAIM: Math. Model. Numer. Anal. 55 (2021), no. 2, 659–687.

[13] S. Caucao, G.N. Gatica, and L.F. Gatica, *A Banach spaces-based mixed finite element method for the stationary convective Brinkman–Forchheimer problem*. Calcolo 60 (2023), no. 4, Article No. 51.

[14] S. Caucao, G.N. Gatica, and L.F. Gatica, *A posteriori error analysis of a mixed finite element method for the stationary convective Brinkman–Forchheimer problem*. Appl. Numer. Math. 211 (2025), 158–178.

[15] S. Caucao, D. Mora, and R. Oyarzúa, *A priori and a posteriori error analysis of a pseudostress-based mixed formulation of the Stokes problem with varying density*. IMA J. Numer. Anal. 36 (2016), no. 2, 947–983.

[16] S. Caucao and P. Zúñiga, *A posteriori error analysis of a mixed FEM for the coupled Brinkman–Forchheimer/Darcy problem*. East Asian J. Appl. Math., to appear.

[17] A.O. Celebi, V.K. Kalantarov, and D. Ugurlu, *Continuous dependence for the convective Brinkman–Forchheimer equations*. Appl. Anal. 84 (2005), no. 9, 877–888.

[18] P. Clément, *Approximation by finite element functions using local regularization*. RAIRO Modélisation Mathématique et Analyse Numérique 9 (1975), 77–84.

[19] P.-H. Cocquet, M. Rakotobe, D. Ramalingom, and A. Bastide, *Error analysis for the finite element approximation of the Darcy–Brinkman–Forchheimer model for porous media with mixed boundary conditions*. J. Comput. Appl. Math. 381 (2021), Article No. 113008.

[20] E. Colmenares, G.N. Gatica, and S. Moraga, *A Banach spaces-based analysis of a new fully-mixed finite element method for the Boussinesq problem*. ESAIM Math. Model. Numer. Anal. 54 (2020), no. 5, 1525–1568.

[21] C.I. Correa and G.N. Gatica, *On the continuous and discrete well-posedness of perturbed saddle-point formulations in Banach spaces*. Comput. Math. Appl. 117 (2022), 14–23.

[22] C.I. Correa, G.N. Gatica, and R. Ruiz-Baier, *New mixed finite element methods for the coupled Stokes and Poisson–Nernst–Planck equations in Banach spaces*. ESAIM Math. Model. Numer. Anal., 57 (2023), no. 3, 1511–1551.

[23] C. Domínguez, G.N. Gatica, and S. Meddahi, *A posteriori error analysis of a fully-mixed finite element method for a two-dimensional fluid-solid interaction problem*. J. Comput. Math. 33 (2015), no. 6, 606–641.

[24] A. Ern and J.-L. Guermond, *Theory and practice of finite elements*. Applied Mathematical Sciences, 159. Springer-Verlag, New York, 2004.

[25] V.J. Ervin and T.N. Phillips, *Residual a posteriori error estimator for a three-field model of a non-linear generalized Stokes problem*. Comput. Methods Appl. Mech. Engrg. 195 (2006), no. 19–22, 2599–2610.

[26] M. Farhloul and A.M. Zine, *A posteriori error estimation for a dual mixed finite element approximation of non-Newtonian fluid flow problems*. Int. J. Numer. Anal. Model. 5 (2008), no. 2, 320–330.

[27] G.N. Gatica, *A Simple Introduction to the Mixed Finite Element Method. Theory and Applications*. SpringerBriefs in Mathematics. Springer, Cham, 2014.

[28] G.N. Gatica, C. Inzunza, and R. Ruiz-Baier, *Primal-mixed finite element methods for the coupled Biot and Poisson–Nernst–Planck equations*. Comput. Math. Appl. 186 (2025), 53–83.

[29] G.N. Gatica, C. Inzunza, R. Ruiz-Baier, and F. Sandoval, *A posteriori error analysis of Banach spaces-based fully-mixed finite element method for Boussinesq-type models*. J. Numer. Math. 30 (2022), no. 4, 325–356.

[30] G.N. Gatica, A. Márquez, and M.A. Sánchez, *Analysis of a velocity-pressure-pseudostress formulation for the stationary Stokes equations*. Comput. Methods Appl. Mech. Engrg. 199 (2010), 1064–1079.

[31] G. N. Gatica, N. Núñez, and R. Ruiz-Baier, *New non-augmented mixed finite element methods for the Navier–Stokes–Brinkman equations using Banach spaces*. J. Numer. Math. 31 (2023), no. 4, 343–373.

[32] V. Girault and P.A. Raviart, *Finite element methods for Navier–Stokes equations. Theory and algorithms*. Springer Series in Computational Mathematics, 5. Springer-Verlag, Berlin, 1986.

[33] V. Girault and M.F. Wheeler, *Numerical discretization of a Darcy–Forchheimer model*. Numer. Math. 110 (2008), no. 2, 161–198.

[34] R. Glowinski and A. Marrocco, *Sur l'approximation, par éléments finis d'ordre un, et la résolution, par pénalisations-dualité d'une classe de problémes de Dirichlet non lineaires*. R.A.I.R.O. 9 (1975), no. 2, 41–76.

[35] F. Hecht, *New development in FreeFem++*. J. Numer. Math. 20 (2012), no. 3-4, 251–265.

[36] F. Hecht, *FreeFem++*, Version 3.58-1, third edition. Laboratoire Jacques-Louis Lions, Université Pierre et Marie Curie, Paris, 2018.

[37] H. Li and H. Rui, *Parameter-robust mixed element method for poroelasticity with Darcy–Forchheimer flow*. Numer. Methods Partial Differential Equations 39 (2023), no. 5, 3634–3656.

[38] D. Liu and K. Li, *Mixed finite element for two-dimensional incompressible convective Brinkman–Forchheimer equations*. Appl. Math. Mech. (English Ed.) 40 (2019), no. 6, 889–910.

[39] H. Pan and H. Rui, *Mixed element method for two-dimensional Darcy–Forchheimer model*. J. Sci. Comput. 52 (2012), no. 3, 563–587.

[40] H. Pan and H. Rui, *A mixed element method for Darcy–Forchheimer incompressible miscible displacement problem*. Comput. Methods Appl. Mech. Engrg. 264 (2013), 1–11.

[41] H. Rui and W. Liu, *A two-grid block-centered finite difference method for Darcy–Forchheimer flow in porous media*. SIAM J. Numer. Anal. 53 (2015), no. 4, 1941–1965.

[42] P. Skrzypacz and D. Wei, *Solvability of the Brinkman–Forchheimer–Darcy equation*. J. Appl. Math. (2017), Article ID 7305230, 10 pp.

[43] C. Varsakelis and M.V. Papalexandris, *On the well-posedness of the Darcy–Brinkman–Forchheimer equations for coupled porous media-clear fluid flow*. Nonlinearity 30 (2017), no. 4, 1449–1464.

[44] R. Verfürth, *A review of a-posteriori error estimation and adaptive mesh-refinement techniques*. Wiley–Teubner, Chichester, 1996.

[45] C. Zhao and Y. You, *Approximation of the incompressible convective Brinkman–Forchheimer equations*. J. Evol. Equ. 12 (2012), no. 4, 767–788.

Centro de Investigación en Ingeniería Matemática (CI^{2}MA)

PRE-PUBLICACIONES 2026

2026-01 Alonso J. Bustos, Gabriel N. Gatica, Ricardo Ruiz-Baier, Benjamín N. Venegas: *A perturbed threefold saddle-point formulation yielding new mixed finite element methods for poroelasticity with reduced symmetry*

2026-02 Jorge Aguayo, Rodolfo Araya: *A Nitsche-type finite element method for the linear elasticity equation with discontinuity jumps*

2026-03 Sergio Caucao, Gabriel N. Gatica, Adrian Suarez, Ivan Yotov: *A skew-symmetry-based mixed formulation for an Oseen-type Kelvin–Voigt–Brinkman–Forchheimer model*

2026-04 Akbar Davoodi, Diana Piguet, Hanka Rada, Nicolás Sanhueza-Matamala: *The asymptotic version of the Erdős–Sós conjecture and beyond*

2026-05 Rodrigo Abarca Del Rio, Fernando Campos, Cristóbal Caro-Ramírez, Jean François Cretaux, Daniel Moreira, Alfredo Ribeiro Neto, Jonas Felipe Santos De Souza, Mauricio Sepúlveda: *First insights into the performance of the SWOT Level 2 River Single-Pass Vector Data Product in rivers with complex morphology: application to the Bíobío River basin, Chile*

2026-06 Juan José Maulén, Fernando Roldán, Cristian Vega: *Relaxed and inertial nonlinear Forward-Backward algorithm*

2026-07 Luis Briceño-Arias, Fernando Roldán: *Optimal leveraging of smoothness and strong convexity for Peaceman-Rachford splitting*

2026-08 Fahim Aslam, Jianghao Hao, Iqra Kanwal, Mauricio Sepúlveda: *Stability and finite-time blow-up for a fractionally damped nonlinear plate equation: numerical and analytical insights*

2026-09 Fahim Aslam, Zayd Hajjej, Jianghao Hao, Iqra Kanwal, Mauricio Sepúlveda, Rodrigo Véjar: *Stability and blow-up for a suspension bridge plate model with fractional damping and memory*

2026-10 Aníbal Coronel, Fernando Huancas, Mauricio Sepúlveda: *Identification of a power-like reaction term in a reaction-diffusion SIS model*

2026-11 Esteban Henriquez, Manuel Solano: *An unfitted HDG method for a distributed optimal convection-diffusion control problem*

2026-12 Sergio Caucao, Gabriel N. Gatica, Luis F. Gatica, Cristian Inzunza: *A priori and a posteriori error analysis of a mixed FEM for stationary convective Brinkman-Forchheimer flows with variable porosity*

Para obtener copias de las Pre-Publicaciones, escribir o llamar a: Director, Centro de Investigación en Ingeniería Matemática, Universidad de Concepción, Casilla 160-C, Concepción, Chile, Tel.: 41-2661324, o bien, visitar la página web del centro: `http://www.ci2ma.udec.cl`



Centro de Investigación en
Ingeniería Matemática (CI²MA)
Universidad de Concepción

Casilla 160-C, Concepción, Chile
Tel.: 56-41-2661324/2661554/2661316
http://www.ci2ma.udec.cl